The Abdus Salam
International Centre for Theoretical Physics

United Nations
Educational, Scientific
and Cultural Organization

International Atomic
Energy Agency

310/1749-44

ICTP-COST-USNSWP-CAWSES-INAF-INFN
International Advanced School
on
Space Weather
2-19 May 2006

The Sun

Natchimuthukonar GOPALSWAMY
NASA Goddard Space Flight Center (GSFC)
Solar System Exploration
Division Code 695
Greenbelt, MC 20771
U.S.A.

A splendid sunset in Hawaii (right) and the Egyptian Sun God Raa. Life on Earth depends on solar energy. The cobra on Raa reminds us of prominences, a phenomenon associated with solar eruptions that can cause severe space weather effects.

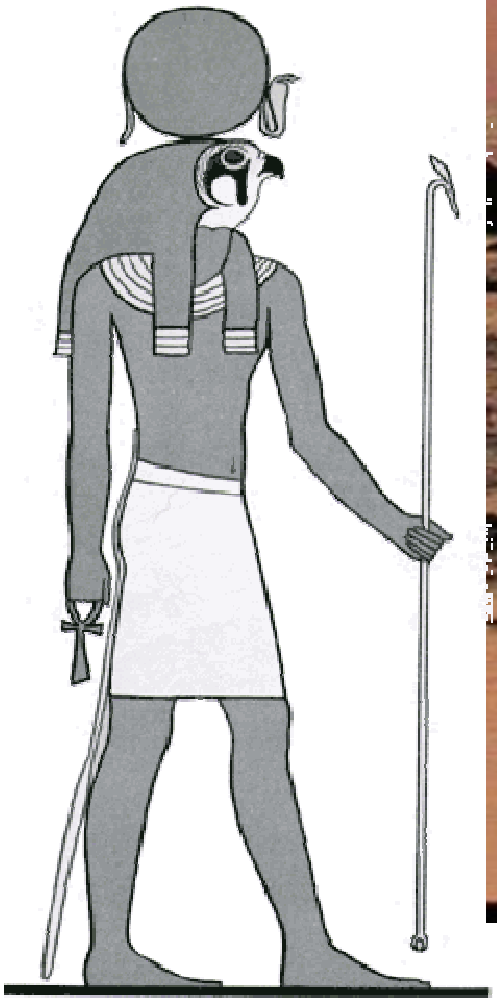

The Sun

N. Gopalswamy
NASA Goddard Space Flight Center

General Content of the Lectures

- Overview of the Sun
- Our Place in the Universe
- Solar Fuel and where does it come from?
- Why Sun is an ordinary star?
- Physics of the Solar Interior: energy generation and transport
- The “standard solar model” and its verification
- Solar magnetism: A consequence of solar rotation and turbulent convection – The Solar Dynamo
- Solar Atmosphere including CMEs and solar wind

Lecture I: Overview of the Sun and our place in the universe

- Sun's impact on the heliosphere
- Sun in the universe
- Solar fuel from Big Bang
- Fusion in the Sun
- Spectral types of stars, HR diagram
- Solar evolution
- The neutrino problem
- The standard solar model

Local and Global Views of the Sun

Sun is studied in two ways:

Global view (Sun as a star – how it evolved over billions of years): Such a view also helps understand other stars and provides a convenient reference for many stellar parameters such as size, mass, luminosity,…

Local view: The only star close enough to view the spatial and temporal variations. e.g. sunspots, active regions, faculae, spicules, granulation, plumes, prominences, coronal holes …

Sun is the basis for all life on Earth: the Sun shines and life thrives

The variability of the solar emissions also affect life on Earth as a source of space weather and possibly climate change. Understanding the solar variability in terms of the known physical laws is a major effort by a large community of solar and solar terrestrial physicists.

Overview of the Sun

A summary of what we know about the Sun from the interior to the atmosphere with various types of electromagnetic radiation and the mass emissions. Coronal mass ejections (CMEs), solar wind and solar energetic particles (SEPs) represent mass emissions

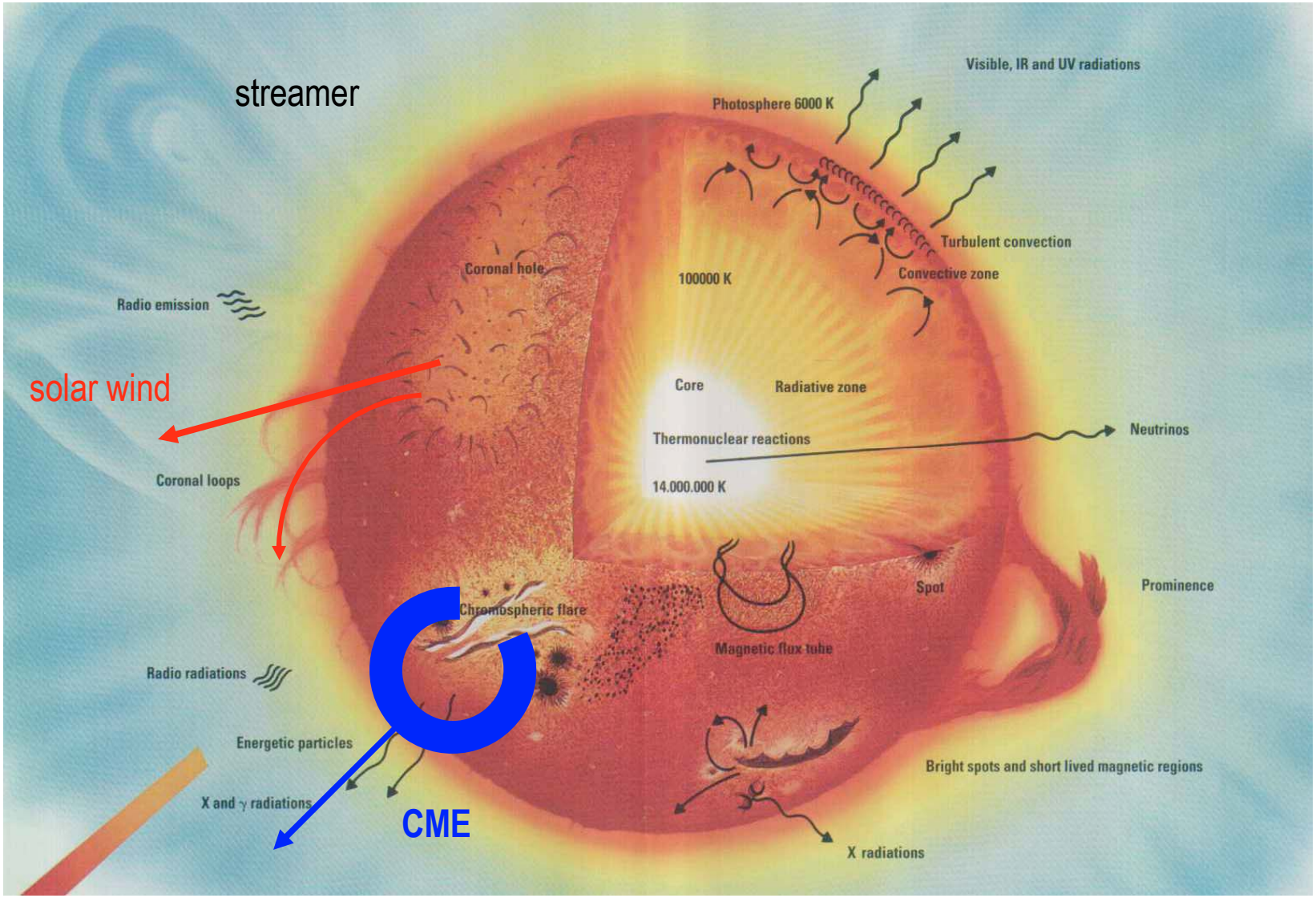

Solar Layers

The structure of the Sun
Consists of seven “layers”
- the core (energy generated)
- the radiative zone
- the convection zone
- the photosphere
- the chromosphere
- the transition zone
- the corona

The transition zone is a thin layer
Where the temperature increases
From tens of thousands of K to
A million K over a very short
distance

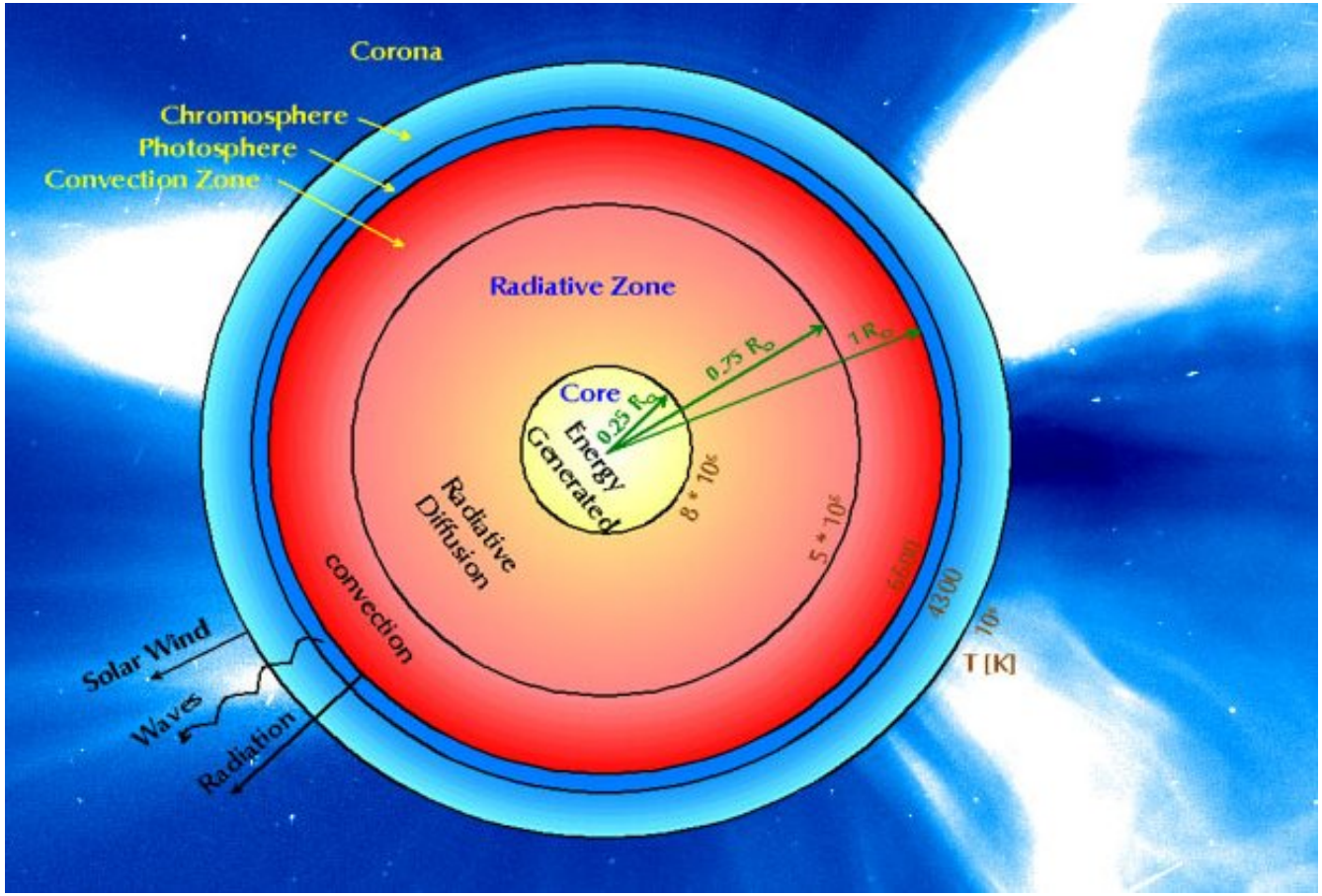

Jussila

Some Vital Statistics of the Sun

- Average, middle aged star (4.5 billion years) on the main sequence
- One among the 400 billion stars in the Milky Way
- The only star that is observable in great detail: units of measurement for stellar quantities
- Likely to become a white dwarf at the end
- Composed of ~72% hydrogen, ~26% helium and ~2% of all other chemical elements (most notably those up to oxygen) in gaseous form.
- Energy source: nuclear fusion at a temperature of ~14 MK
- Approximate sphere of radius ~696000 km (compare Earth radius 6400 km)
- Rotation rate: $13.45 - 3.0 \sin^2\varphi$ deg per day [φ = latitude] or rotation period ~26.7 days at the equator
- Rotation speed ~ 2 km/s at the equatorial photosphere
- mass ~2×10^{30} kg
- Average density ~ 1.4 g/cm^3
- Gravitational acceleration 274 m/s^2
- Luminosity (energy radiated by the sun in one second) $L_\odot$: 4×10^{26} W → 1.4 kW/m^2 at Earth's orbit
- Surface temperature ~5770 K [at this temperature a black body radiation peaks in visible light]
- An extended atmosphere known as corona at 2 million K → emits predominantly in X-rays
- Sun is at an average distance of ~1.5×10^8 km from Earth
- Sun emits the entire electromagnetic spectrum

Solar Variability & its Impact on the Solar System

Sun puts out -
electromagnetic radiation
(blackbody + flare)
and mass
(solar wind, CMEs, SEPs)

Mass Chain:
CMEs
Solar Wind
SEPs

Aspects of CMEs related to Space Weather :
- ability to cause Geomagnetic storms (geoeffectiveness)
- ability to drive shocks that accelerate SEPs (SEPeffectiveness)

Climate effects mainly from variability in electromagnetic radiation with a contribution from the mass chain

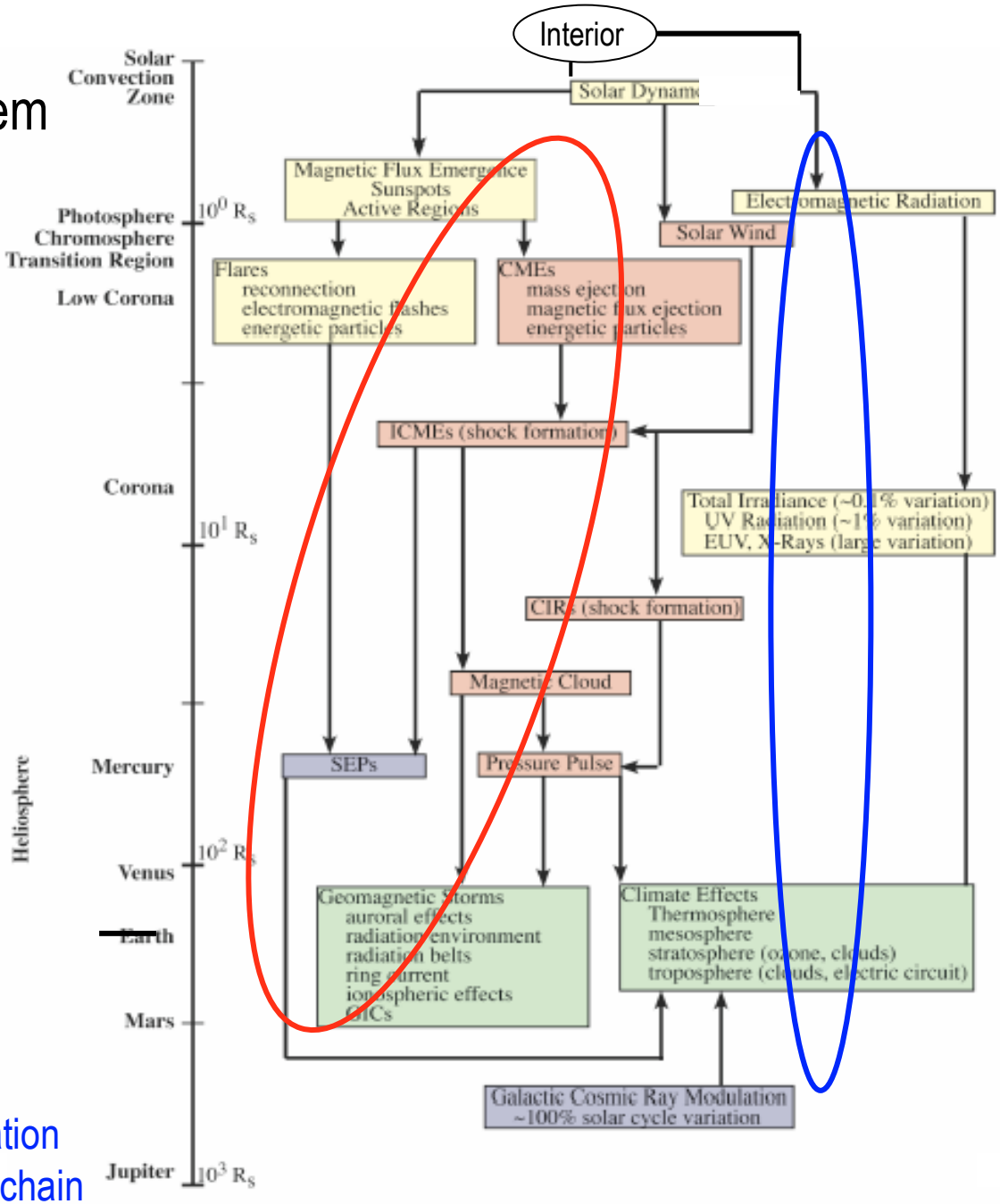

Position of the Sun in the Universe

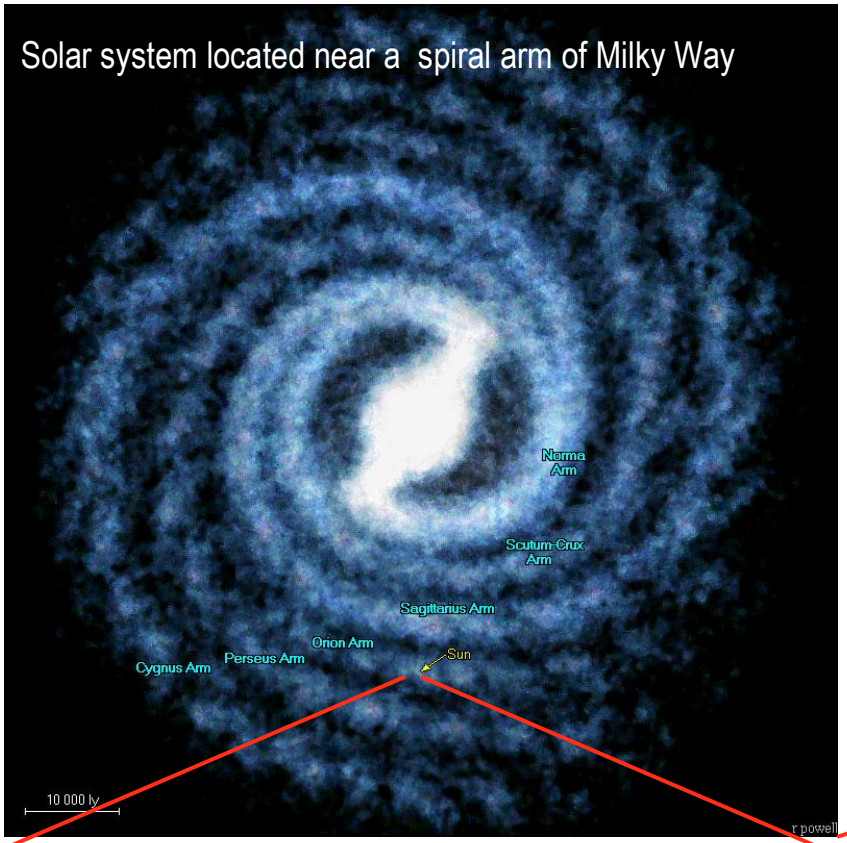

M83 – a galaxy similar to ours

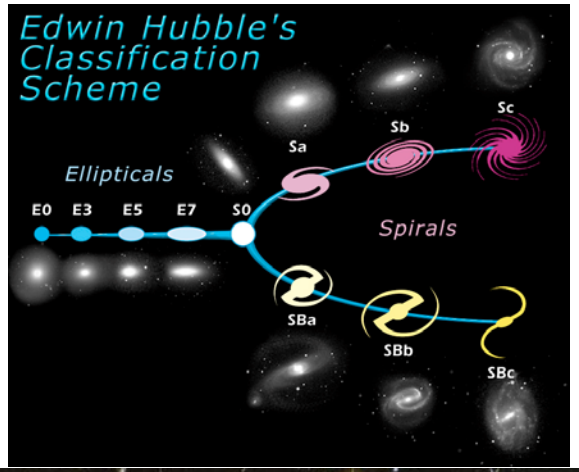

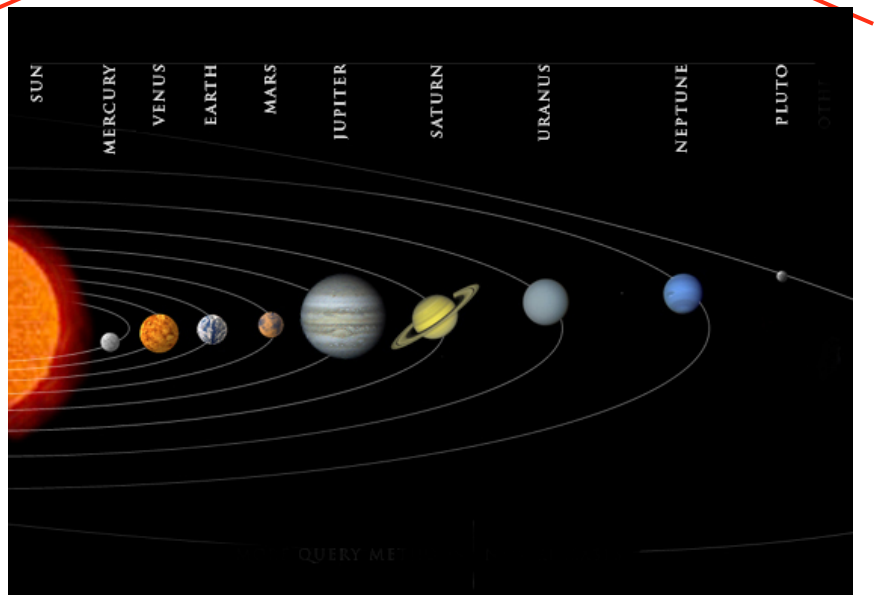

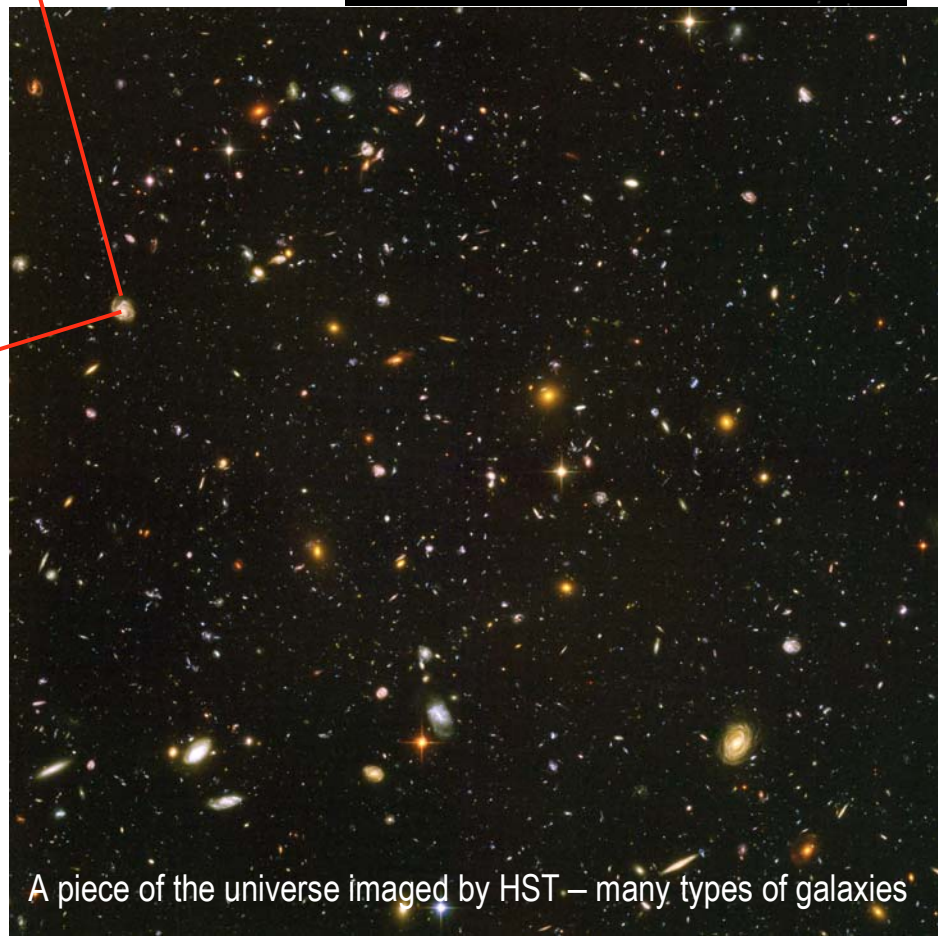

A piece of the universe imaged by HST – many types of galaxies

Our place in the Milky Way

sun is located at a distance of 26000 ly from the galactic center & slightly displaced from the galactic plane (by 20 ly)

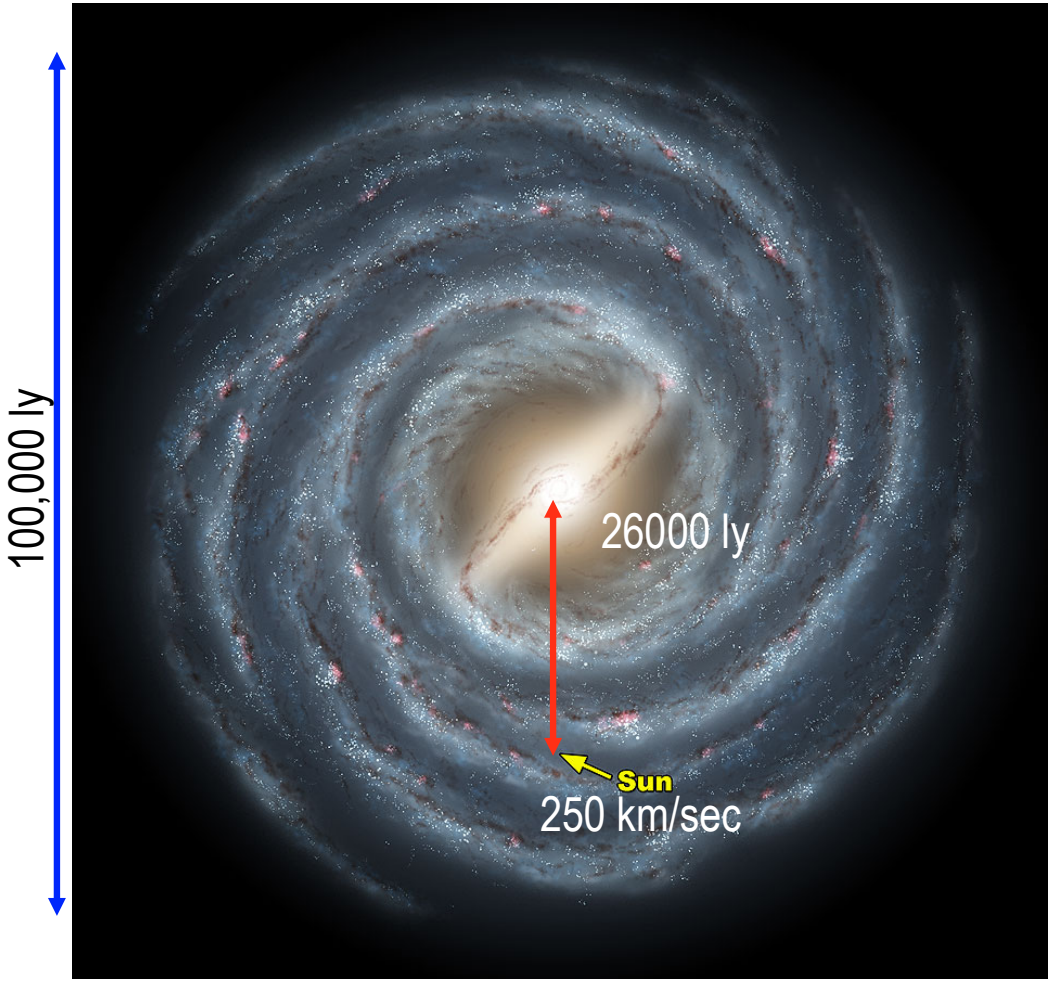

Orbital period (Galactic year) 220 million years

Galaxies:
- Basic units of larger, organized structures
- Sites of star formation from raw gas
- Factories synthesizing heavy elements from Hydrogen & Helium

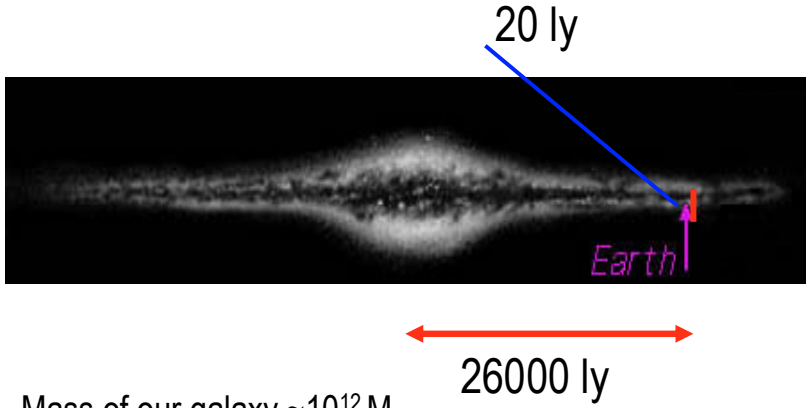

Mass of our galaxy ~10^{12} $M_{\odot}$

stars (~ 400 billion) and their planets, and thousands of clusters and nebulae, gas, dust

1 ly = 10^{13} km, distance traveled by lightin one year

Solar Fuel

- Protons (hydrogen nuclei) fusing to form alpha particles (helium nuclei) and releasing energy in the process seems to be the primary source of energy for the Sun
- But what is the origin of H and He in the Universe?
- One of the acceptable answers is the Big Bang
- The formation of H and He occurs as the universe starts expanding after the Big Bang
- A definite ratio between H and He results from Big Bang
- These become key ingredients in the galaxies formed eventually

Big Bang

- Hydrogen, helium, and some lithium formed moments (~ 3min) after the Big Bang

T = Temperature (K); k = Boltzmann constant; kT = thermal energy; 1 ev ~10,000 K
1 MeV = 10^6 eV ~ 10^{10} K or 10 BK

History of the Universe according to the Big Bang theory

Cosmic time	Temperature	Events
$t \approx 10^{-4}$ s	$kT \approx 10^2$ MeV	Quarks form neutrons and protons
$t \approx 1$ s	$kT \approx 1$ MeV	Neutrinos decouple
$t \approx 4$ s	$kT \approx 0.5$ MeV	Electron–positron annihilation
$t \approx 3$ min	$kT \approx 0.1$ MeV	Helium and other light nuclei formed
$t \approx 3 \times 10^5$ years	$kT \approx 0.3$ eV	Atoms formed and photons decouple

10^9 K

p- protons
n- neutrons
ν_e – neutrinos
ν_e~ – antineutrinos
e^- - electrons
e^+ - positrons

Universal He Abundance

- When the universe was at T~10 BK, only p and n exist. They were continually transformed into one another by:
  $\nu_e + n \leftrightarrow e^- + p$ and $\nu_e\sim + p \leftrightarrow e^+ + n$
- n are heavier so it is easier to produce p. At a temperature T, the ratio is, #n/#p = exp $(-\Delta mc^2/kT)$, where
- $\Delta m = (m_n - m_p) \sim 1.3$ MeV/c^2 the differenve between n and p masses.
- What happened when the universe cooled below 10BK? The n ↔ p reactions cease when #n/#p ~1/5. Further neutron decay reduces the ratio to 1/7 when T=1 BK.
- n+p → d+γ dominates the reverse reaction (photo-dissociation of deuterium nucleus (d) to n and p)
- By capturing more n and p, d turns into tritium and He3 nuclei, respectively.
- Further n & p capture transform these to He4. Once He4 forms, the n are locked up because He4 is a stable nucleus. No stable elements with mass 5 and 8. Some trace amounts of Li7 produced.
- The resulting #n/#p ~1/7 from big bang thus correctly predicts the universal abundance of He: 25% He and 75% H
- 1n/7p → 2n/14p → 2n+2p/12p → 1He/12H. By mass, He/(He+12H) = 4/16=25%; 12H/(He+12H) → 12/16 = 75% This was the raw material for the first stars
- Sun made of recycled stellar material.

Nucleosynthesis: Big Bang, stellar fusion, neutron capture

- Hydrogen, helium, and some lithium formed moments (~ 3min) after the Big Bang; how about heavier elements found on Earth and in the solar system?
- Fusion in stars produces elements up to ^{56}Fe. Beyond ^{56}Fe, fusion reactions do not release energy
- Slow (or s) process of neutron capture followed by beta decay can produce heavier elements: e.g., $^{56}Fe \rightarrow {}^{57}Fe \rightarrow {}^{58}Fe \rightarrow {}^{59}Fe$ (3 successive neutron captures), followed by $^{59}Fe \rightarrow {}^{59}Co$ (beta decay).
- S-process goes on until ^{208}Pb and ^{209}Bi are reached; no more slow neutron capture possible because the new nuclei decay fast before they can capture neutrons.
- The rapid (or r) process breaks past ^{208}Pb. The stable actinides may be produced directly from a neutron-rich precursor, or from α-decay of even heavier elements. [needs lots of neutrons – wind from neutron stars?]

We are stardust!

Elements up to Li can be explained as a consequence of the Big Bang. Higher mass elements up to Fe can be explained by fusion reactions taking place in the interior of stars. Heavier elements up to Uranium seem to be created in novae and super novae (neutron capture makes them in Asymptotic Giant Branch (AGB) stars; convection brings them to the surface and supernovae to the ISM; r –process in winds from neutron stars). Fe is the most stable element. So, all the elements our body were made in the interior of stars.

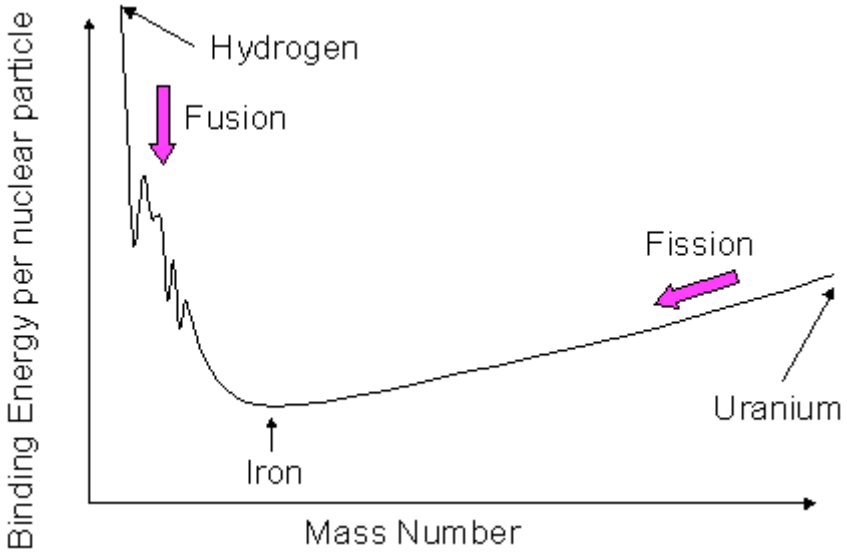

The universe is slowly becoming Fe rich

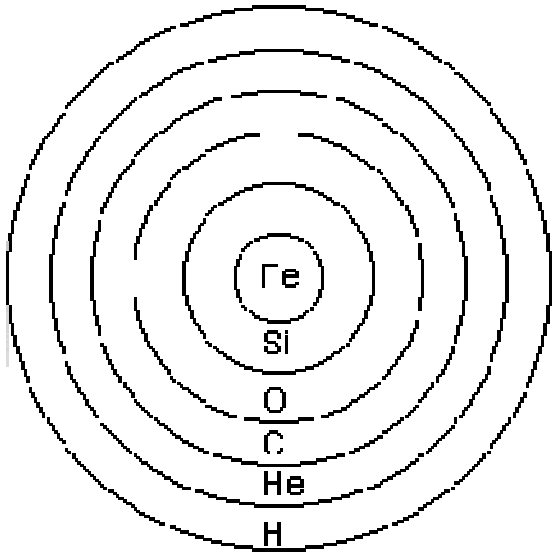

Structure of massive stars

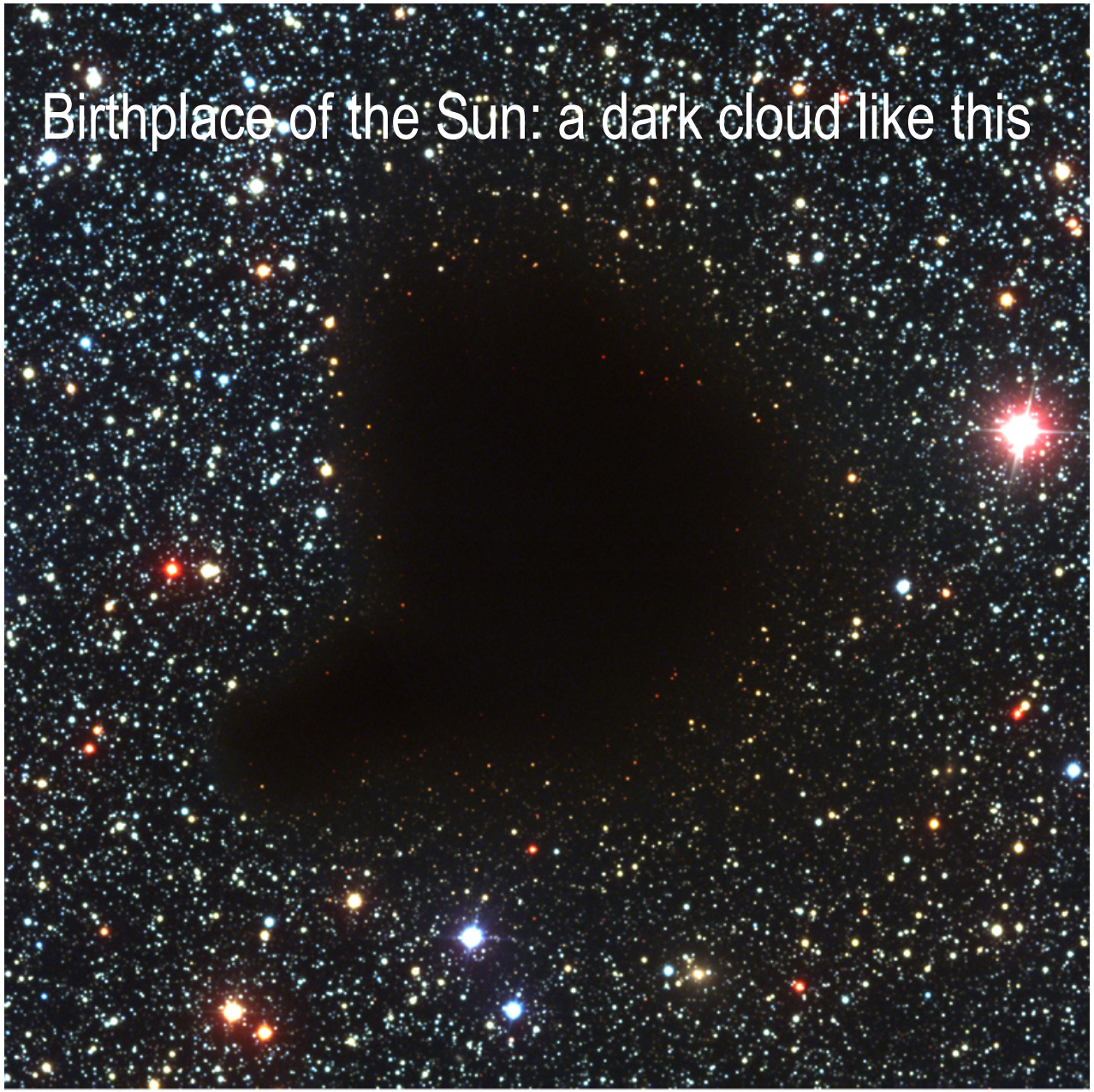

The "Black Cloud" B68
(VLT ANTU + FORS1)

ESO PR Photo 20a/99 (30 April 1999)

Early life

1 AU = 1.5×10^8 km

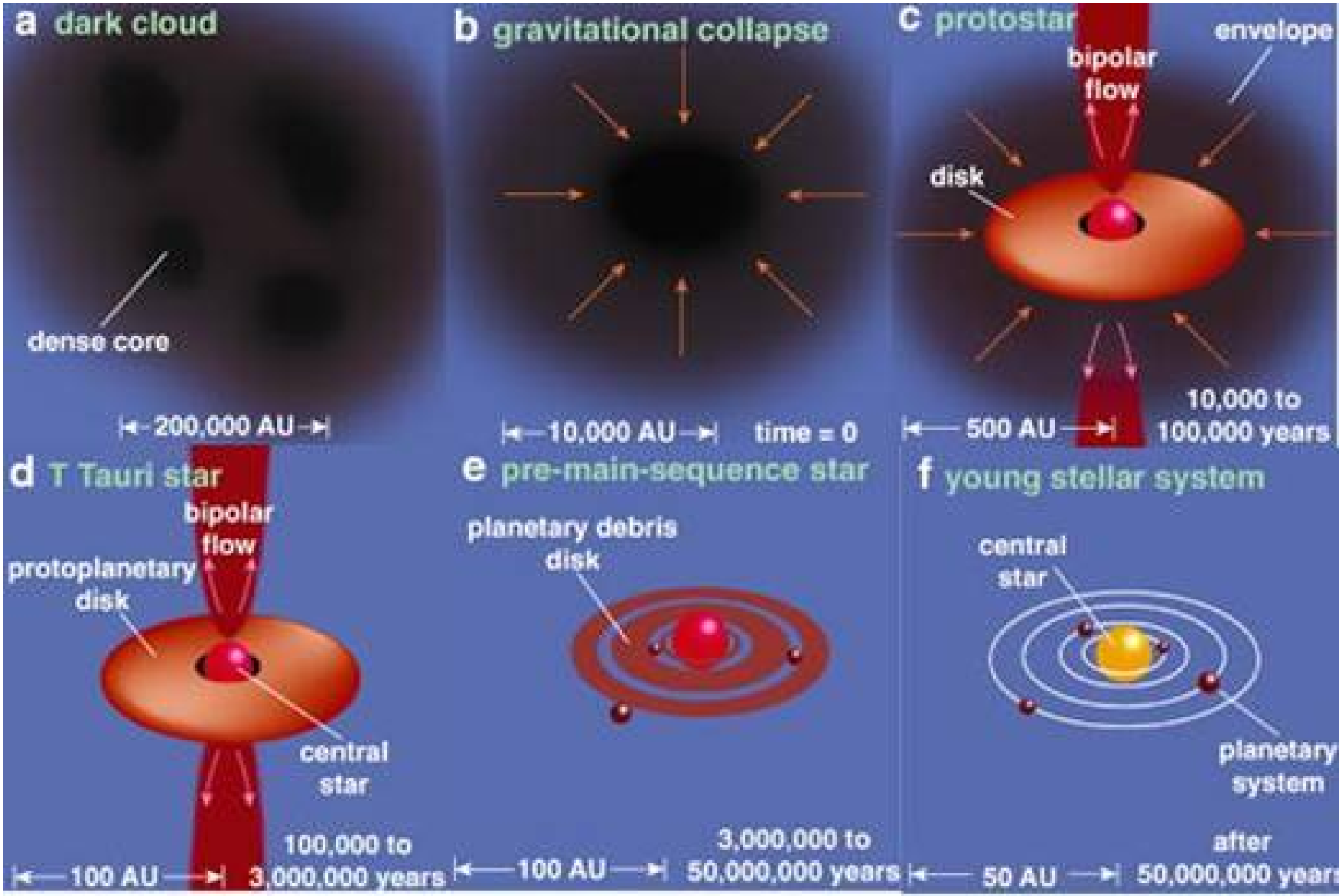

J. Christensen-Dalsgaard

Fusion: electrostatic repulsion vs. Nuclear attraction

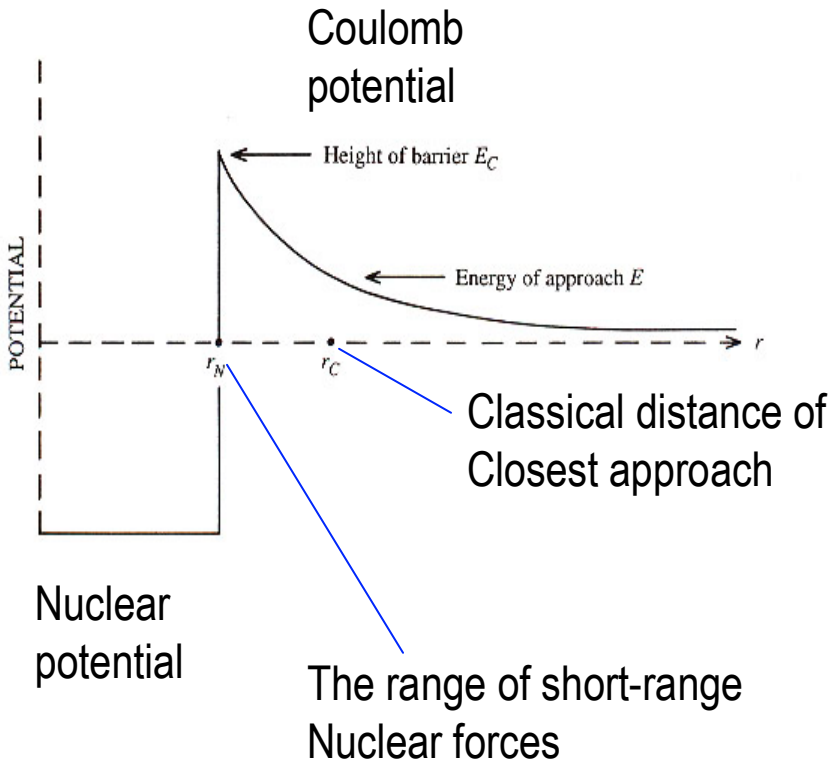

(adapted from A. C. Philips)

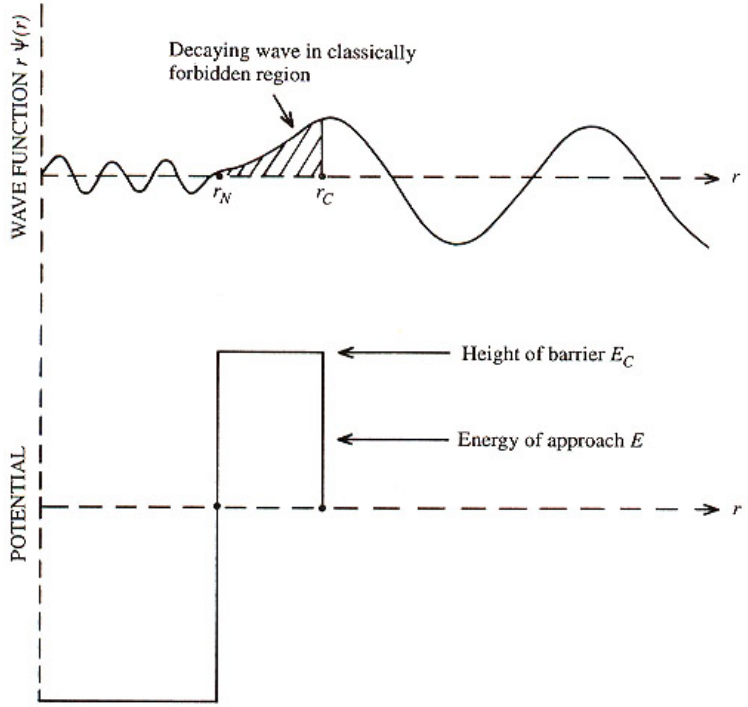

Quantum mechanical tunneling can cause fusion even for particle energy < Ec

Fusion inside the Sun

contribution to $L_\odot$ from the reactions

Energy of the neutrinos produced

$^1H + {}^1H$	$^2D + e^+ + \nu_{e\ (0.263)}$	$0.85L_\odot$
$^1H + {}^1H + e^-$	$^2D + \nu_{e\ (1.44)}$	
$^2D + {}^1H$	$^3He + \gamma$	
$^3He + {}^3He$	$^4He + {}^1H + {}^1H$	
$^3He + {}^4He$	$^7Be + \gamma$	$0.15L_\odot$
$^7Be + e^-$	$^2D + \nu_{e(0.8)}$	
$^7Li + {}^1H$	$^4He + {}^4He$	
$^7Be + {}^1H$	$^8B + \gamma$	$1.5 10^{-4} L_\odot$
^8B	$^8Be + e^+ + \nu_{e(7.2)}$	
^8Be	$^4He + {}^4He$	

Most of the reaction rates are determined in the laboratory and extrapolated to the Sun. The error in rates ±1% (Parker 1986).

Kinetic energy of protons brings them close; Coulomb repulsion takes them apart. When the thermal energy wins, fusion occurs

$4\ H^1 \rightarrow He^4$ + energy

- mass of $4\ H^1 = 6.693 \times 10^{-27}$ kg
- mass of $1\ He^4 = 6.645 \times 10^{-27}$ kg
- mass diff ~0.048×10^{-27} kg per reaction
- $E = mc^2 = 0.048 \times 10^{-27}$ kg x $(3 \times 10^8$ m/sec$)^2$
- $E \sim 4.3 \times 10^{-12}$ Joules (26 MeV)
- $L_\odot$ ~4×10^{26} W → 10^{38} reactions needed per second
- ~4×10^{38} protons consumed every second
- ~2×10^{38} electron neutrinos released per sec. - can be detected as evidence for fusion
- Converting the hydrogen into helium for the Sun would produce about 10^{44} J of energy enough to keep Sun burning for 10 billion years

CNO cycle (for >1.2 $M_\odot$)

CNO Chains

$$^{12}C + {}^{1}H \rightarrow {}^{13}N + \gamma$$
$$^{13}N \rightarrow {}^{13}C + e^{+} + \nu$$
$$^{13}C + {}^{1}H \rightarrow {}^{14}N + \gamma$$
$$^{14}N + {}^{1}H \rightarrow {}^{15}O + \gamma$$
$$^{15}O \rightarrow {}^{15}N + e^{+} + \nu$$
$$^{15}N + {}^{1}H \rightarrow {}^{12}C + {}^{4}He$$

or

$$^{15}N + {}^{1}H \rightarrow {}^{16}O + \gamma$$
$$^{16}O + {}^{1}H \rightarrow {}^{17}F + \gamma$$
$$^{17}F \rightarrow {}^{17}O + e^{+} + \nu$$
$$^{17}O + {}^{1}H \rightarrow {}^{14}N + {}^{4}He$$

For $M/M_\odot = 1.2$, the energy production rates are equal $\varepsilon_{pp} = \varepsilon_{CNO}$
For the Sun ε_{pp} is dominant ($M/M_\odot = 1$).

Main Sequence Star

- H → He happens at ~5 MK; This is a very slow process and the lonest in the life of a star (90% of stellar life). This phase is known as the main sequence. A star in this phase is known as a main sequence star.
- Other fusion reactions need higher temperature and the corresponding phases are shorter-lived

Further evolution:
- When H is exhausted, the core shrinks.
- It heats up but can not yet burn He, which needs 100M K!
- The high temperatures ignites a shell of H around the core.
- The increased pressure drives the envelope of the star outward.
- Creating a giant or supergiant

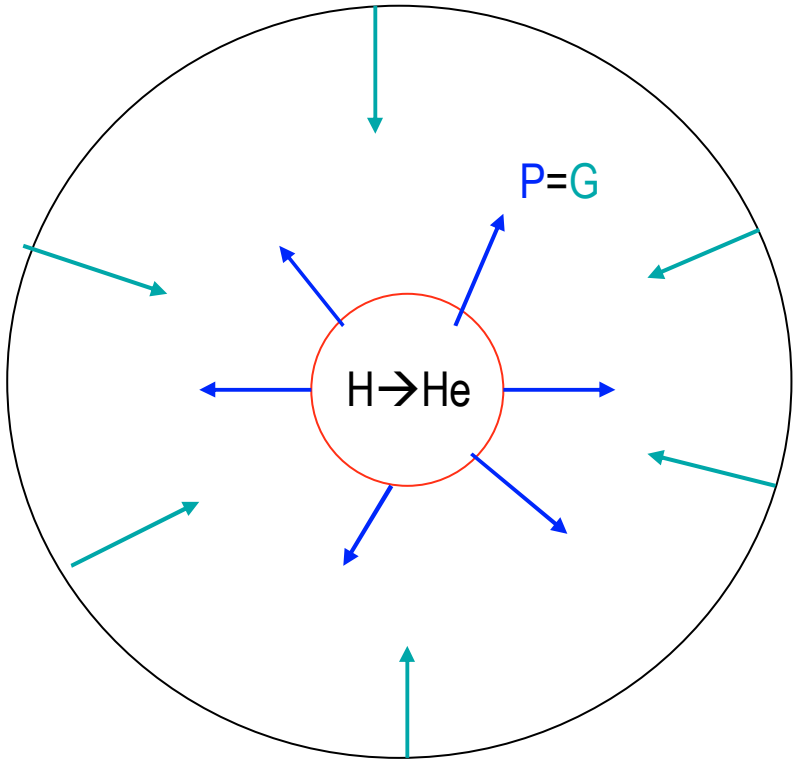

Force balance in a main sequence star:
The pressure force (P) in the interior is balanced by the gravitational force (G)

Hertzsprung-Russell (HR) Diagram

- In 1911, Ejnar Hertzsprung, a Danish astronomer plotted the luminosities of stars against their colors. The color tells you the star's surface temperature.
- In 1913, Henry Norris Russell of Princeton University plotted the luminosities of stars against their spectral types. Spectral types are also a measure of temperature
- Essentially, Russell made the same diagram that Hertzsprung made. The diagram became known as the Hertzsprung-Russell (or "H-R") diagram. By studying H-R diagrams, one can figure out the life cycles of stars.

Class I-IV giants; class V main sequence

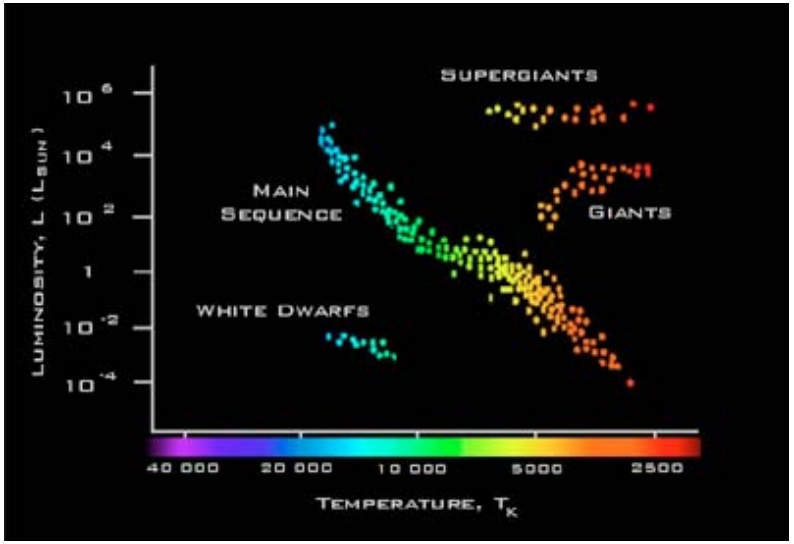

HR Diagram describes stellar evolution

Recall that $\lambda_{max}T = 0.29$ cmK holds for a black body at a temperature T. The maximum radiation occur at a wavelength λmax. At lower temperature the wavelength is larger (red). At higher temperature, the wavelength is shorter (blue).

Spectral Classification of Stars

- In the 1890s, Edward C. Pickering at Harvard University and his assistant Williamina P. Fleming started classifying stars according to their Hydrogen content: A-type stars had the most Hydrogen, B-type had the next most, and so on. They had 22 letters. But it was not clear what it meant.
- In 1901, Annie Jump Cannon, another assistant of Pickering realized that the classification became simpler if ordered according to temperature. The stars grouped according to decreasing temperature as: OBAFGKMRNS

Type	O	B	A	F	G	K	M0	M5
Teff 1000 K	50	25	11	7.6	6	5.1	3.6	3

Sun is a G2V star, because it is a G-star of intermediate temperature and belongs to main sequence (class V)

Stellar Evolution & the Sun

S. Chandrasekhar 1910-1995

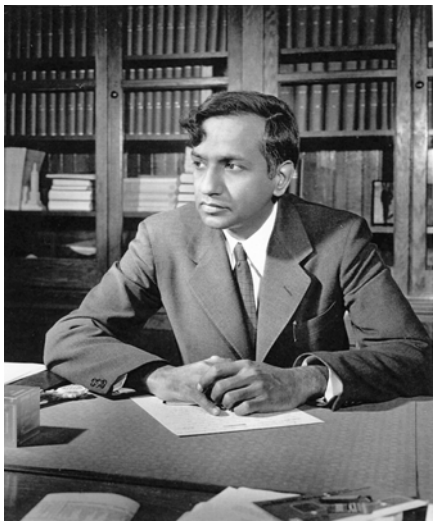

Chandrasekhar limit $1.4M_\odot$

$M_\odot < 1.4M_\odot$ → White Dwarf

No WDs with $M > 1.4\ M_\odot$

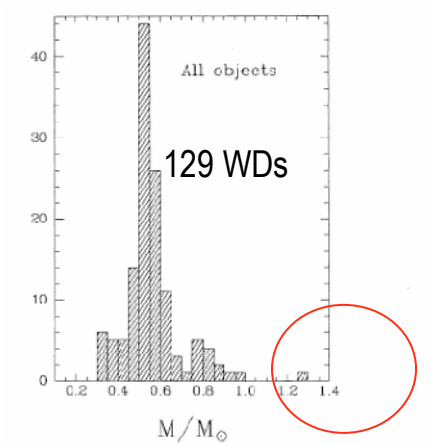

Bergeron et al. 1992, ApJ

Massive stars on the main sequence have a higher luminosity ($L \sim M^4$) and surface temperature

Earth is at 214 $R_\odot$!!
The Sun will expand to a size bigger than the solar system in the red giant phase and then slowly shrink to ~0.01 $R_\odot$ as a white dwarf.

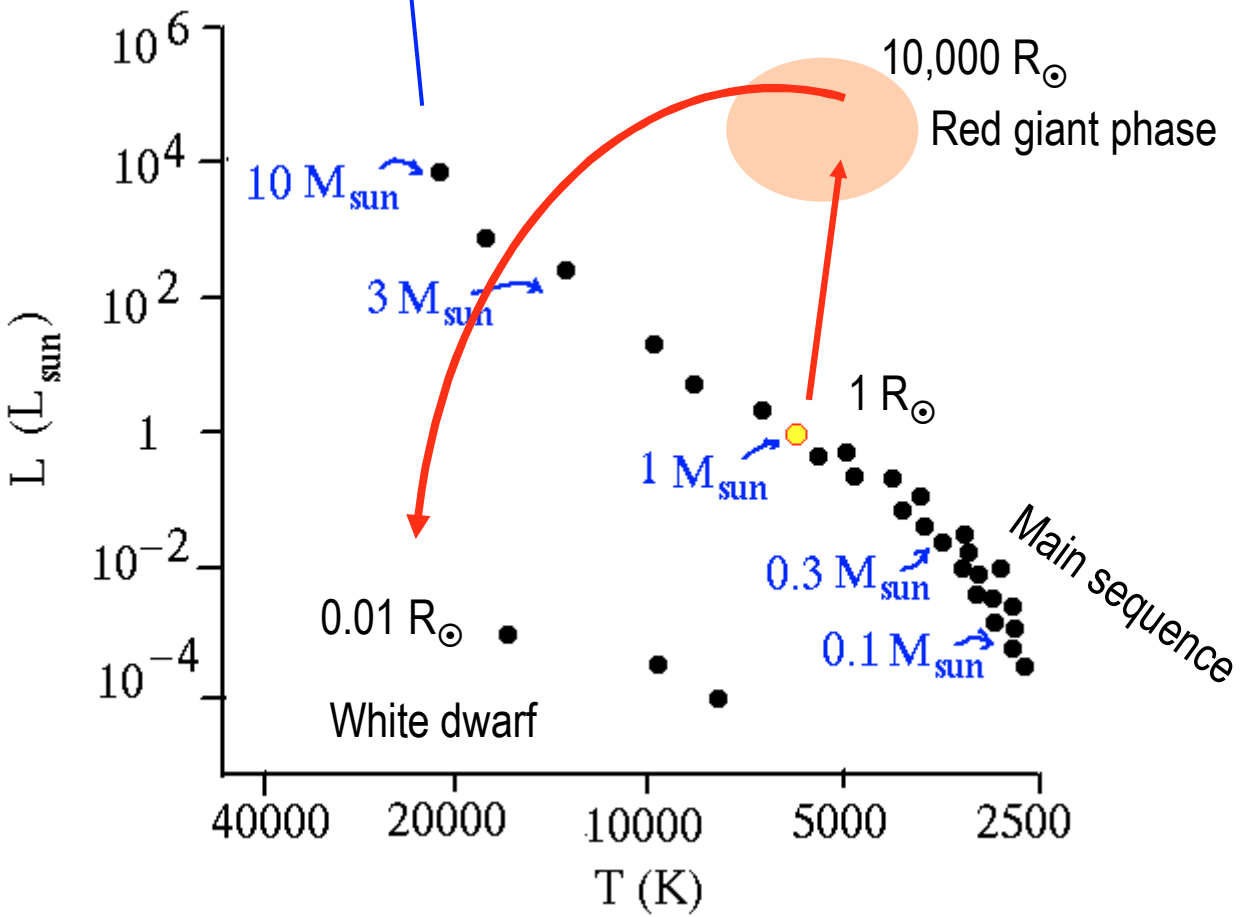

N. Gopalswamy Abdus Salam ICTP 5/3/2006

$R_\odot \sim 7 \times 10^5$ km $M_\odot$ 1.99×10^{30} kg

The Neutrino Problem

We saw that the nuclear fusion inside the sun produces ~2x10^{38} neutrinos are produced every second. Since neutrinos do not interact significantly with matter, almost all of them escape from the interior. Clever experiments designed to detect the neutrinos, did detect them, but not a expected.

$$\nu_e \leftrightarrow \nu_\mu \leftrightarrow \nu_\tau$$

Problem: Low flux (~1/3) observed compared to what the standard solar model predicts
Solutions:
- nonstandard solar models
- problem with observations

Most nonstandard models cannot explain all the observations
Helioseismic measurement of sound speed strongly supports standard model
The first results (June 2001) from the Sudbury Neutrino Observatory (SNO) in Canada have finally indicated solution of a problem that remained a puzzle for 30 years. SNO detected three types of neutrinos: electron, muon and tau
The results confirmed that e-neutrinos produced by nuclear reactions inside the Sun "oscillate" or change flavor on their way to Earth.
Neutrino oscillations are only possible if the three flavors of neutrinos have mass.
- SNO result therefore has important implications for cosmology and particle physics as well.

In 2002 Raymond Davis Jr. and Masatoshi Koshiba won part of the Nobel Prize in Physics for experimental work that found the number of solar neutrinos was ~ a third of the number predicted by the Standard Solar Model.

The solution of the neutrino problem is an ultimate victory to the Standard Solar Model, already proven correct by helioseismology.

The Standard Solar model

- Conservation laws of physics (mass, momentum, and energy), the energy transport equation and the equations describing the nuclear reaction network constitute the complete set of equations which describe the evolution of a star.
- The standard solar model assumes spherical symmetry (rotation, magnetic field ignored; mass reduction due to fusion [<0.7%] and wind ignored).
- Dynamical time-scale ~1 h: enough time (4.5 by) to establish hydrostatic equilibrium
- For any volume element, the weight is balanced by pressure gradient (mainly gas pressure; the radiation pressure is < 0.05%)
- Only convective and radiative transport are important in the Sun
- When the temperature gradient required to transport all the energy by radiation exceeds the adiabatic temperature gradient, the layer is unstable to convection and the material physically transports the energy outwards.
- mixing length: length traveled by a convective element before it loses its identity (mixing length theory to deal with Temperature gradient).
- The four equations in five variables: pressure P, temperature T, density ρ, mass $M(r)$, and luminosity L are solved with the help of the equation of state which provides a relation between P, T, and ρ.
- In the interior of the Sun, where hydrogen and helium are fully ionized, the simple ideal gas law provides an adequate equation of state (except for the outer layer)
- Constraints: The standard solar model must have the Sun's luminosity, mass and radius (all measurable) at the Sun's age (inferred from the ages of the oldest meteorites).
- The abundance of helium is adjusted to produce a solar model with the Sun's luminosity
- The spectrum of *p*-modes have been used to test and constrain the standard solar model.

Solar Structure

$F_{net} = F_g - F_p$

$F_g = -GM(r)\,\delta M/r^2 = -GM(r)\rho(r)\delta r\delta A/r^2$

$F_p = (dP/dr)\delta r\delta A$

At Equilibrium, $F_{net} = 0$ or $F_g = F_p$

$dP/dr = -GM\rho/r^2$ (1)

$\delta M = \rho(r)\delta r\delta A$

$= \rho(r)\,\delta r.4\pi r^2$

$dM/dr = 4\pi r^2\rho$ (2)

Equations describing the Standard Solar Model

$M = 4\pi R^3\rho/3$

$Pc = \rho gh$, with $h=R$, $g=GM/R^2$

$Pc = 3GM^2/4\pi R^4$

For Sun, $M = 1.99\times10^{30}$ kg, $R=7\times10^8$ m

$Pc = 3\times10^{14}$ Nm^{-2}

Earth's atmospheric pressure: 10^5 Nm^{-2}

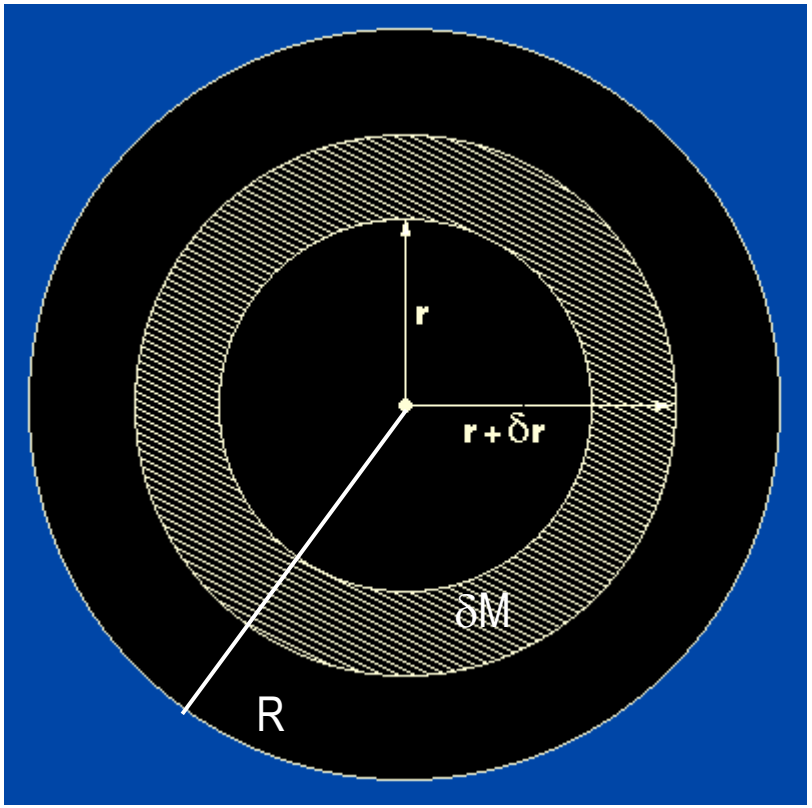

Rotation, element diffusion, and magnetic fields ignored

Include these for improved standard model

the energy equation,

$dL/dr = 4\pi r^2\rho\varepsilon$, (3)

ε nuclear energy generation rate/ unit mass

the energy transfer equation,

$dT/dr = -(3/4ac)(\kappa\rho/T^3)\,(L/4\pi r^2)$ (4)

a - Stefan's constant, *c* - speed of light,

κ - Rosseland mean opacity

The energy output of the shell from nuclear fusion reactions
and its "evolved" composition are then input as constants into the equations.

Solutions

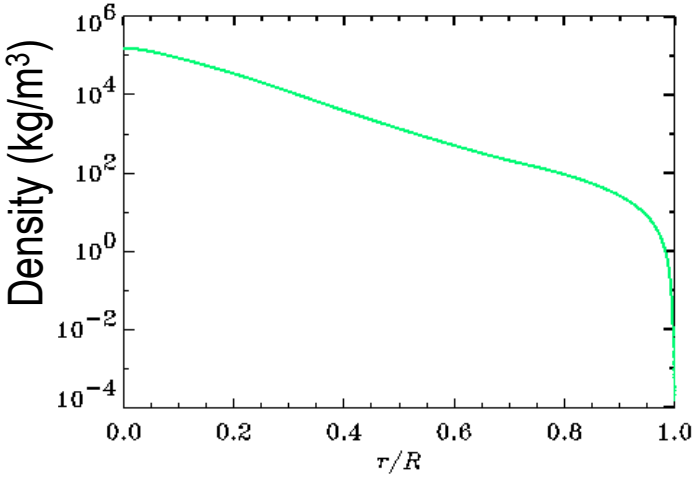

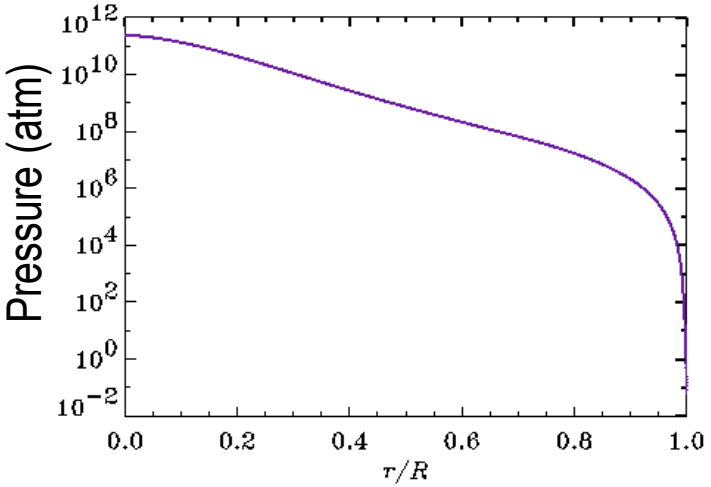

r/R =0 corresponds to sun center
r/R = 1 corresponds to the solar surface

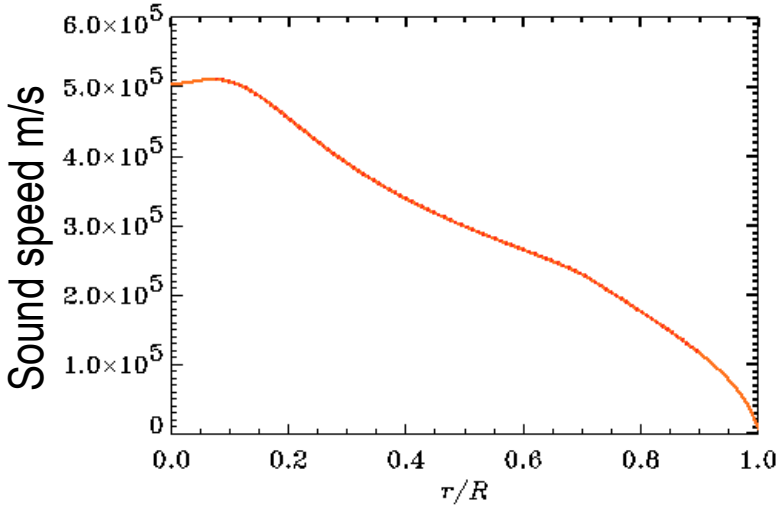

Helioseismology has validated the standard solar model
Solution of the neutrino problem is another strong support for the standard model
We will just show how closely the sound speed shown here compares with helioseismic observations

Christensen-Dalsgaard, 2003

Solar Interior: Summary

Inner Core:
- The energy is generated by fusion reactions.
- Temperature ~15 MK
- density ~150 g/cm^3
- Extends to 0.25 $R_\odot$

Radiative Zone:
- The energy is transported by electromagnetic radiation.
- density decreases from ~20 g/cm^3 to ~ 0.2 g/cm^3
- Extends from 0.25 $R_\odot$ to 0.7 $R_\odot$

Interface Layer (Tachocline)**:**
- The Sun's magnetic field is generated.
- The changes in chemical composition are observed.

Convection Zone:
- The temperature gradient is such that energy transport has to occur by convection.
- Temperature 2 MK (at the base) to ~5700 K (at the top – same as photosphere)
- density ~2x10^{-7} g/cm^3
- The convection at the surface is observed as granules.
- It extends from 0.7 $R_\odot$ (a depth of 200 000 km) up to the visible surface.

Lecture II
Helioseismology and Solar Dynamo

- Solar oscillations
- p-modes and g-modes
- p-modes and the standard solar model
- Differential rotation
- Local helioseismology

Helioseismology

- The oscillations in the Sun are sound waves, generated by the convection much like the sound made by the vessel with water boiling in it
- Helioseismology is the study of solar oscillations to understand the internal structure from surface observations
- Discovered in 1962 by R. Leighton
- Ulrich (1970) proposed that the waves are the surface manifestation of sound waves trapped beneath the surface of the Sun
- Confirmed as global oscillations by Deubner in 1975
- Useful to probe the interior of the Sun where the modes of these oscillations are trapped
- Provided a strong confirmation of the standard solar model

R. Leighton (left)
(from Sheeley 2005)

Solar Oscillations

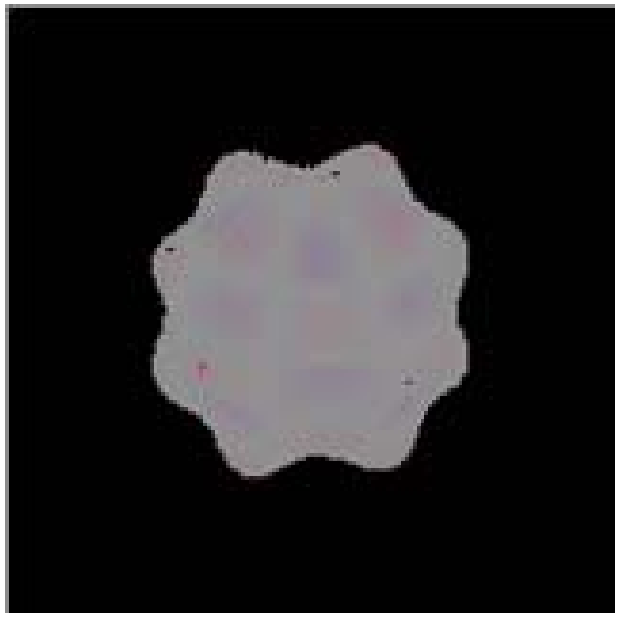

Movie showing oscillations with greatly exaggerated amplitudes

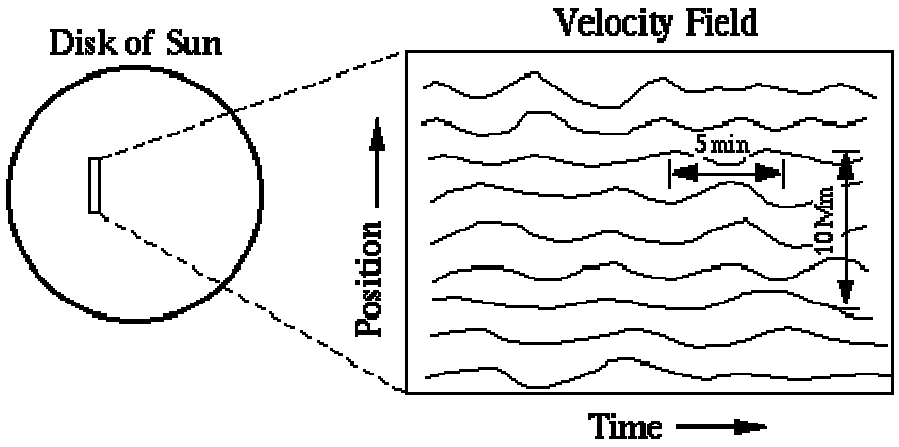

A simple description of observations that show solar oscillations.

Courtesy: D.B. Guenther & P. Demarque 1996

Dopplergrams

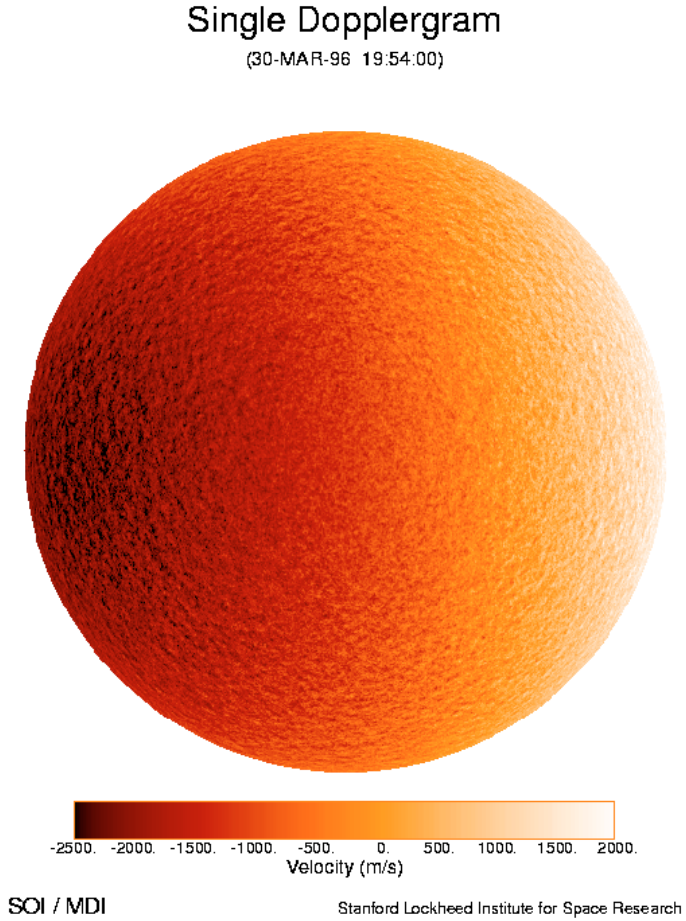

Includes Doppler velocities due to rotation
dark: blue shift; light: red shift. East limb is dark because it moves towards the observer (blue shift)

dark and light grains indicate up and down motion of the solar surface

Superposition of many different natural modes of the Sun. The modes are driven by turbulent motions in the outermost layers of the convective envelope of the Sun (rotation removed by averaging)

Observed Power Spectrum

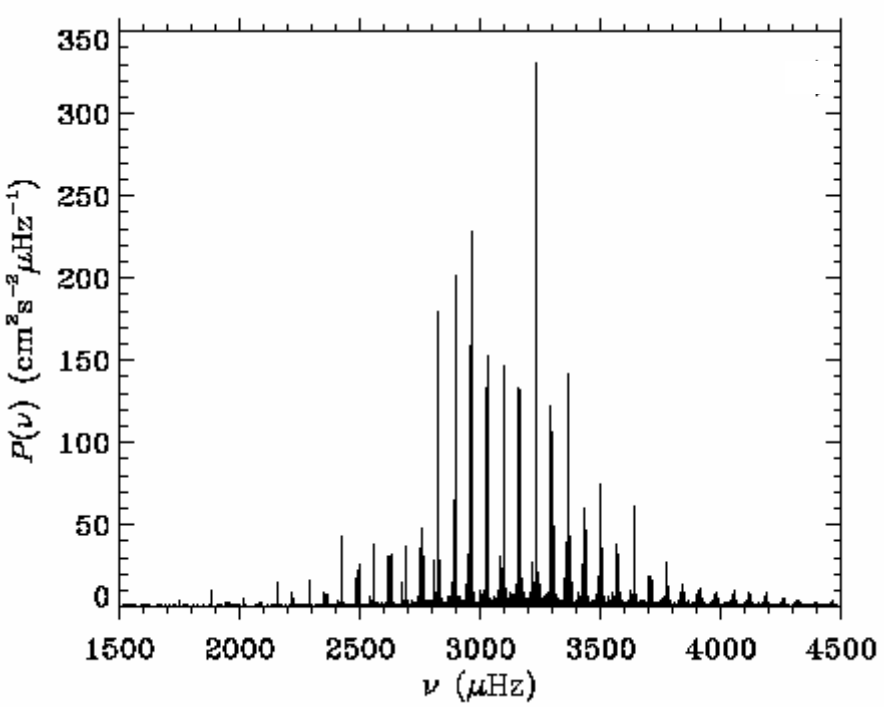

Power spectrum of solar oscillations, obtained from Doppler observations in light integrated over the solar disk. The data were obtained from six observing stations and span approximately four months. Note the peak power around 3000 micro Hz or 3 milli Hz corresponding to an oscillation period of about 5 minutes (hence the name 5 –minute oscillations

J. Christensen-Dalsgaard, 2003

Observations

SOHO/MDI

Superposition of millions of modes

A sequence of "Dopplergrams" - maps of motion made by observing the Doppler effect. Light areas are moving up and darker areas are moving down. The region shown is about 1/6 the diameter of the Sun wide. The motions oscillate with a period of about 5 minutes.

Properties of Oscillations

Property	Value
Life time	A few days
period	3-12 min
frequency	1-8 milliHz
Normal modes observed	Several million

The presence of oscillations at the solar surface was first established by Leighton, Noyes and Simon (1962) ApJ 135, 474.

Theory of Solar Oscillations

- Start with basic equations

$$d\mathbf{v}/dt = -\nabla p + \rho\nabla\Phi \text{ [motion]}$$

$$d\rho/dt + \nabla\bullet\mathbf{v} = 0 \text{ [continuity]}$$

$$(1/P)dP/dt = (\Gamma/\rho)d\rho/dt \text{ [adiabatic]}$$

$$\nabla^2\Phi = -4\pi\rho \text{ [Poisson]}$$

$\mathbf{v}$ = fluid velocity,

Φ = gravitational potential,

Γ = effective ratio of specific heats ($\rho dP/Pd\rho$) which becomes γ when constant. $d/dt = \partial/\partial t + v\bullet\nabla$

- In equilibrium, $\rho = \rho_o(r)$, $P = P_o(r)$, $\Phi = \Phi_o(r)$, $\mathbf{v}=0$

- For small perturbations ($x = x_o + x'$ with $x' << x_o$) they can be expanded in spherical harmonics $Y^l_m(\theta,\phi)$ using the Legendre polynomials $P^m_l(\theta)$:

$$x' = \text{Re}\,[\exp(i\omega_{nl}t)\, x'_1(r)Y^l_m(\theta,\phi)] \quad \text{with} \quad Y^l_m(\theta,\phi) = P^m_l(\theta)\exp(im\phi),\ \omega_{nl} \text{ is the oscillation frequency}$$

- The spherical harmonic functions provide the nodes of standing wave patterns. n – order (number of nodes in the radial direction), l- degree (the number of node lines on the surface), m - is the number of nodal lines crossing the equator ($-l \le m \le l$).

Some low-l modes

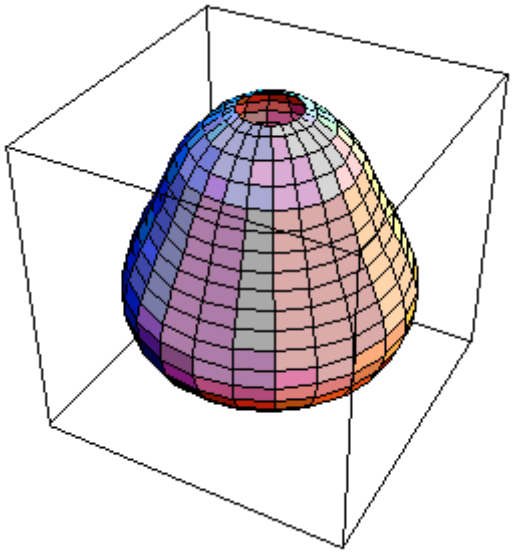

l=3 m=0

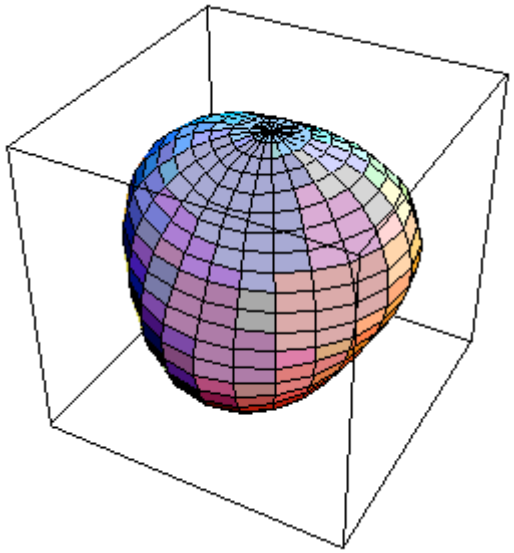

l=3 m=2

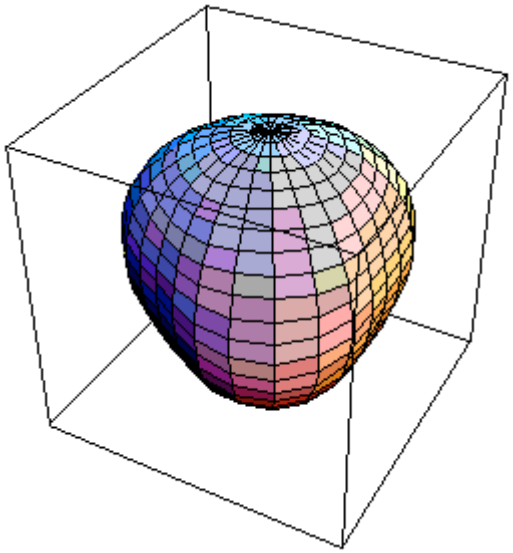

l=3 m=3

Courtesy: D.B. Guenther & P. Demarque 1996

Observations

In the real Sun, millions of modes are combined, giving the observed oscillation pattern. It is possible to extract the modes from the observations to derive a spectrum of the oscillations as shown on the right.

Spectrum from SOHO/MDI

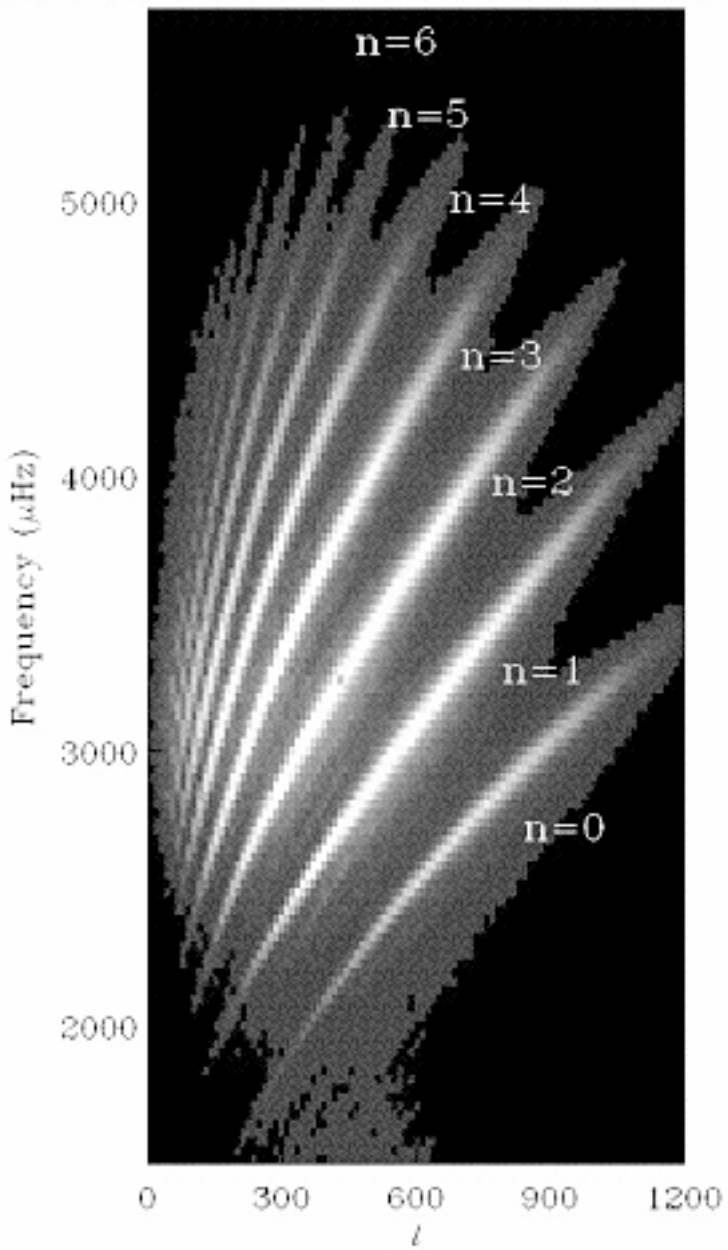

Simplified Equations

- The equations reduce to the following linearized equation for the perturbations in pressure (P'), position (ξ), and gravitational potential (Φ') as

$$(1/\rho)dP'/dr + (g/c^2\rho)P' + (N^2 - \omega^2)\xi + d\Phi'/dr = 0$$

$$(1/r^2)d(r^2\xi)/dr + (1/\Gamma)(d\ln P_o/dr)\xi + (1-L_l^2/\omega^2)(P'/c^2\rho) - [l(l+1)/(\omega^2 r^2)]\Phi' = 0$$

$$(1/r^2)d(r^2 d\Phi'/dr)/dr - [l(l+1)/r^2]\Phi' - 4\pi G\rho\,[P'/c^2\rho + (N^2/g)\xi] = 0$$

L_l = the Lamb frequency given by $L_l^2 = l(l+1)c^2/r^2$
N = Brunt-Väisälä frequency, given by $N^2 = g[\Gamma^{-1} d\ln P_o/dr - d\ln\rho_o/dr]$ - also known as the buoyancy frequency

- For high modes (n or l large), Φ' can be neglected (compared to other perturbations - Cowling's approximation). Introducing new variables, $\tilde{\xi}, \tilde{\eta}$:

$$\tilde{\xi} = r^2\xi\exp[-\int_0^r (g/c^2)dr], \quad \tilde{\eta} = \omega^2 r\xi\exp[-\int_0^r (N^2/g))dr], \quad \text{we get}$$

$$d\tilde{\xi}/dr = h(r)(r^2/c^2)(L_l^2/\omega^2 - 1)\,\tilde{\eta}$$

$$d\tilde{\eta}/dr = (1/h(r)r^2)(\omega^2 - N^2)\,\tilde{\xi}$$

with $h(r) = \exp[-\int_0^r (N^2/g - g/c^2)dr] > 0$

p- and g-modes

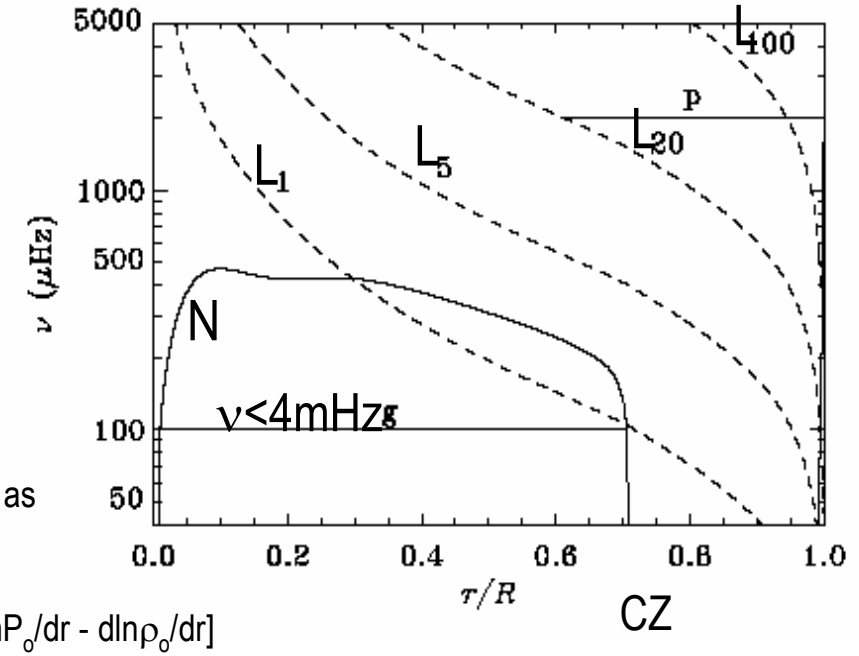

- Under WKB approximation, the solutions can be written as
  $\xi\tilde{},\eta\tilde{} \sim \exp(i\int k_r dr)$ with

$k_r^2 = (1/\omega^2c^2)(\omega^2 - L_l^2)(\omega^2 - N^2)$; $L_l^2 = l(l+1)c^2/r^2$; $N^2 = g[\Gamma^{-1}d\ln P_o/dr - d\ln\rho_o/dr]$

Properties of the oscillations can be understood from this dispersion relation.

- for $k_r>0$, we have sinusoidal behavior with radius (propagating mode). For $k_r<0$, we have evanescent mode.
- For a given frequency, L_l and N define regions of the Sun where modes can propagate
- If $\omega > L_l$ and $\omega > N$, $k_r > 0$, the modes are acoustic (restoring force is pressure) p-modes
- If $\omega < L_l$ and $\omega < N$, $k_r > 0$, they are gravity modes, because the restoring force is gravity

- For $\omega^2 >> N^2$ $k_r^2 = \omega^2/c^2 - L_l^2/c^2$ or $k_r^2 = \omega^2/c^2 - l(l+1)/r^2$

- When r decreases, $l(l+1)/r^2$ becomes larger. The wave cannot propagate inward when $k_r=0$, at which point it travels horizontally. $k_r=0$ happens at $r = r_t$, the turning point: $r_t = (L/\omega)c$ with $L^2 = l(l+1)$

- For $r < r_t$ the wave decays exponentially [$\exp(-k_i r)$], $k_i >0$
- For large l, r_t is large → close to the surface
- For small l, $k_r > 0$ always → goes through the center

Trapping of p-modes

- We just saw that there is an inner boundary r_t at which p-modes are reflected
- There is a natural outer boundary arising from the acoustic cutoff frequency near the surface:
  $\omega_c = c/2H_\rho$, $H_\rho = (d\ln\rho/dr)^{-1}$ is the density scale height
- The outward increase of ω_c thus provides the upper boundary of the cavity required to trap acoustic waves in the Sun.
- In the solar photosphere H_ρ ~120 km, so $\omega_c \sim 0.03\ s^{-1}$ (3 min period; $f_c = \omega_c/2\pi = 5$ mHz).

Most of the p-modes have a frequency of ~3 mHz and hence will be reflected back into the interior

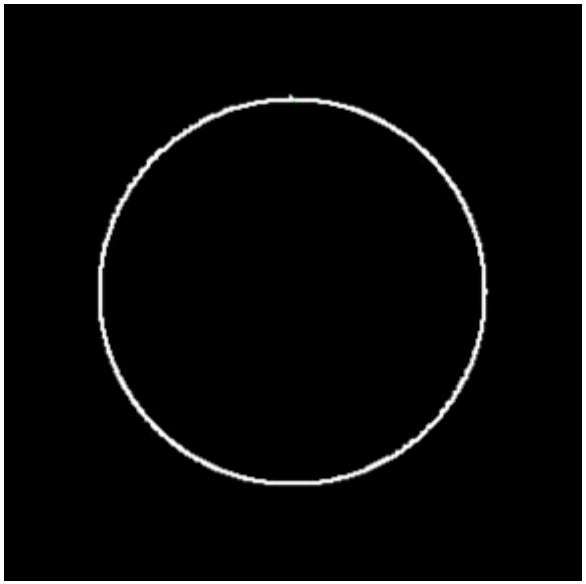

Movie illustrating the ray path for mode with a particular l-value
The distance from the sun center where the ray turns is the inner trapping boundary

Christensen-Dalsgaard

Probing the interior using p-modes

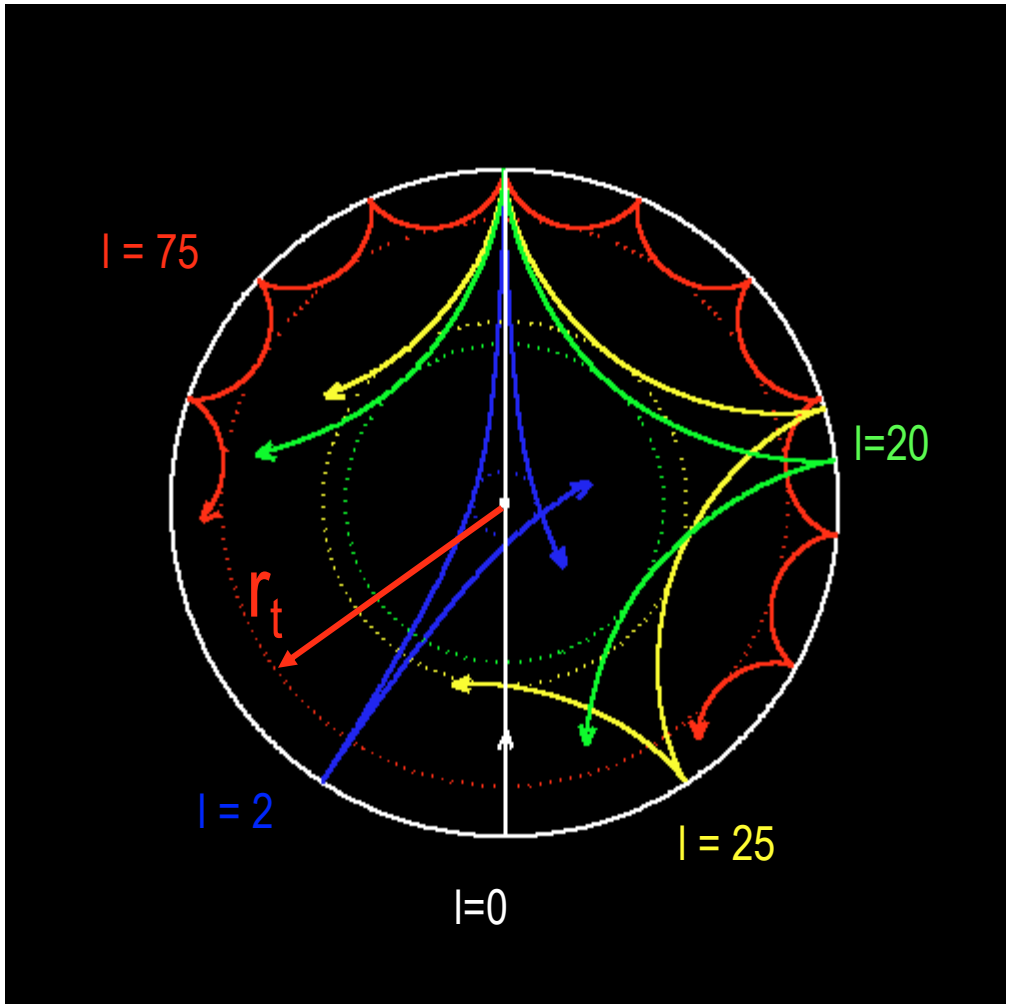

p-modes: acoustic waves trapped in the interior of the Sun

Lower the l value (horizontal wave number), the deeper the sound waves penetrate

Using different l values, the entire Interior can be probed.

The photosphere is the upper boundary for most of the sound waves (acoustic cutoff)

Christensen-Dalsgaard

g-modes

- In the limit $\omega^2 << L_l^2$,

  $k_r^2 = (1/\omega^2 c^2)(\omega^2 - L_l^2)(\omega^2 - N^2)$ becomes

  $k_r^2 = L_l^2/c^2\,(N^2/\omega^2 - 1)$ or

  $k_r^2 = l(l+1)/r^2\,(N^2/\omega^2 - 1)$

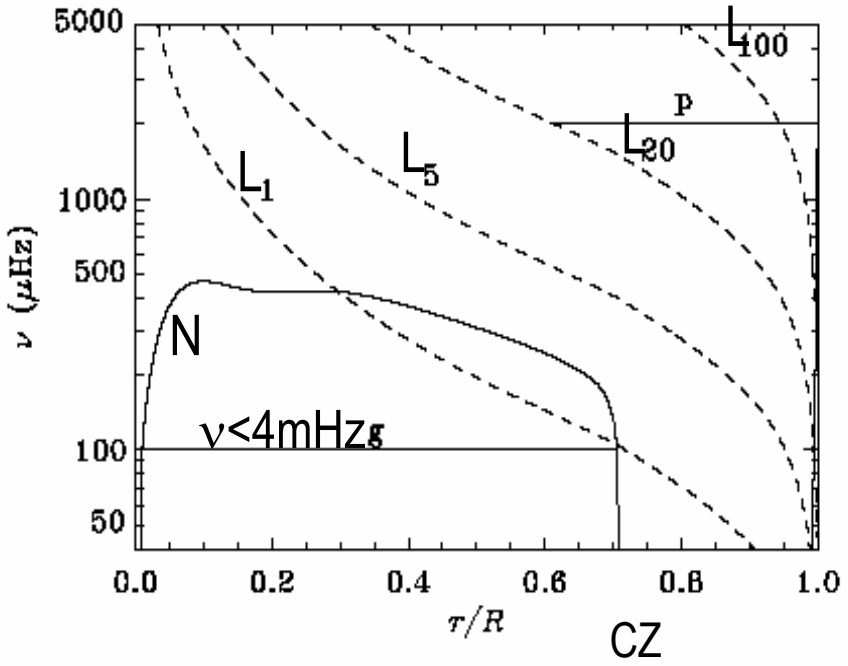

- Remember we need $k_r > 0$ ($\omega < N$) for propagation
- $N = \omega$ gives the turning points: one just below the convection zone and the other very near the centre of the Sun.

- The p and f modes have now been detected to frequencies as low as 0.5mHz (e.g. Schou 1998; Bertello et al. 2000)

- Claims of even lower frequency modes have not been substantiated. They could be g-modes!

Wave paths for p- and g modes

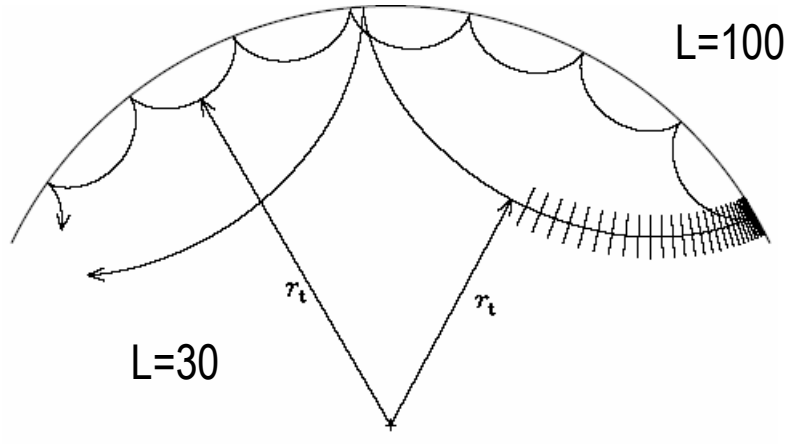

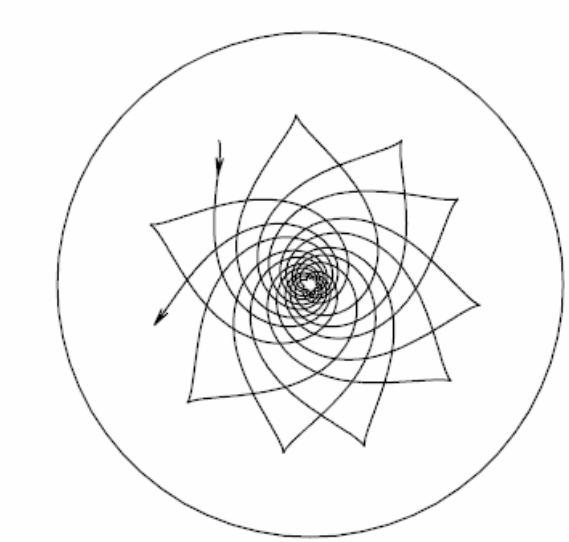

Propagation of acoustic waves (p modes), corresponding to modes with *l* = 30, *n* = 3mHz (deeply penetrating rays) and (*l* = 100*; n* = 3mHz (shallowly penetrating rays). The lines orthogonal to the former path of propagation illustrate the wave front.

Wave paths for a g-mode of *l* = 5*; n* = 192.6*m*Hz.g-modes mostly in central region of Sun.

Convective instability

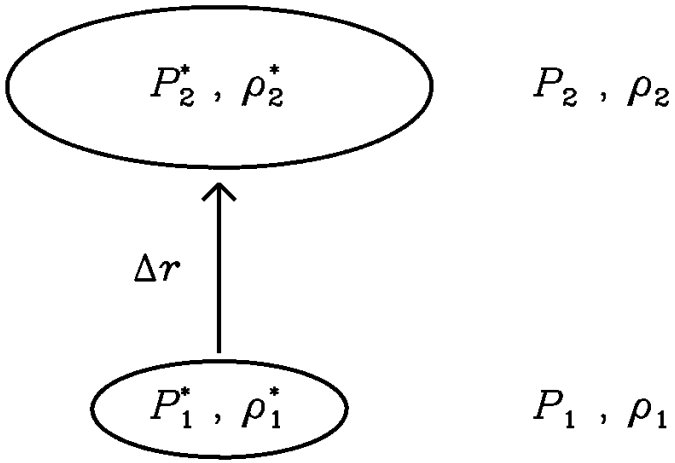

Buoyancy force:

$$\rho \frac{\mathrm{d}^2 \Delta r}{\mathrm{d}t^2} = f_{\mathrm{buoy}} = -g(\rho_2^* - \rho_2)$$

$$= -g\rho \left(\frac{1}{\Gamma_1} \frac{\mathrm{d} \ln p}{\mathrm{d}r} - \frac{\mathrm{d} \ln \rho}{\mathrm{d}r} \right) \Delta r$$

$$\equiv -\rho N^2 \Delta r$$

Instability towards convection when

$$N^2 < 0 \qquad \text{or} \qquad \frac{1}{\Gamma_1} \frac{\mathrm{d} \ln p}{\mathrm{d}r} < \frac{\mathrm{d} \ln \rho}{\mathrm{d}r}$$

Brunt-Väisälä frequency

or

$$\frac{\mathrm{d} \ln \rho}{\mathrm{d} \ln p} < \frac{1}{\Gamma_1} \equiv \left(\frac{\partial \ln \rho}{\partial \ln p} \right)_{\mathrm{ad}}$$

Duvall Law

- The p-mode solution can be written as
- $\int_t^R (\omega^2 - L_l^2)^{1/2} c^{-1} dr = (n+\alpha)\pi$ (α is a phase constant) condition for standing waves

Or

- $\int_{l_t}^R [1 - l(l+1)c^2/\omega^2 r^2]^{1/2} c^{-1} dr = (n+\alpha)\pi/\omega$
- set $w = \omega[l(l+1)]^{-1/2}$ so that
- $(n+\alpha)\pi/\omega = F(w)$ with $F(w) = \int_{l_t}^R [1 - c^2/w^2 r^2]^{1/2} c^{-1} dr$
- The observed and computed frequencies in fact satisfy relations like $(n+\alpha)\pi/\omega = F(w)$ quite closely, first noticed by Duvall (1982) for the observed frequencies. Thus, one can invert the observed F(w) to get c(r).

Helioseismology: Model Solutions

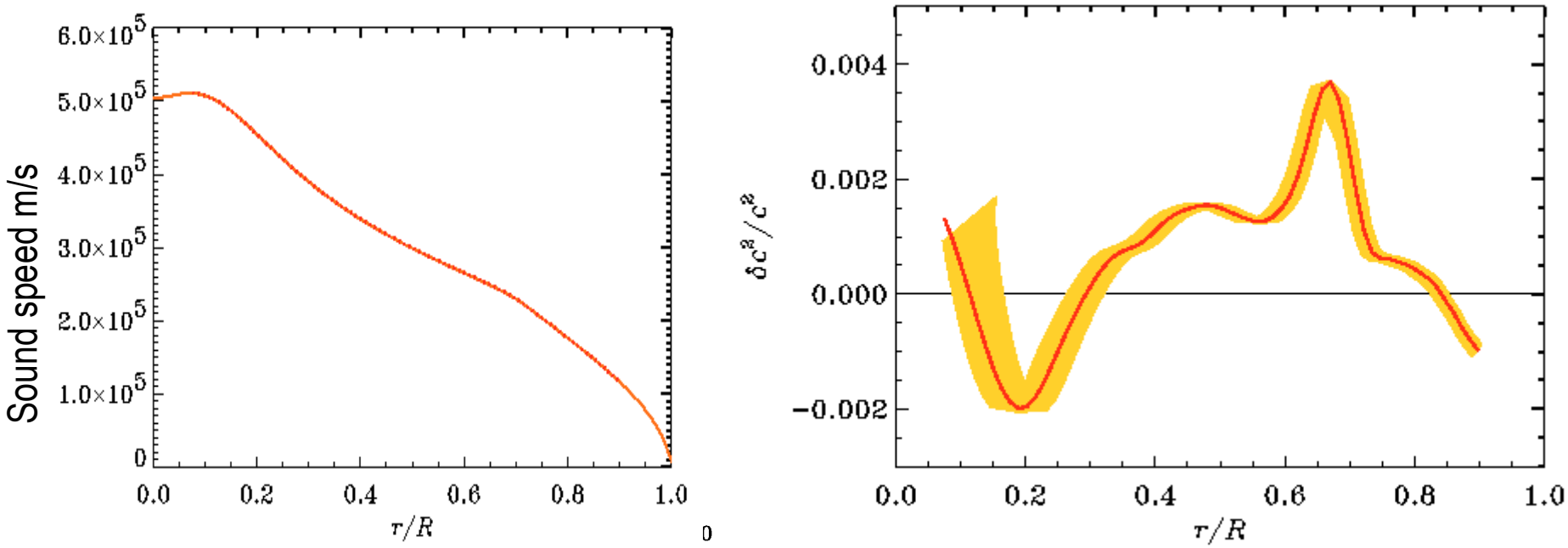

The relative differences between the Sun and the standard solar model in the squared sound speed, c^2, inferred from the solar frequencies determined from the 360-day series of SOHO MDI data. Note that the error is less than 0.4%. That is the standard solar model is in extremely good agreement with the helioseismic observations

Effect of Rotation

- So far we considered the Sun without rotation. Rotation will affect the quantum number m. If the Sun rotates with a uniform frequency Ω, then one can see that the inertial frame $((r,\theta,\phi))$ and the rotating frame $((r',\theta',\phi'))$ are related by

  $$(r',\theta',\phi') = (r,\theta,\phi-\Omega t)$$

- Therefore, the perturbations in the rotating frame $\cos(m\phi' - \omega t)$ will be $\cos(m\phi - m\Omega t - \omega t)$ or $\cos(m\phi-\omega_m t)$ where $\omega_m = \omega - m\Omega$

- Thus rotation causes the oscillation frequencies to split as $\pm m\Omega$. Waves propagating in the direction of rotation have a higher frequency $(\omega+m\Omega)$ compared to those propagating in the opposite direction $(\omega-m\Omega)$.

- For each (n,l) m takes values from –l to l. i.e., there is (2l+1)-fold degeneracy, lifted by rotation.

- The inversion discussed before for no-rotation case can be performed to include rotation. This way one can probe the rotation in the interior of the Sun

Rotation in the interior

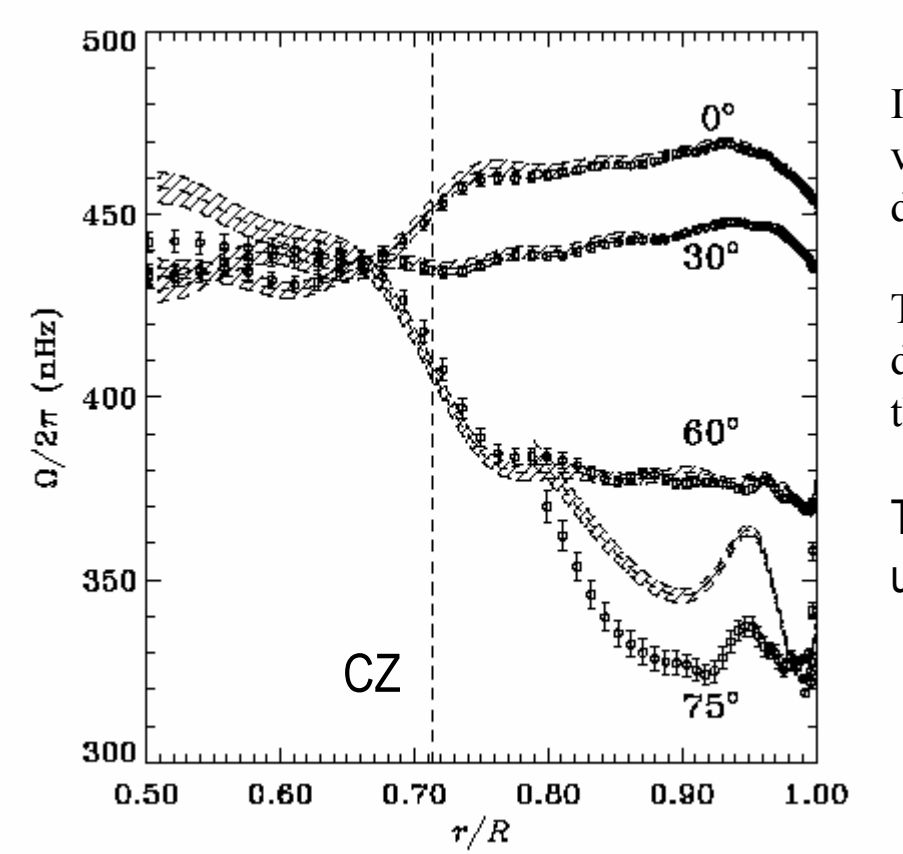

Inferred rotation rate as a function of radius at various latitudes, obtained from the inversion of 144 days of MDI data. (from Schou et al., 1998.)

The differential rotation on the surface is also seen down to the convection zone (CZ). Rigid rotation in the radiative zone

The sun has a differentially-rotating envelope and a uniformly-rotating radiative interior.

r/R =0 corresponds to sun center
r/R = 1 corresponds to the solar surface

Christensen-Dalsgaard, 2003

Other Applications of Helioseismology

- Sunspots and solar active regions were found to be strong absorbers of incident acoustic (p-mode) power (Braun, Duvall and Labonte, 1987, 1988)
- In sunspots, the p-mode travel times for outward propagating waves are smaller, by ~1min, than the corresponding inward travel times. Duvall et al. (1996) interpreted this as evidence of down flows within the spot and in its immediate surroundings. They also inferred higher magnetic field beneath the sunspot (2 kG at the surface and 4 kG at a depth of 600 km).
- Helioseismic tomography: technique to distinguish between ray paths which encounter the sunspot and the quite Sun. The resultant difference in travel time for the two different rays contains diagnostic information about the subsurface structure of the sunspot. Also could be used for far side imaging

Active Regions in Acoustic Power

Acoustic Power map

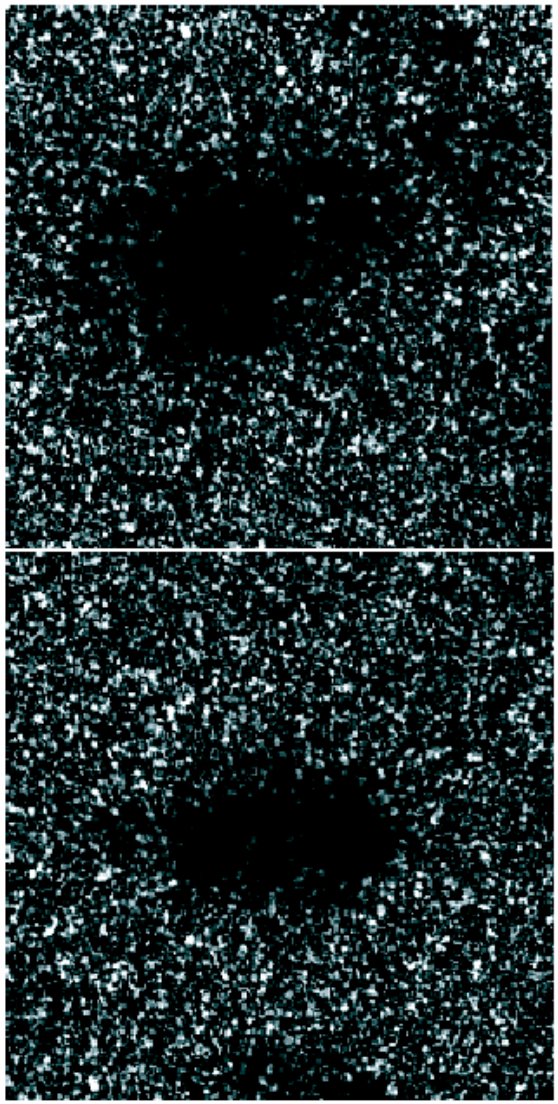

H. Moradi, 2004

Magnetogram

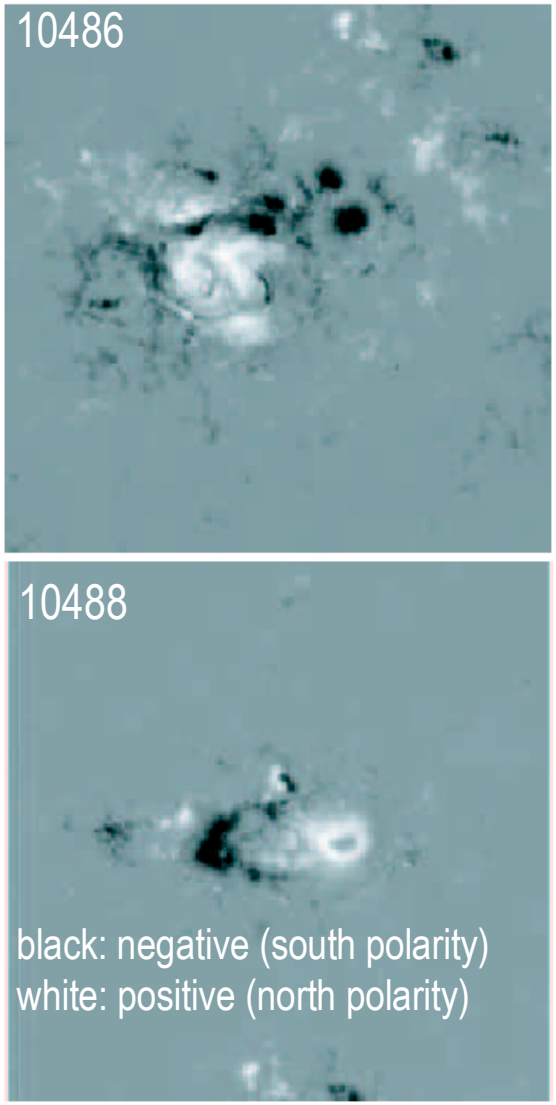

N. Gopalswamy Abdus Salam ICTP 5/3/2006

The amplitudes of p-modes are reduced in magnetic field regions (Leighton, Noyes and Simon, 1962). Acoustic power maps are now used to study the absorption of p-mode energy by sunspots (Braun et al. 1990).

Examples of acoustic power maps for two famous active regions (top-10486, and bottom-10488) compared with SOHO/MDI magnetograms

Active regions are compact regions on the sun with very high magnetic field, mainly from sunspots.

Note that the acoustic power is significantly reduced in the region occupied by active regions

Lecture III: The solar dynamo

- Solar magnetism and solar activity cycle
- A simple dynamo

The solar dynamo

- **A dynamo can be defined as the process by which the magnetic field in an electrically conducting fluid is maintained against dissipation.**
- **The motion of the conducting fluid (u) in the Sun across the magnetic field (B) regenerates and hence sustains the magnetic field.**
- **The base of the convection zone (aka tachocline) is the seat of the dynamo**
- **The tachocline is a transition layer between the differentially-rotating solar envelope and the uniformly-rotating radiative interior. Thus the tachocline represents a transition in the rotation profile.**

Two Basic Magnetic Properties

- 1. Existence of magnetic field.
- 2. Magnetic cycle (field reversal every 22 yrs).
- The differential rotation and convection in the outer layers are sufficient explain these.
- Let us first look at what observations tell us about the existence of magnetic field and the magnetic cycle

Surface Magnetic Field

- The photospheric field is organized in patches of strong field embedded in an overall weak field. The strong field has a hierarchy of magnetic elements with same field strength but different fluxes. Sunspots (3000 G; 10^22 Mx)) to bright network elements (~1500 G 10^18 Mx).
- During solar maxima, the large scale field is in active regions (ARs): two spots of opposite polarity surrounded by faculae. Occur in bands parallel to the equator (active region belts).
- Hale's Law: tendency of leading polarity in the active region fields to differ in northern and southern hemispheres
- ARs originate from CZ and decay in a few months as small-scale magnetic elements
- ARs tend to originate in the sites of existing or previous ARs
- AR emergence in the butterfly pattern: the solar cycle can be regarded as a wave with a period of 22 years

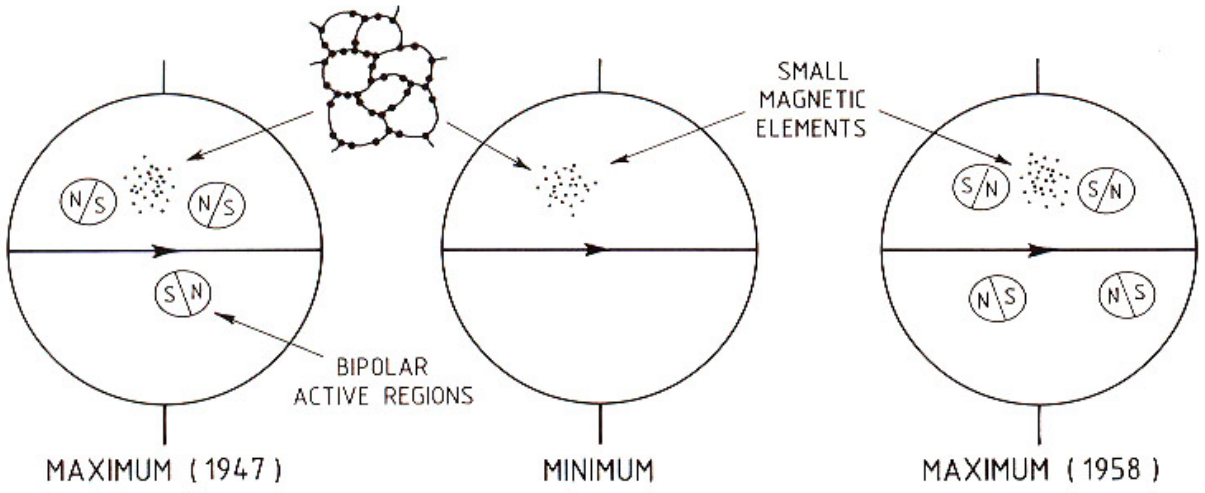

Hoyng, 1992

Butterfly Diagram

AR emergence at ~40 deg in new cycle
Emergence at progressively lower latitudes

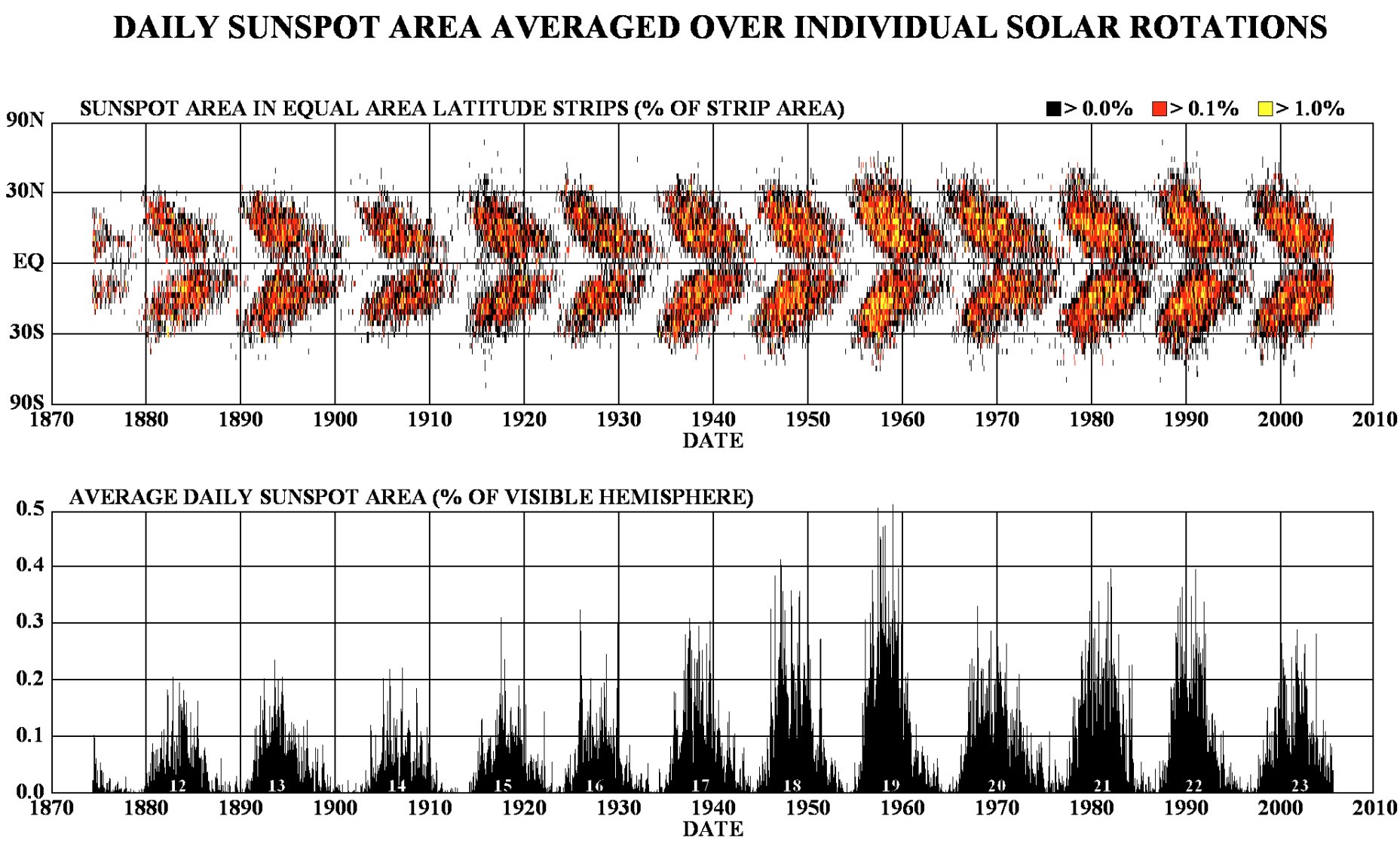

Flux emergence

- Flux emergence is the key to the connection between magnetic field generation in the Sun, and its consequence on the surface and above.
- Assume an east-west flux tube is embedded in the CZ which has a fluid pressure p_i. The magnetic field itself has a pressure, $B^2/8\pi$. For pressure balance, $p_e=p_i+ B^2/8\pi$, where p_e& p_i are external and internal gas pressures. Since $B^2/8\pi >0$, $p_e> p_i$, so the buoyancy force will lift the flux tube to low density region. Penetration of this field through the solar surface produces the observed bipolar structure.
- How the east-west flux rope is produced inside the Sun is the business of the dynamo theorists.

The two tubes reach equator in 11 years and disappear

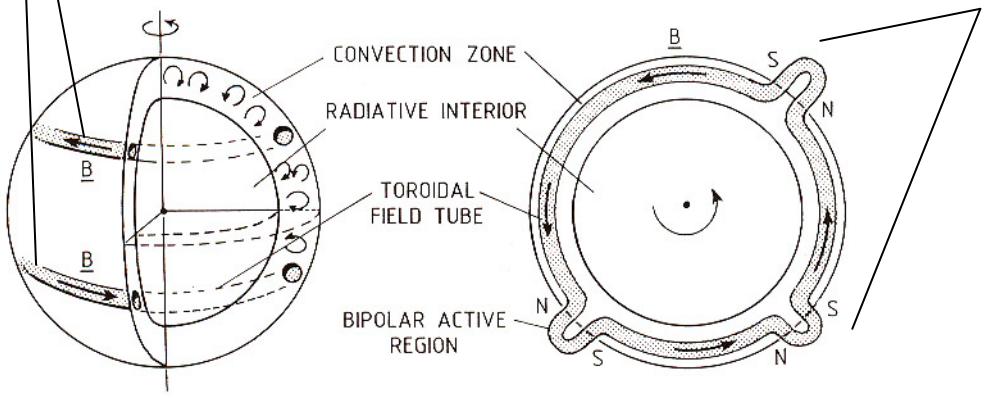

Hale's Polarity law

Differential Rotation

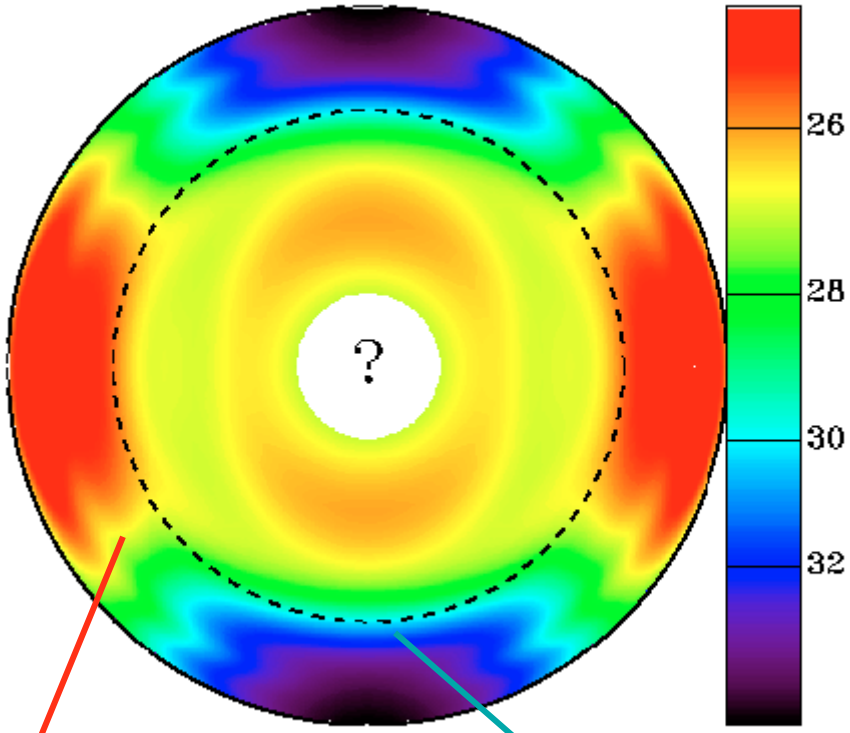

Rotation rate varies with latitude and radius.
The surface pattern more are less seen in the Interior down to the convection zone. The Equator rotates in ~25 days, while the pole in ~30 days
The rotation corresponds to an angular frequency.

The difference between the equatorial and polar rotation rates can be expressed as

$\Delta\Omega_r$ (diff rot pole to equator) ~$6 \times 10^{-7} s^{-1}$

Radial pattern

At the poles, the interior rotates faster than the surface

Thompson et al. 2003

Dynamo: α–Ω dynamo

Twisting of field lines is caused by the effect of the Sun's rotation on the rising "tubes" of magnetic field from deep within the Sun. This is called the alpha-effect after the Greek letter that looks like a twisted loop. The twist produced by the alpha effect makes sunspot groups that obey Joy's law and also makes the magnetic field reverse from one sunspot cycle to the next (Hale's law).

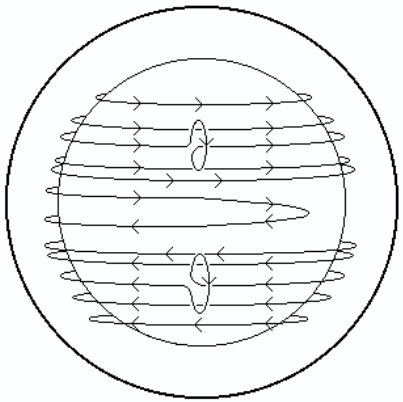

Hathaway

The α-effect

Magnetic fields within the Sun are stretched out and wound around the Sun by differential rotation. This is called the omega-effect after the Greek letter used to represent rotation. It takes ~8 months for a north-south field line to wrap once around the Sun. The field will have different directions in the northern and southern hemispheres.

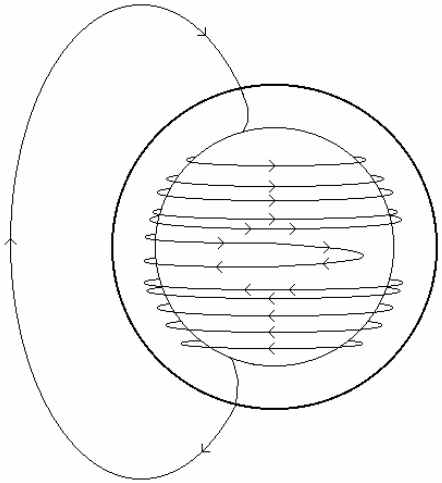

The ω-effect

Animation

This animation illustrates how differential rotation converts poloidal flux into toroidal flux

Simplified Dynamo Equation

Here we shall look at a simple dynamo known as the alpha-omega dynamo. Toroidal (T) & Poloidal (P) components of mean magnetic field are governed by the following equations with : α and β determined by the turbulent velocity field superposed on mean flow u_o

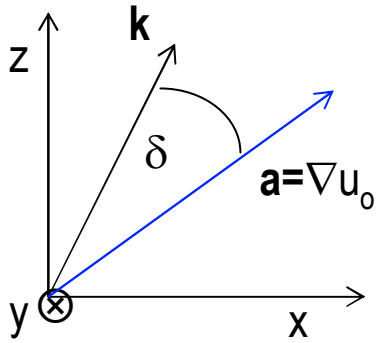

New T field — From T by alpha effect — Diffusion

$$\partial P/\partial t = \alpha T + \beta \nabla^2 P$$

$$\partial T/\partial t = (\mathbf{e}_y \times \mathbf{a}) \cdot \nabla P - \alpha \nabla^2 P + \beta \nabla^2 T$$

New T field — From P by Omega effect — From P by alpha effect — Diffusion

Hoyng 1992

T from P in two ways (α, Ω); P from T only by alpha; Both T and P diffuse; When $|\alpha \nabla^2 P| << |(\mathbf{ey} \times \mathbf{a}) \cdot \nabla P|$, we have $\alpha\Omega$ dynamo. Note that P can only decay when $\alpha T = 0$, so αT crucial.

Dynamo waves

Let us seek plane wave solutions to the above equations.
Substituting $(P,T) = (P_o,T_o)\exp(ik.r - i\omega t)$ for an $\alpha\Omega$ dynamo, we get the dispersion relation:

$$\omega^2 + 2i\beta k^2\omega - (\beta k^2)^2 - i\alpha k s = 0;\ s = a\sin\delta$$

This quadratic equation has the following roots:

$$\omega = i\beta k^2 \pm (i\alpha k s)^{1/2} = i\beta k^2 \pm (1+i)(\alpha k s/2)^{1/2}$$

Frequency of the dynamo wave = $\mathrm{Re}(\omega) = \pm(\alpha k s/2)^{1/2}$

Growth rate of the dynamo wave = $\mathrm{Im}(\omega) = \beta k^2 \pm (\alpha k s/2)^{1/2}$

Let us see if this frequency and growth rate are consistent with the solar data

Application to the Sun

The quantity s can be obtained from the differential rotation as follows:

$s = a\sin\delta \sim |\nabla u_o| \sim \Delta u_o/R_\odot \sim \Delta\Omega_r$ (diff rot) $\sim 6\times10^{-7} s^{-1}$

The wave number can be obtained from the size of the Sun: $k \sim 1/R_\odot = (1/7)\ 10^{-10}\ cm^{-1}$

The butterfly diagram gives the dynamo period $P_r = 22\ y = 2\pi\ Re(\omega) = 2\pi(\alpha ks/2)^{-1/2}$

Substituting for *s* and k on the right hand side of the above expression, we get $\alpha = 10$ cm/s

For marginal stability, Im (ω) ~0, which gives

$\beta k^2 \sim (\alpha ks/2)^{1/2} = 2\pi/P_r$ or $\beta \sim 2\pi R_\odot^{\ 2}/P_r$ or $\beta \sim 4 \times 10^{13} cm^2 s^{-1}$

Numerical models find similar values for α and β. Surface diffusion of magnetic elements also give a diffusion rate very similar to the above value of β.

Lecture IV: The atmosphere

- Detailed description of the photosphere, chromosphere, and the corona
- Mass emissions in the form of solar wind and coronal mass ejections
- Properties of coronal mass ejections and heliospheric impact

Solar Atmosphere

- We discussed the interior of the Sun. Now we describe the 4 atmospheric layers.
- Photosphere (T ~5770 K) visible. In reality it is a layer with T ranging from 6400 K to 4400 K. 100 km thick. Fraunhofer absorption lines indicate we are looking at a hotter source thru a cooler gas.
- Chromosphere: Envelope of gas surrounding the photosphere. Only 10,000 km thick. Many emission lines, but the H-alpha is the strongest Balmer line, so the chromosphere appears reddish.
- Transition region: The non-homogeneous layer between the chromosphere and the hot corona. T rises from 20, 000 K to ~1 MK. Hydrogen is ionized
- Corona: The extended hot atmosphere with a temperature of ~2 MK

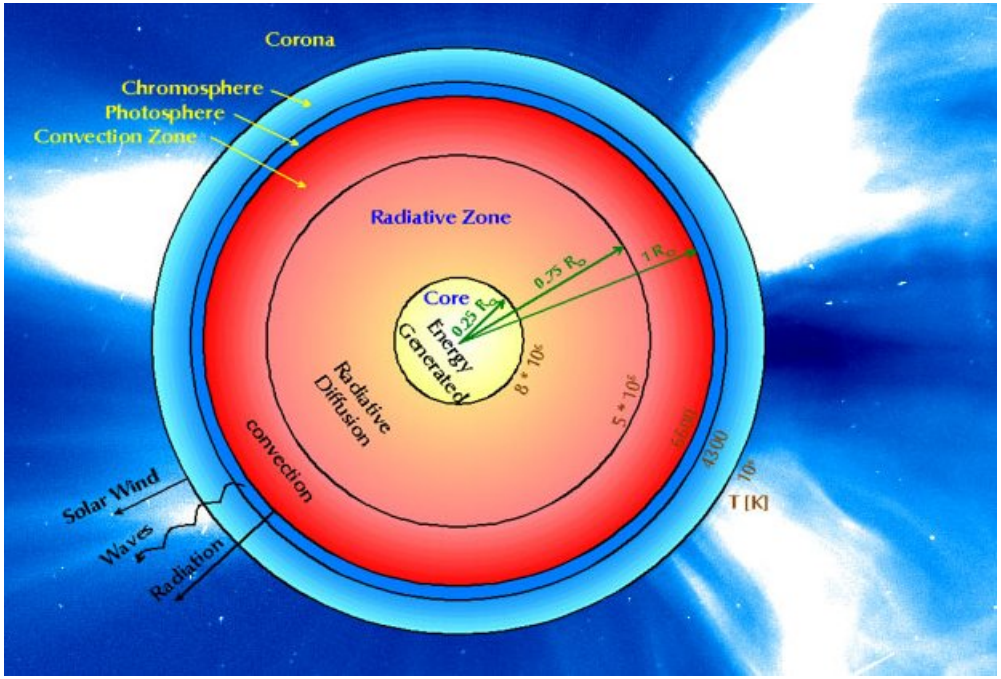

Jussila

Structure	Mean diameter	Lifetime
Spot	1000 km	100 days
- umbra	10-20 Mm	
-Penumbra	20-60 Mm	15-30 min
- Umbral dot	1000 km	
- Flux tube	<100 km	
- Fibril	200 km	2 h
Plage		150 days
- Facula		
-Ephemeral AR		
Prominence		
-Quiescent		months
-Active region Pr		weeks
-Threads	<300 km	minutes
Coronal Hole		200 days
-Bright Point		

Resolved structures on the Sun

Topologies and length scales – related to observed magnetic fields

A hierarchy of magnetic elements from the photosphere to the corona

The formation of the structures on the Sun involves the magnetic field and its interaction with the solar plasma

All ultimately linked to the convection zone

Photosphere

- The visible layer of the solar atmosphere, only about 100 km thick
- 6000 K black body
- contains the granular pattern, sunspots and faculae

Photospheric Fine Structures: Evidence of Convection

Granules, mesogranules, supergranules, bright points, filigree

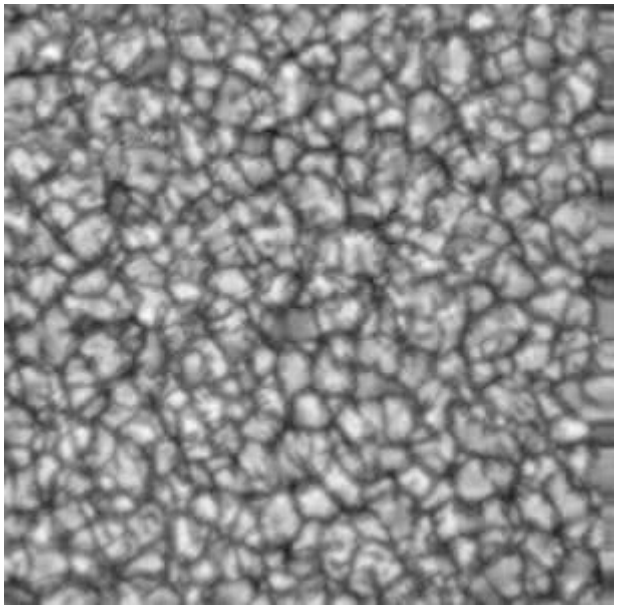

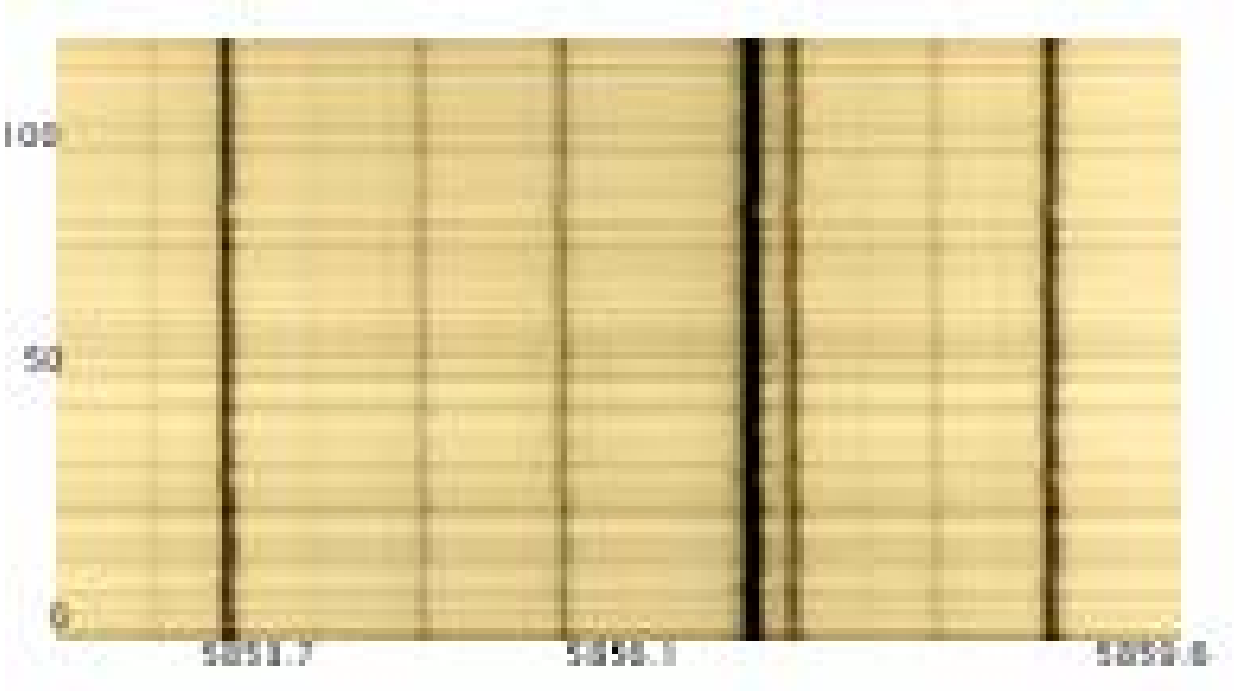

Granules: blobs of gas coming up at bright regions from below the surface (convection) Cools at the surface and sinks back along dark areas. So granules are the tops of convection cells in the photosphere

The wiggly-line spectrum. The wiggles indicate organized motion on the solar surface, amounting to ~ 2 km/s (Doppler shift). The associated temperature fluctuation is ~200 K

Supergranulation

The bright dots in the intergranular region
and at the boundaries of the supergranualtion
are intense magnetic filed regions

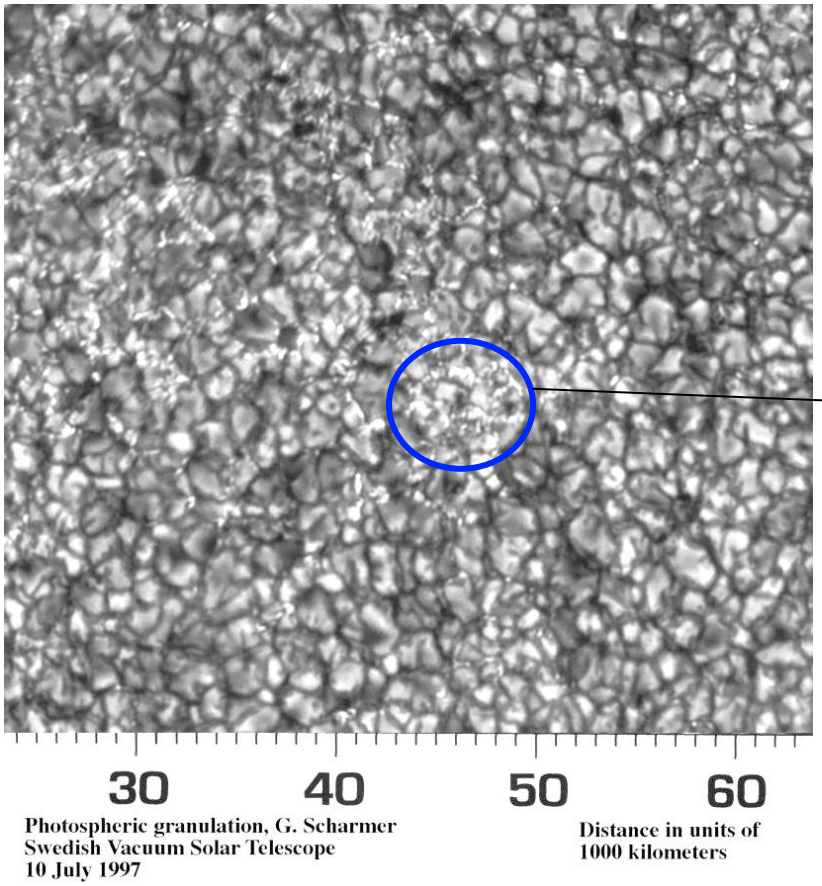

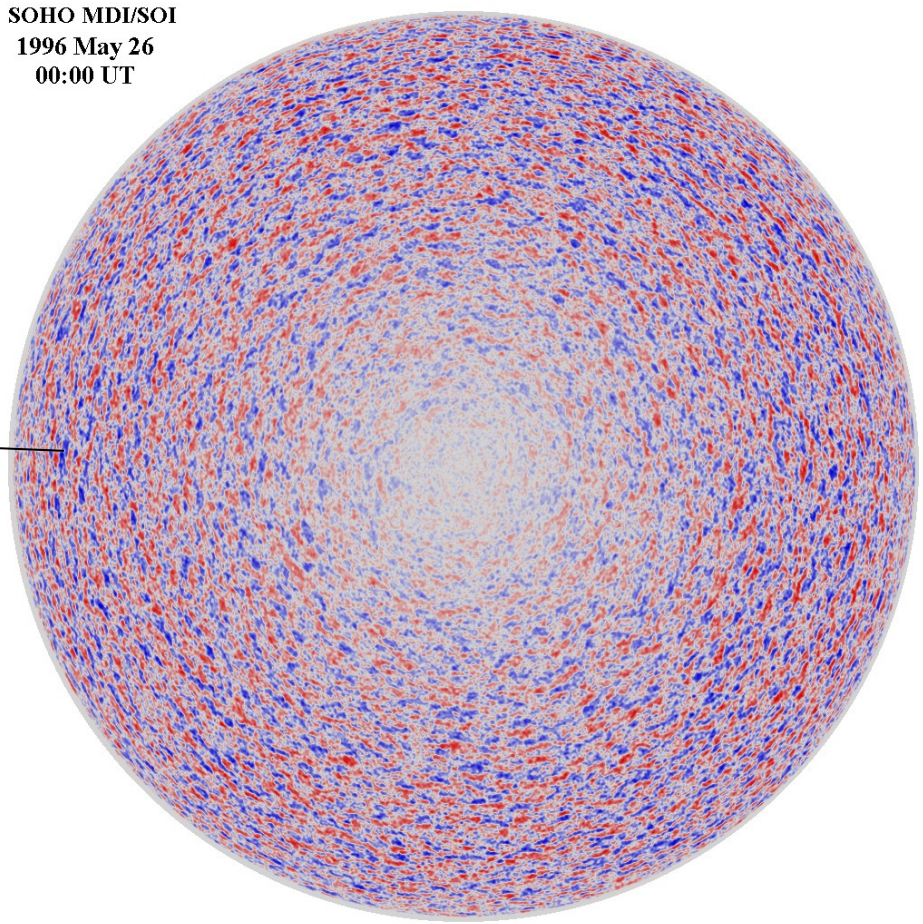

Simulations confirm the granulation pattern

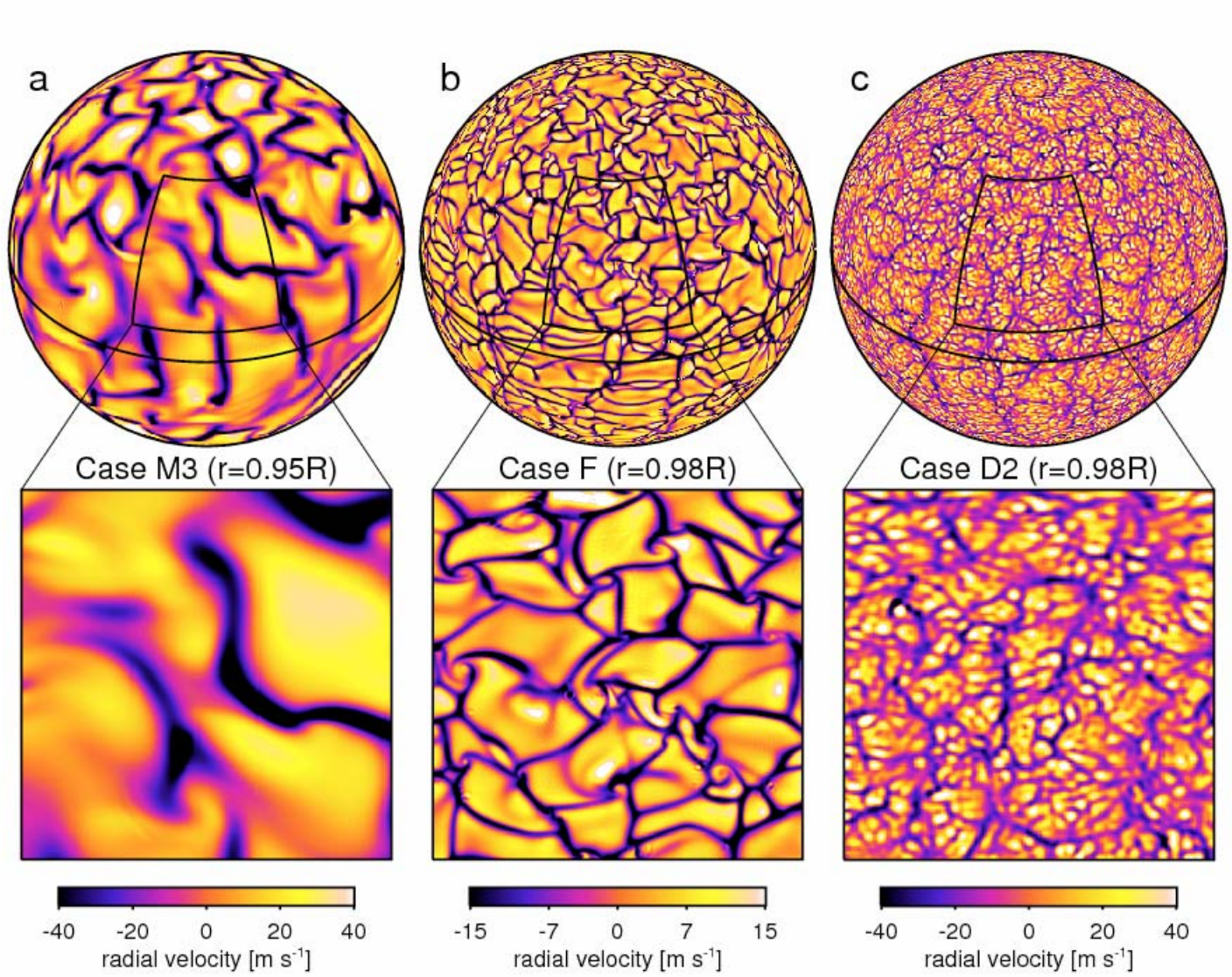

Association with Magnetic field regions

- Magnetic field is concentrated along the edges of the supergranular cells (also known as photospheric network
- The flux tubes have ~1 kG fields
- The photospheric fine structure provide information on convection and its interaction with magnetic field to decide the size and number of flux tubes
- Faculae are magnetic regions smaller that appear bright near the limb

Structure	Mean diameter	Speed	Lifetime	Remarks
Granules	1000 km	1-2 km/s	8 min	Small convective cells (CC)
Mesogranules	5000-10000 km		2 h	Larger CC
Supergranules	30,000-35,000 km	0.1 km/s	20 h	Large CC
Network BPs	150 km?			Chains of BPs known as filigree

Interaction of the flow with magnetic field

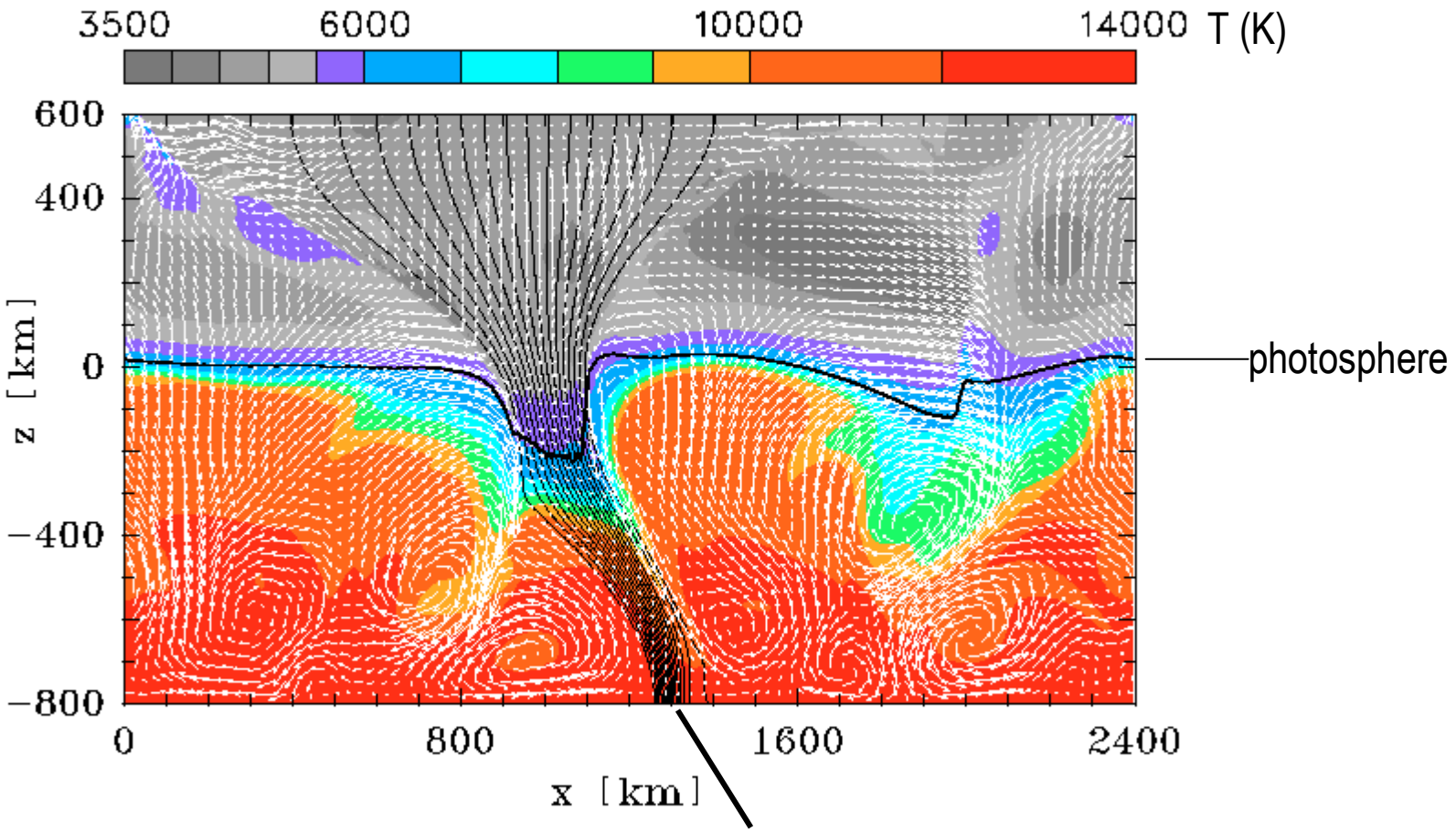

O. Steiner

Sunspots

Multiple umbrae
SVST La Palma

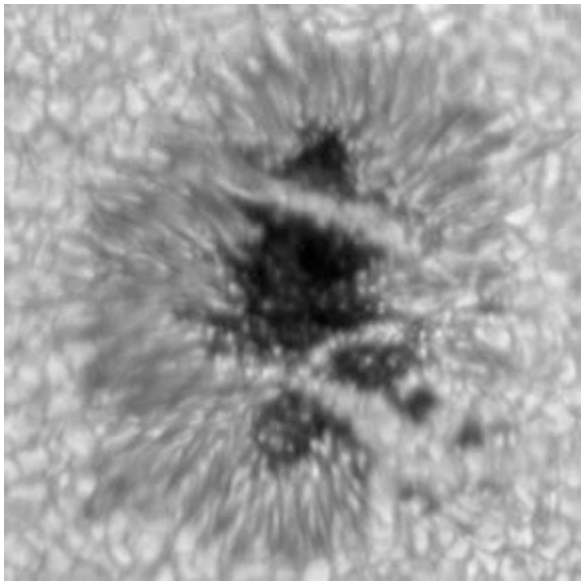

Dark and bright filaments; Evershed flow (1-2 km/s)

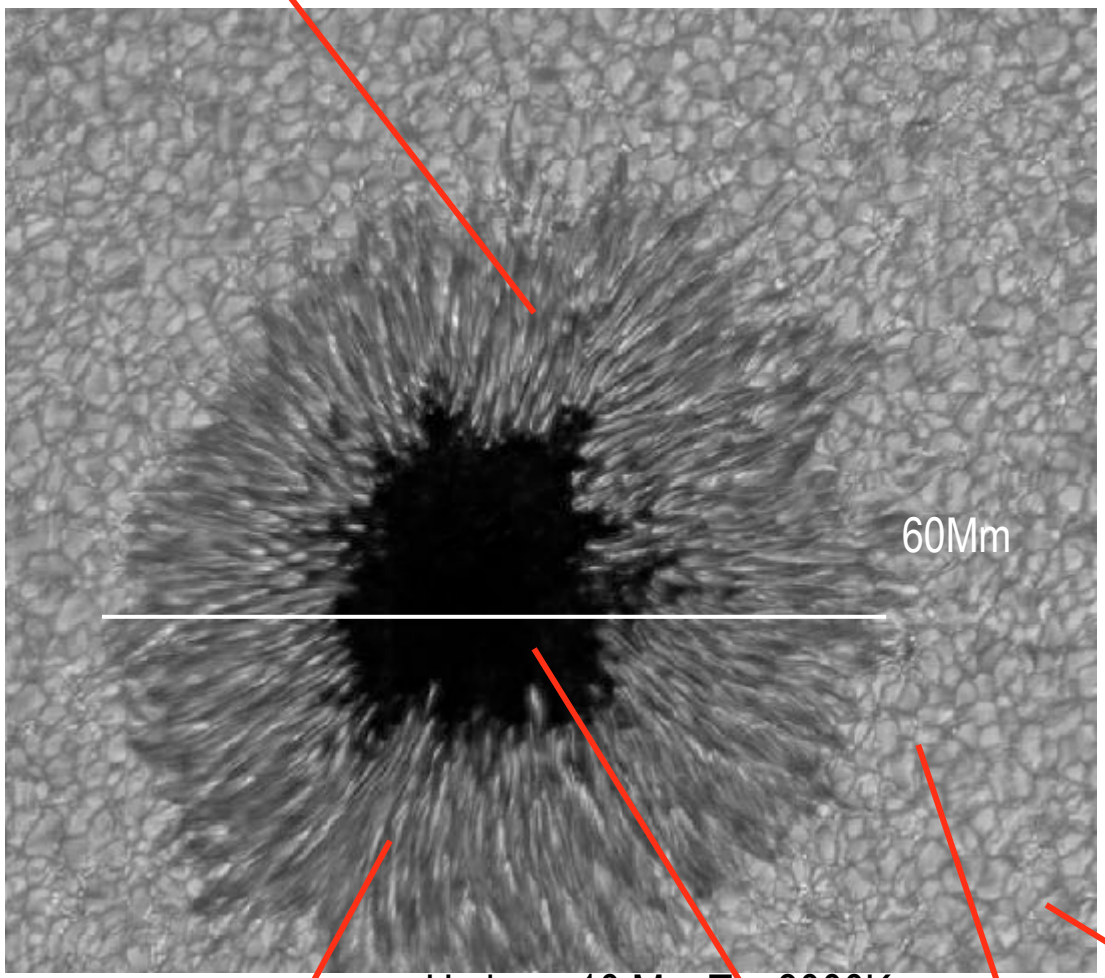

Sunspots - depression below the photosphere (600-1000 km)
Cooler than the quiet chromosphere, therefore emits less per unit area
Sunspot observations indicated differential rotation
Have high magnetic filed ~3-4 kG (using Zeeman Effect in 1908 by Hale) vertical in the umbra
Pores: small spots without penumbra

Penumbra ~15,000 km
T ~ 4500 K; B~ 1 kG

Umbra ~10 Mm T ~ 3000K;
B~3-4KG

T~6000K

granulation

Some more properties of sunspots

- Umbrae with < 7” size have higher temperatures (1” ~725 km)
- Umbral minimum intensity I_{min} ~ (0.03-0.3)I_{ph}, the mean photospheric intensity at 540 nm wavelength
- High magnetic field umbrae are darker and cooler
- Penumbral elongated features are due to inclined magnetic field. The fields in dark fibrils are stronger and more horizontal than the bright ones (see sketch below)
- Flow is toward the umbra (0.3 – 0.5 km/s) in bright filaments; away from the umbra in dark fibrils (3.5 km/s)
- Sometimes a “light bridge” is observed in the umbra. It is a narrow weak field region separating two segments of the strong-field umbra
- Spots generally appear as groups with opposite magnetic polarity, separated by a polarity inversion line (PIL) or neutral line. The vertical component of the field vanishes along this line (see sketch blow)
- The leading spots are typically bigger; the trailing spots have the polarity of the solar pole in their hemisphere
- Sunspots follow Hale’s law: leading spots in the N & S hemispheres have opposite polarities
- Generally confined between +30 deg and -30 deg latitude
- The line connecting the leader and follower is tilted away from the equator by ~12 deg (Joy’s law)
- Sunspots do not survive for more than 2-3 rotations
- No granules in the umbra: convection is suppressed by the magnetic field
- The spot equilibrium is dominated by magnetic pressure: $Pi + B^2/8\pi = Pe$; $Pi < Pe \rightarrow$ T lower inside the spot

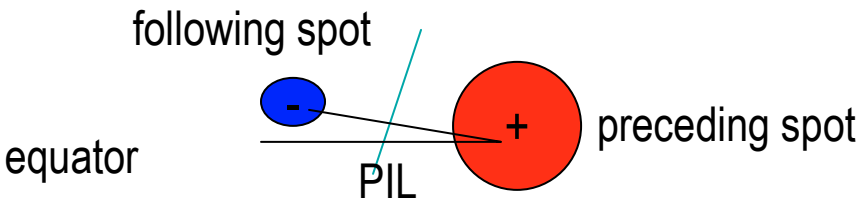

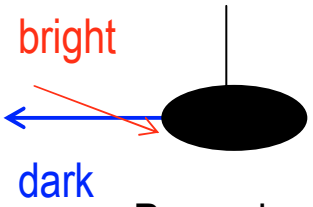

Penumbral fibrils

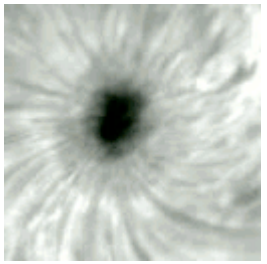

Sunspot Motions

A spiral-shaped sunspot captured on February 19th 1982, using the Kitt Peak Vacuum Telescope. The sunspot had a diameter of ~ 80000 km and held its shape for about two days before it broke up and changed its form.

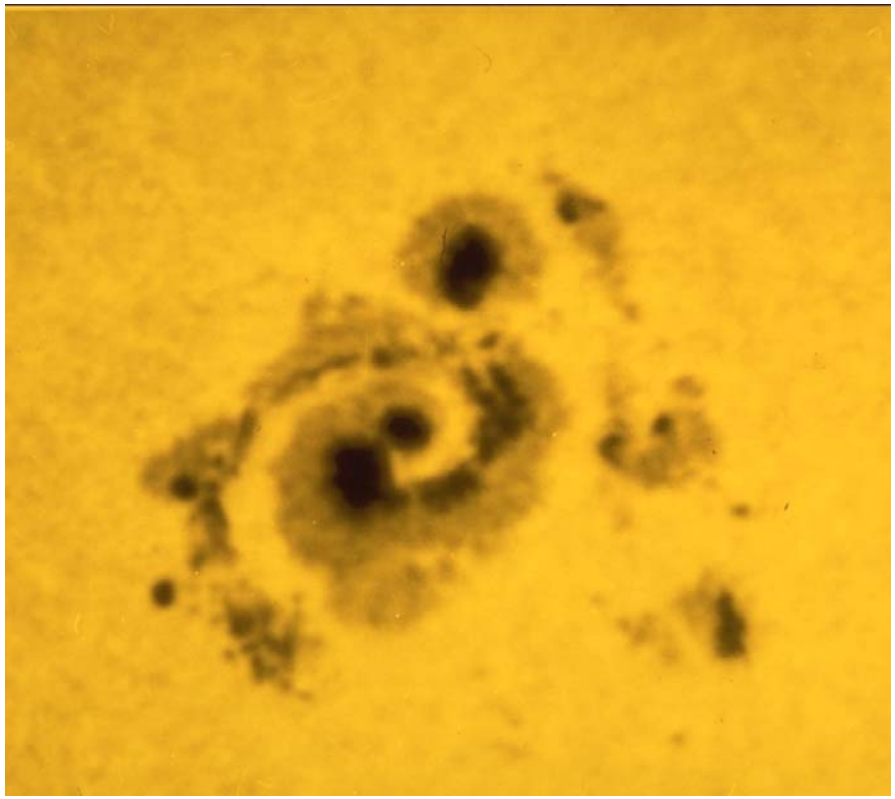

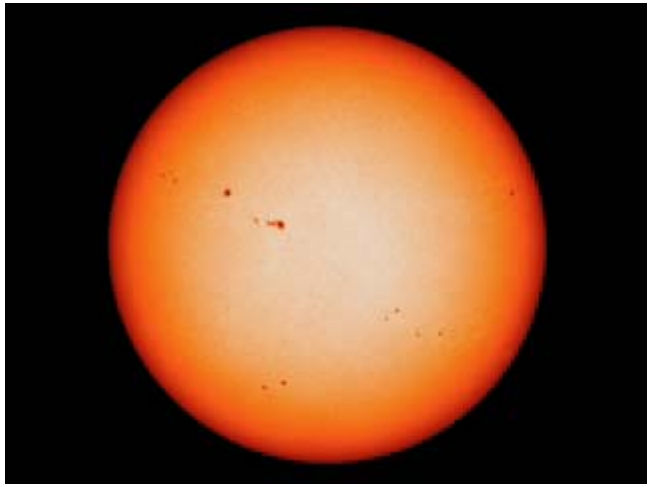

Movie showing sunspot rotation

NSO/AURA/NSF

Mount Wilson Sunspot Classification Scheme for Sunspot Groups

alpha: A unipolar sunspot group.

beta: A sunspot group having both positive and negative magnetic polarities (bipolar), with a simple and distinct division between the polarities.

gamma: A complex active region in which the positive and negative polarities are so irregularly distributed as to prevent classification as a bipolar group.

beta-gamma: A sunspot group that is bipolar but which is sufficiently complex that no single, continuous line can be drawn between spots of opposite polarities.

delta: A qualifier to magnetic classes (see below) indicating that umbrae separated by less than 2 degrees within one penumbra have opposite polarity.

beta-delta: A sunspot group of general beta magnetic classification but containing one (or more) delta spot(s).

beta-gamma-delta: A sunspot group of beta-gamma magnetic classification but containing one (or more) delta spot(s).

gamma-delta: A sunspot group of gamma magnetic classification but containing one (or more) delta spot(s).

beta-gamma-delta groups are most complex and prone to producing eruptions

Chromosphere

- The layer where the temperature ranges from 6000 K to ~20,000K
- Contains the following features, some of them closely related to photospheric features:

- Chromospheric network
- Filaments
- Plage
- Prominences
- Spicules

Chromospheric Features: network

- The chromospheric network: a web-like pattern most easily seen in H-alpha and the ultraviolet line of calcium (Ca II K). The network outlines the supergranules and is due to the presence of bundles of magnetic field lines that are concentrated there by the fluid motions.

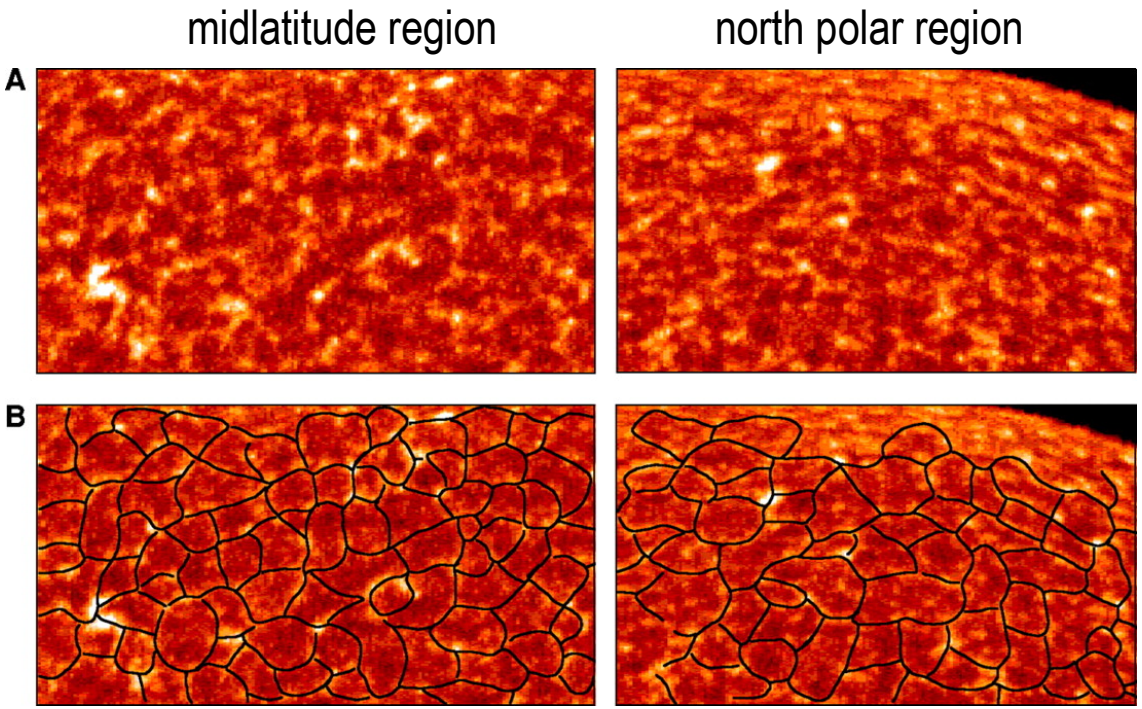

540”x 300” images
Bright: hotter plasma
Upflow at cell center
Downflow towards the edges

In the bottom, sketches of the network are superposed

Hassler et al. 1999: SOHO/SUMER chromospheric Si II 1533 Å images

Plage

Plage: “beach" in French, bright patches surrounding sunspots that are best seen in H-alpha. Plage are also associated with concentrations of magnetic fields and form a part of the network of bright emissions. Important contributors to irradiance variation.

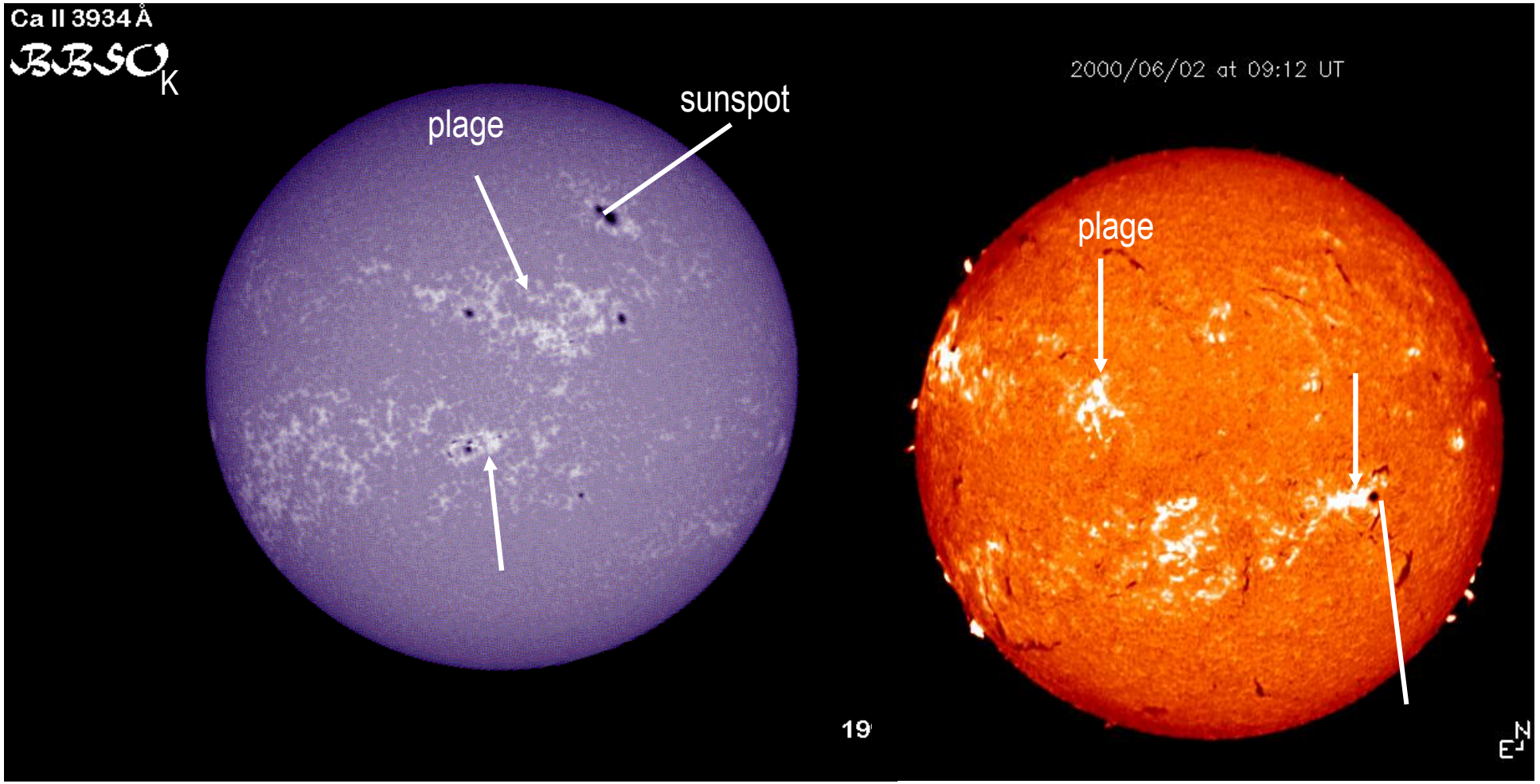

H-alpha

Prominences & Filaments

Prominences: dense clouds of cool material (~7000K) suspended in the corona by loops of magnetic field. Prominences and filaments are actually the same things except that prominences are seen projecting out above the limb of the Sun. Both filaments and prominences can remain in a quiescent state for days or weeks. However, as the magnetic loops that support them slowly change, filaments and prominences can erupt and rise off of the Sun over the course of a few minutes or hours.

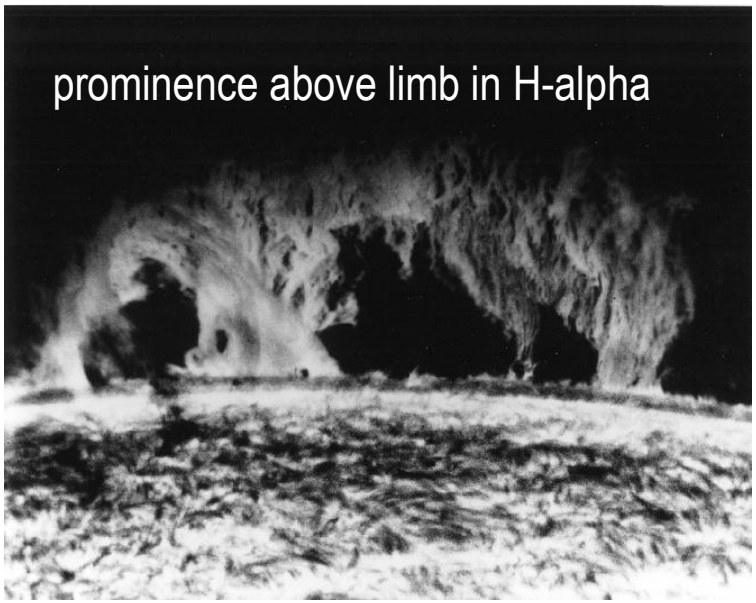

Dark Filament on the disk & its disappearance (eruption)

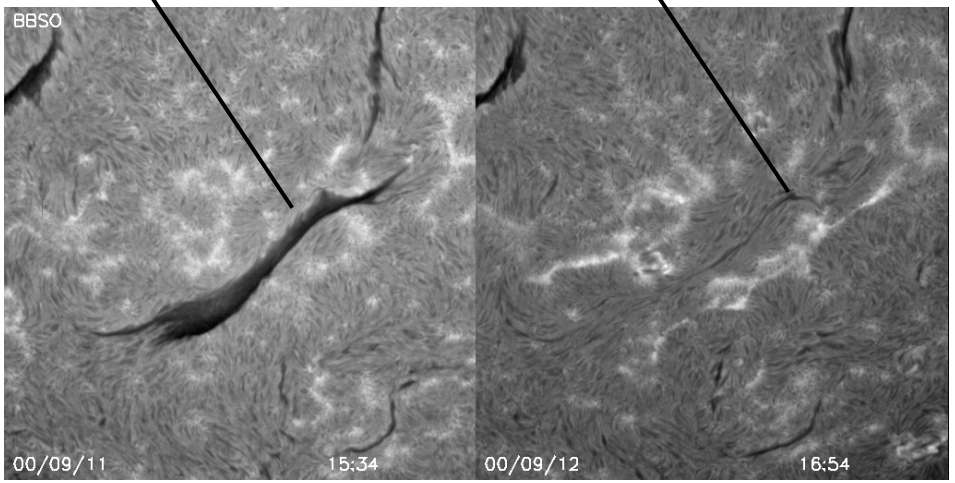

BBSO

More on Prominences

- Thin sheets of cool (~8000K) dense (density ~$10^{10\text{-}11}$cm^{-3}) plasma suspended in the corona.
- Quiescent prominences are located between active regions or in polar regions
- Active (or plage) prominences are in located in active regions
- Length ~200 Mm; height ~50 Mm; thickness ~2 Mm
- Magnetic field ~5-10 G in quiescent prominences; 20-150 G in active region prominences, highly sheared (<20 deg deviation from PIL)
- Rising motions: a few km/s; counterstreaming
- Prominence Mass: Mp = NpVpm$_p$ ~3x10^{15} g [N~ 10^{11}cm^{-3}]
- Mass of the corona: Mcor = Ncm$_p$AH ~ 1.5 x10^{17} g [coronal density Nc ~ 3x10^8cm^{-3}; A = area at the coronal base ~ solar surface area; H= coronal scale height ~ 5 x10^9 cm]
- Prominence supported by jxB force against gravity (j – electric current, B - magnetic filed)
- Prominence material probably comes from the chromosphere due to transient jets or continuous evaporation. Coronal condensation is another idea, but the mass may be a problem

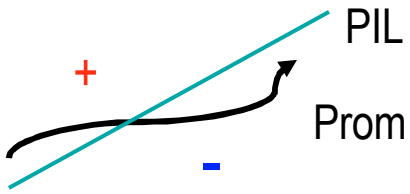

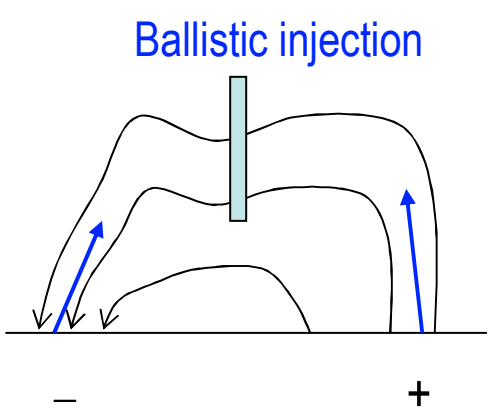

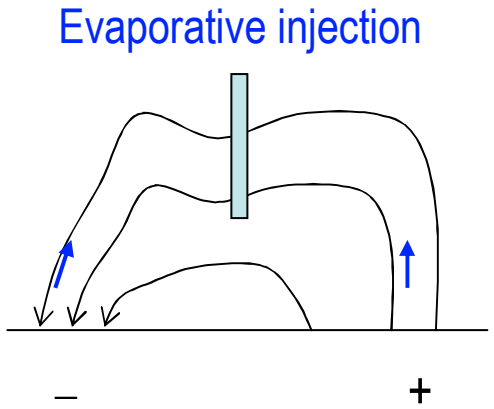

Spicules

Spicules: small, jet-like eruptions seen throughout the chromospheric network. They appear as short dark streaks in H-alpha images. They last for a few minutes but in the process eject material off of the surface and outward into the hot corona at speeds of 20 to 30 km/s.

They appear at network junctions, from where the magnetic field spreads out

Note the relation to the chromospheric network and supergranules.

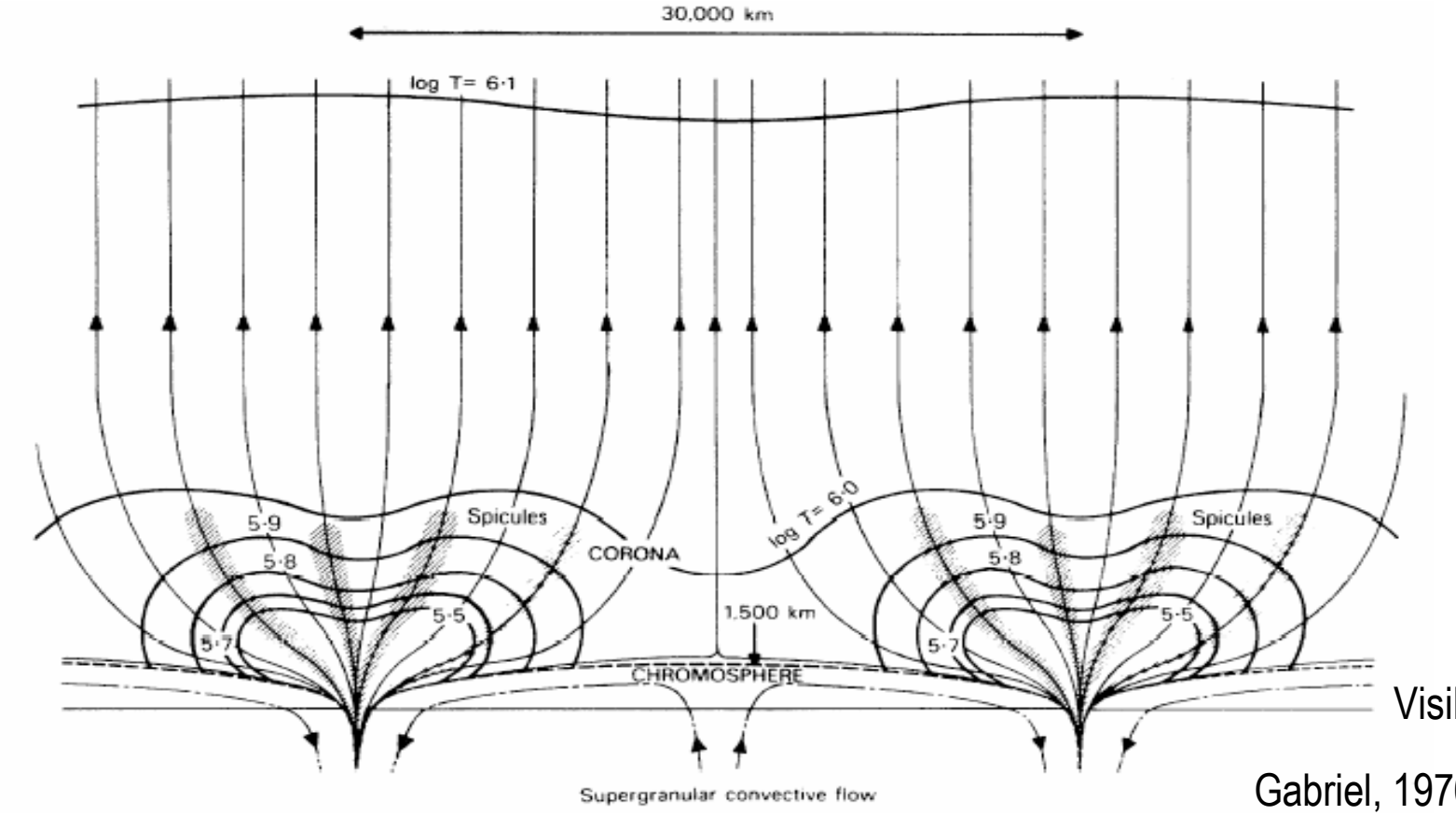

Visible limb

Gabriel, 1976

Spicules on the disk

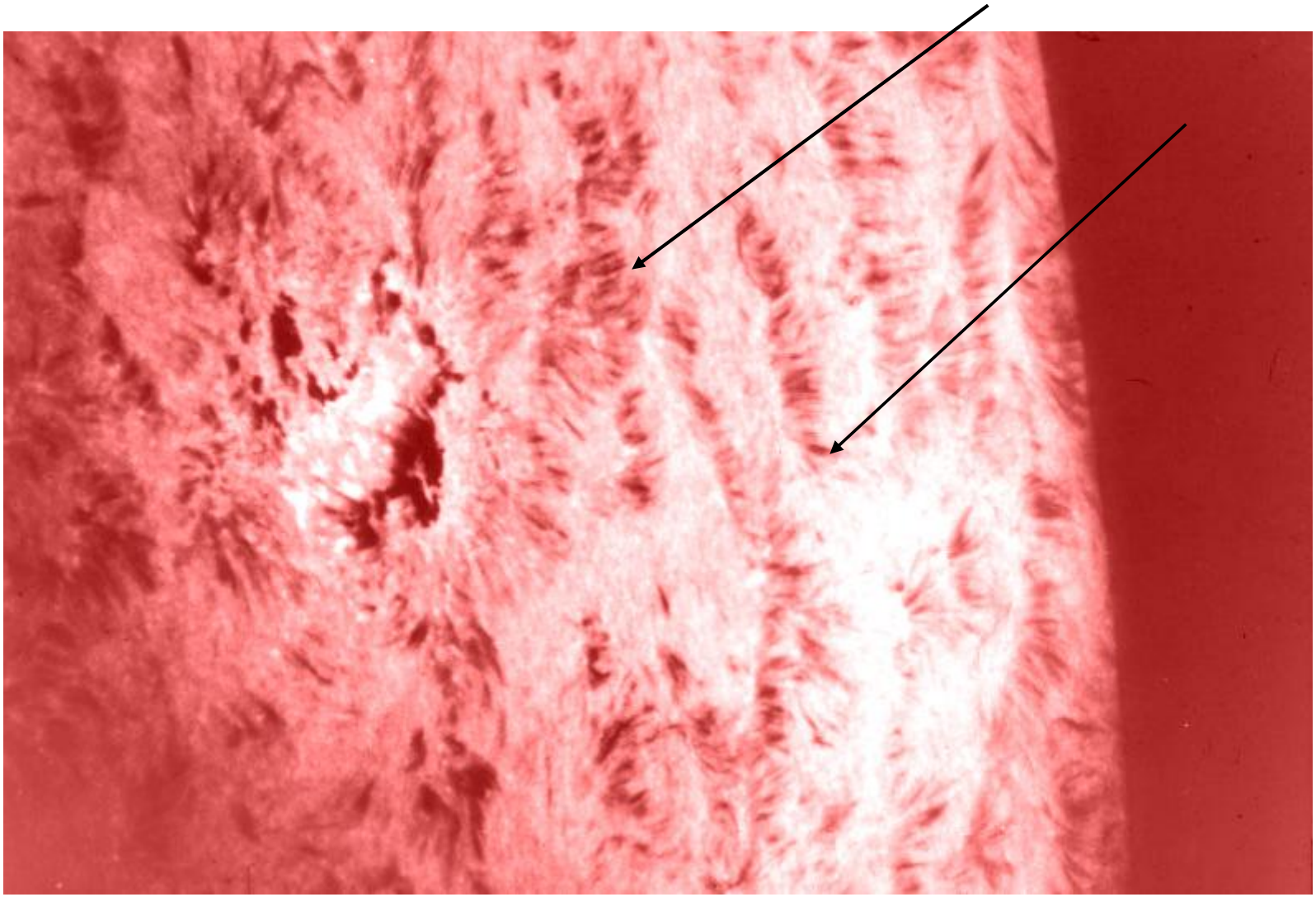

Fine Structure of the quiet Chromosphere

Structure	Mean diameter	Speed	Lifetime	Remarks
Spicules	500-1500 km	20-25 km/s	5 min	Transport mass upwards (10^{15} protons/cm^2/s)
Network	(30-35)x1000 km	0.8km/s	20 h	down flow
- Bright mottles	1,500-4,000 km		11-12 m	Parts of network boundaries
- Dark Mottles	1000-8000 km		5-15 m	Disk version of spicules
- Fibrils	1000-2000 km		6-12 m	Elongated horizontal structures
Supergranular cells	(30-35)x1000 km			Overly the ph. supergranules
- BPs	1000 km		3-4 m	

Thermal Structure of solar atmosphere

The temperature initially falls from ~6000 K and then increases to attain a few MK. The only place where the temperature can exceed the interior (15 MK) is compact flare regions in the corona. The flare plasma can attain tens of MK.

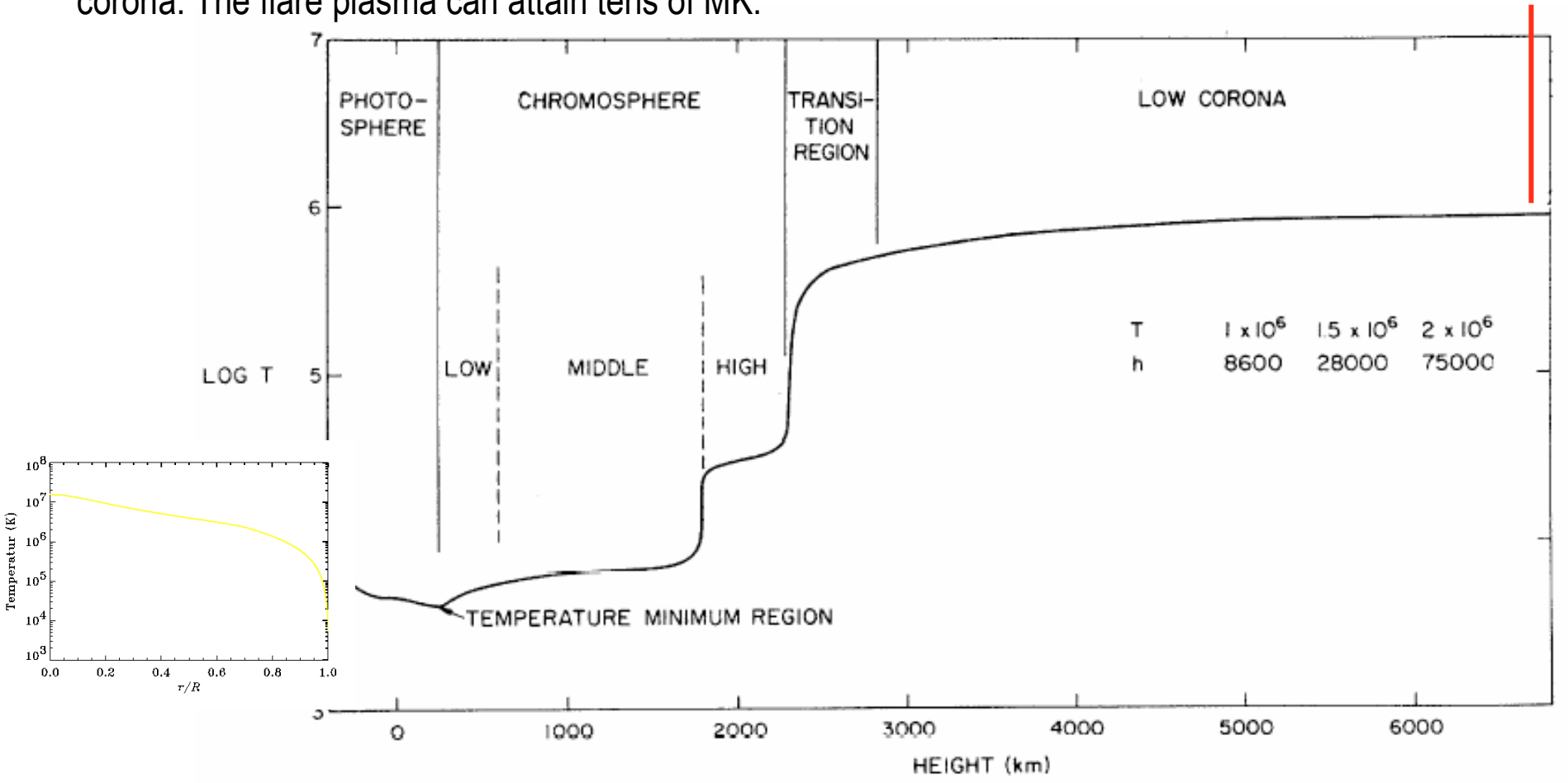

The Corona

- Most of the space Weather Events originate in the corona, although they have clear connection to underlying structures.
- Flares happen in the corona, but many of them have chromospheric counterparts
- Flux emergence from below the photosphere and photospheric motions are thought to be responsible for build up of energy in coronal magnetic fields that can be released as flares and coronal mass ejections
- The emission lines in the corona, as those in the chromosphere and transition zone, indicate the high temperature. The lines are formed at certain heights where the temperature is appropriate. By assembling a set of lines formed at various temperatures, one can study various layers of the chromosphere, transition zone and the corona, analogous to using various oscillation modes to probe the interior.
- There are also other ways of probing the atmosphere using X-rays and radio waves

Emission Lines showing the existence of

Chromosphere

Ion	Line (Å)	T (10^4 K)
H I	1215.67	1-2
HI	6562.8 (H-alpha), 3970.07(H-epsilon)	0.6-1
He I	10830, 5875.7	2
C II	1334.532,1335.708	2
Si III	1206.51, 1892.03	3.5
Si II	1304.372, 1309.227,	1.2
Si II	1526.708,1533.432	1.2
Ca II	3933.66 (K), 3968.47(H) 8542.09, 8662.14, 8498.02	0.6-0.8
Mg II	2795.53(k),2802.70 (h)	0.6-0.8
O I	1302.169,1304.875	0.6
C I	1560.683, 1657.008	0.6

Transition Region, & Corona

Ion	Line (Å)	T (10^4 K)
Mg X	609.76, 624.03	1200
NeVII	465.221	50
OVI	1031.912	32
OIV	554.51	15
NV	1238.821, 1242.804	16
He II	303.78	8
He II	1640.332,1640.474	8
C IV	1548.185, 1550.774	10
Si IV	1393.755,1402.770	6
C III	1175.711,1174.933	5

EUV (<900 Å) very useful. SOHO EIT uses 195, 171, 284 Å lines

Visible: ground based; UV, EUV from space

From Schatzman & Praderie 1990

Sun in X-rays

- Recall that, $\lambda T = 0.29$cmK. For T =2 MK, $\lambda \sim 1.5 \times 10^{-7}$ cm or 15 Å (soft X-rays)
- Sun has been known as an X-ray source since 1945, but the Skylab mission (1973) provided main results on solar X-ray emission.
- Yohkoh mission confirmed a lot of Skylab results and demonstrated the dynamic nature of the corona (1992-2001)
- Nonthermal emission was also imaged by Yohkoh's hard X-ray telescope and the current RHESSI mission
- X-ray observations provide information on magnetic field topology
- Largely agree with potential field extrapolations of the photospheric magnetic field into the corona
- Einstein (1980), EXOSAT(1983), and ROSAT (1990) satellites confirmed X-ray emission from many stars.

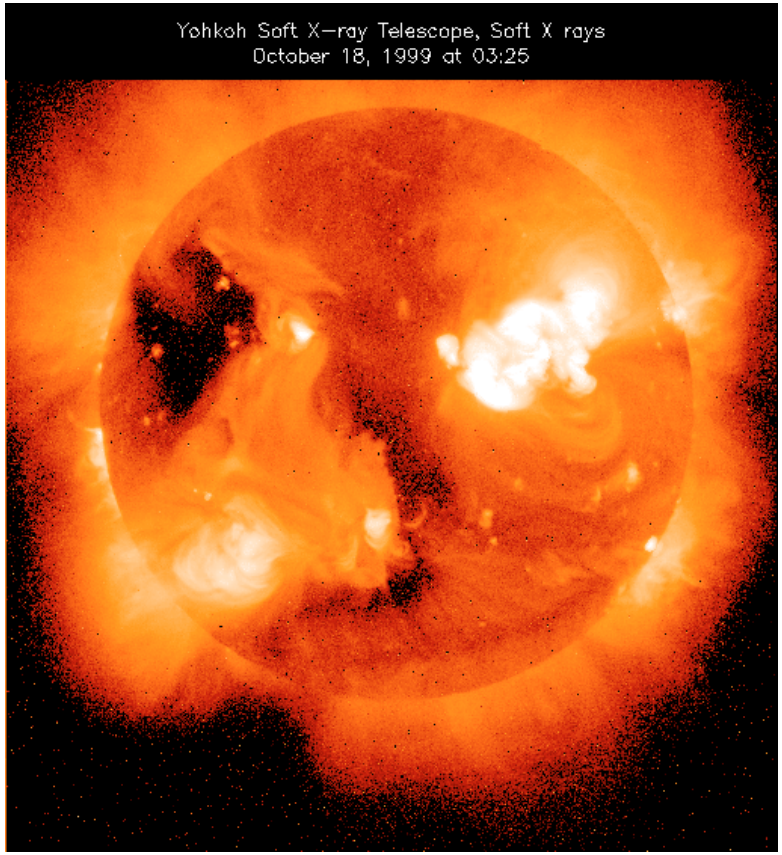

Sun in Radio

- Sun emits radio waves at mm – km wavelengths
- Radio window allows observations from ground from mm to tens of m. Longer wavelengths have to be observed from space because of the ionospheric cutoff around 30 m
- Thermal and nonthermal emissions can be observed. Thermal tells us about the quiet atmosphere. Nonthermal emissions tells us about accelerated charged particles and the associated physical processes.
- Can probe the entire Sun-Earth distance by choosing appropriate wavelengths
- Good proxy for solar activity: 10 cm emission from active regions
- Large-scale structure of the corona and its variability with solar cycle

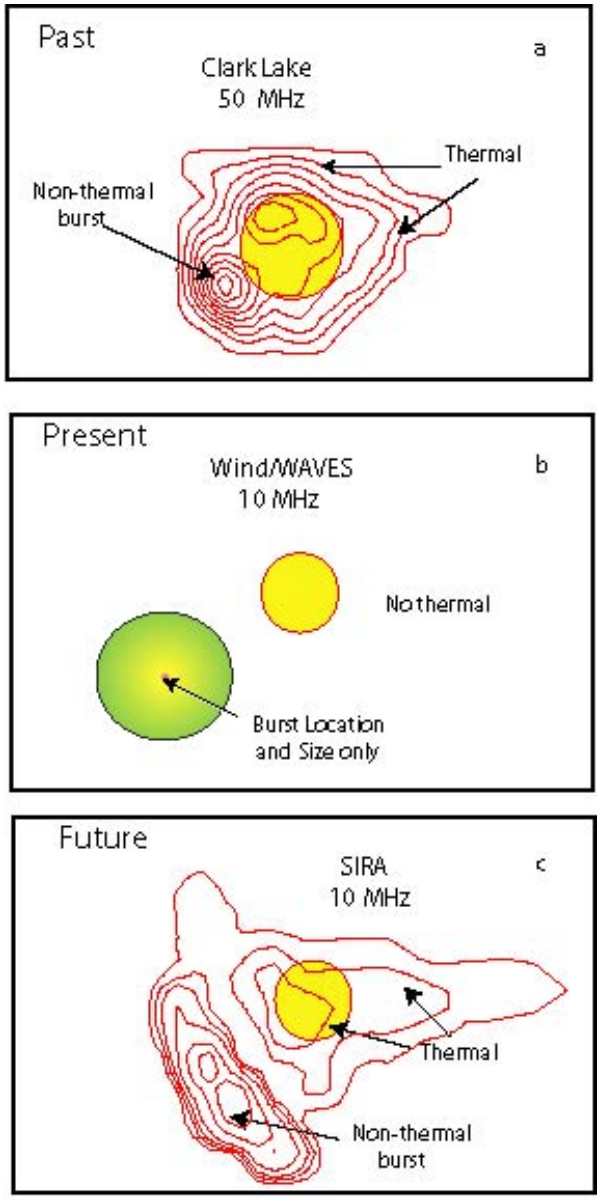

Sun in cm radio wavelengths

- Quiet Solar disk at 10,000 K (most pixels are at this temperature): QS
- Gyroresonance emission from corona above sunspots. Magnetic field info
- Small bright areas on the disk: active regions (AR), post-eruption arcades (AF)
- Dark areas on the disk: Filaments (F) because Tb ~ 8000K
- Bright regions outside the disk: Prominences (P) Tb ~8000 K>> optically thin corona (~200 K); Sometimes mounds consisting of AR loops (Tb > 10000K)
- Dimming (deficit of free-free emission) can be observed in some limb events.
- Prominences and filaments erupt as part of coronal mass ejections
- 100s of eruptions documented on the NoRH web site
- Selected references: Hanaoka et al., 1994; Gopalswamy et al., 1996; 1999; 2003; Hori et al. 2000; 2002; Kundu et al. 2004

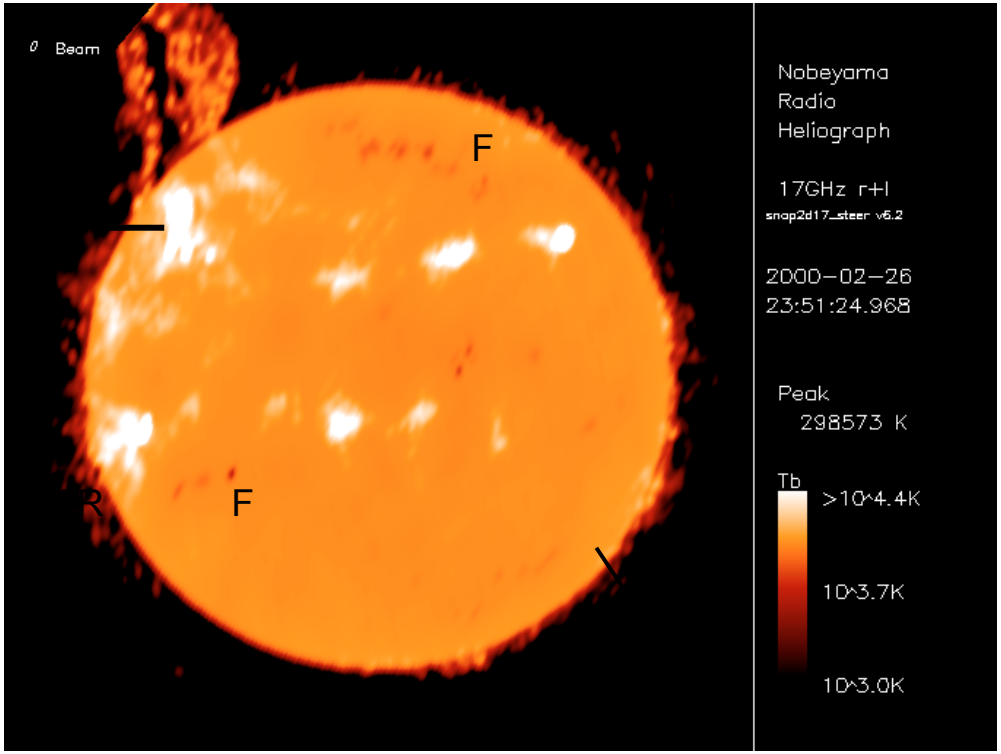

Unlike spectral observations, structures at different temperatures can be imaged in radio. Both chromospheric and coronal phenomena can be observed in microwaves. Both thermal and nonthermal emissions can be observed

From Nobeyama radioheliograph in Japan

Coronal Features

- Coronal Holes : source of high-speed solar wind
- Coronal Loops: closed magnetic field line loops around sunspots and active regions. can last for days or weeks if not associated with solar flares
- Helmet Streamers: source of low-speed solar wind; network of magnetic loops with dense plasma connecting the sunspots in active regions typically occurring above prominences
- Polar Plumes: long thin streamers associated with open magnetic field lines at the poles. Plume and interplume regions have different properties near the Sun. fast wind in the interplume region
- Coronal Mass Ejections (CME): huge magnetized plasma structures ejected from the Sun over the course of several hours
- Solar flares: huge explosions with time scales of only a few minutes

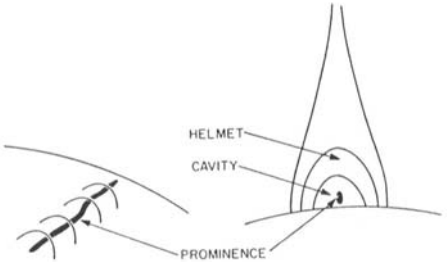

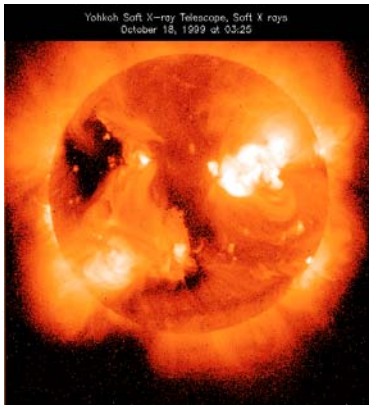

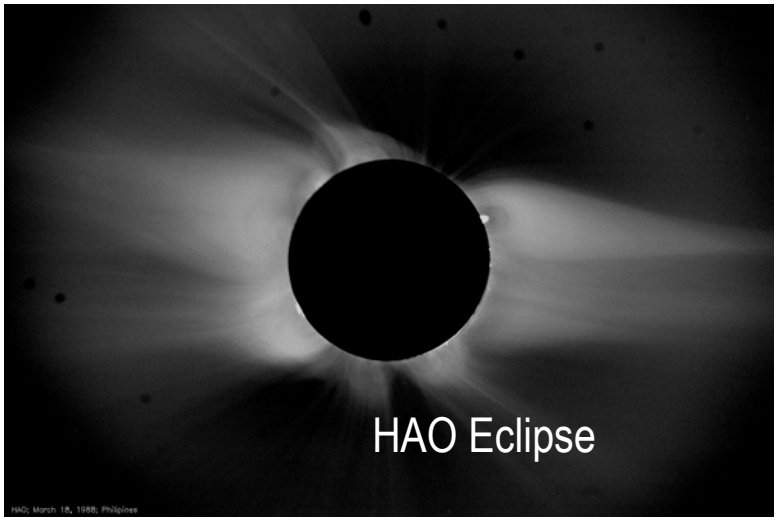

TRACE loops

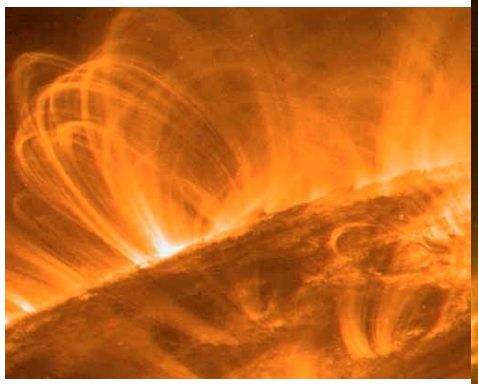

TRACE Flare loops

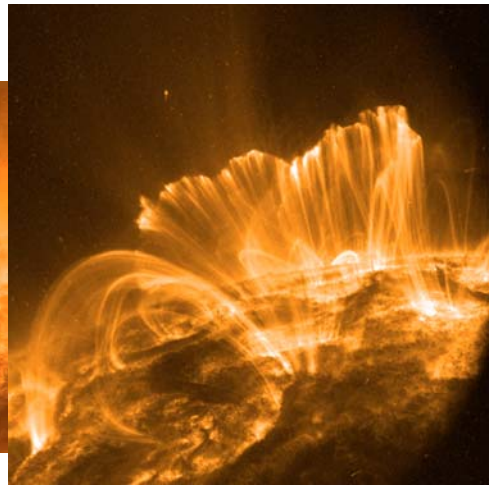

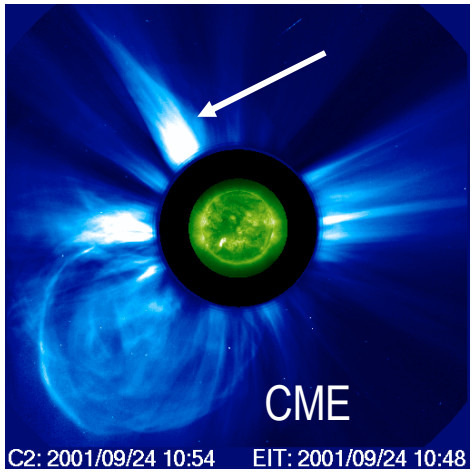

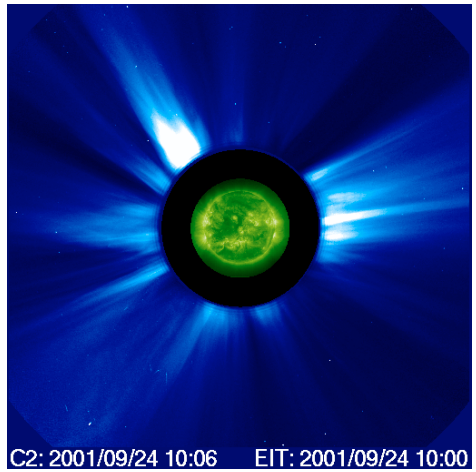

Coronal Holes

- Large-scale regions of the corona observable in X-rays (a few Å) & EUV fainter than the surrounding corona.
- Polar CHs can cover up to 10% of solar surface; low-latitude ones from 1 to 5%
- Polar holes, largest during solar minimum shrink toward and disappear during solar maxima
- Unlike sunspots, CHs display rigid rotation (27 days)
- The formation of coronal holes are linked to the evolution of active regions. The unipolar regions in CH are due to the mergers of the similar polarity regions of active regions (Timothy, 1975)
- Extended NS holes occur when low-latitude holes link up with the polar hole of the same polarity
- The coronal holes have a higher unipolar flux compared to the surrounding quiet Sun
- Bartol called these M-regions from which high speed winds originate. Skylab observations confirmed this
- The transition region is ~5 times thicker in CH than in quiet regions; dT/dz is ~5-10 times lower; pressure is 2-3 times lower
- Coronal hole chromosphere different from quiet chromosphere observed in microwaves

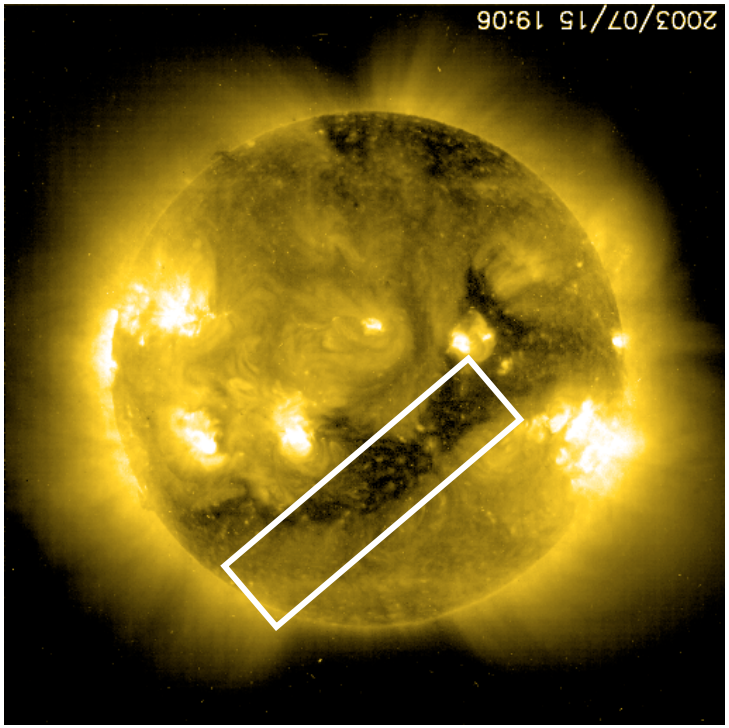

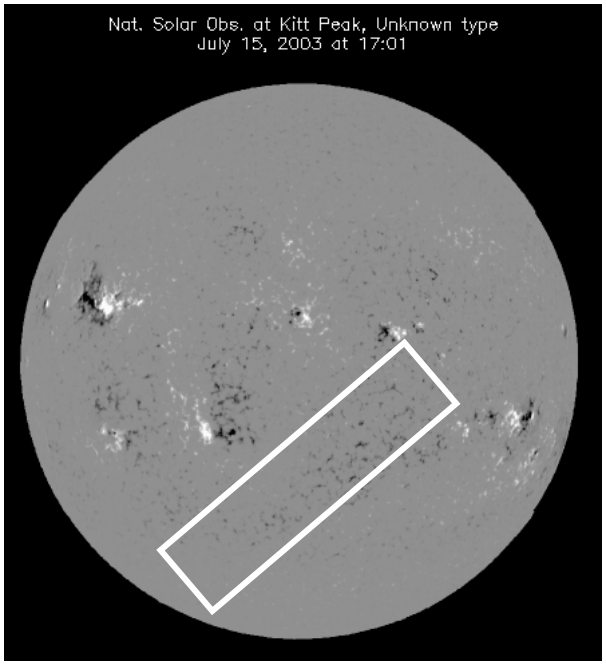

Coronal holes longer radio wavelengths

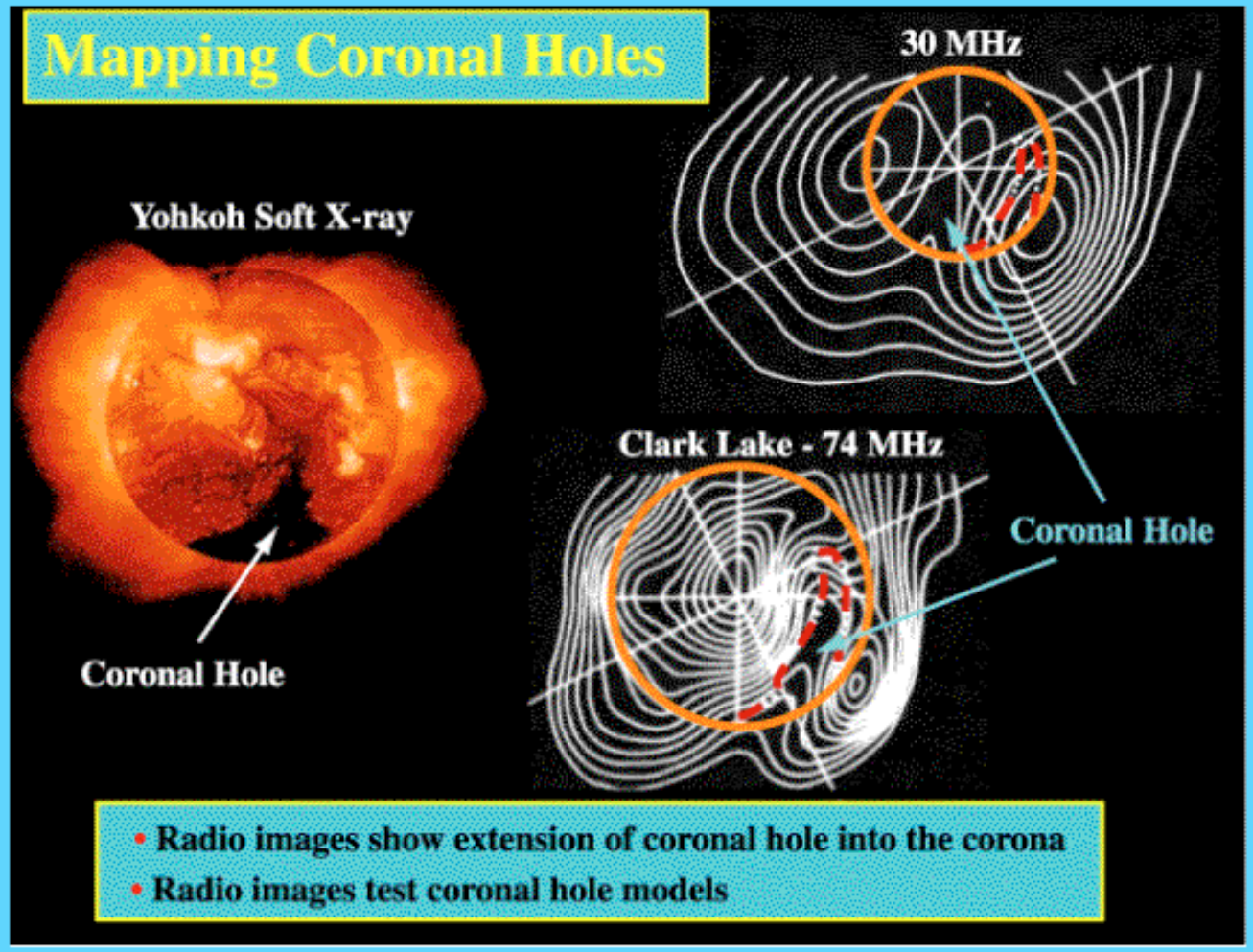

Coronal holes appear as holes at wavelengths > 3 cm. This figure compares a coronal hole in X-rays with that in meter wavelengths (E. J. Schmahl)

Polar coronal hole in microwaves

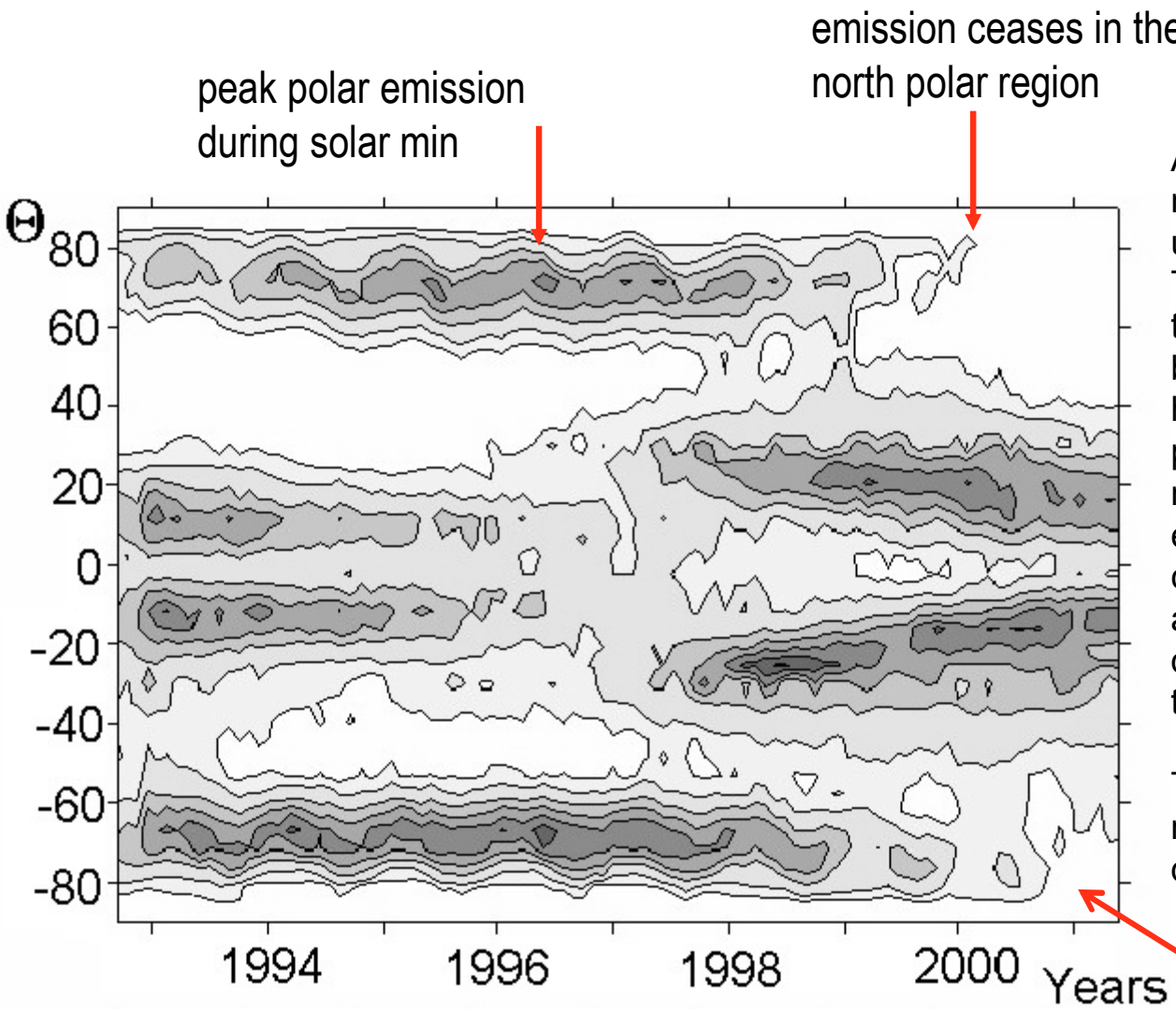

Gelfreikh et al. 2002

A long-term synoptic map of microwave emission at 17 GHz using Nobeyama radioheliograph. The low-latitude emission is due to the coronal active regions (the butterfly pattern), whereas the high-latitude emission is due to polar coronal holes. Note that the northern and southern polar emissions disappear when the coronal holes disappear. There is a north-south asymmetry in the disappearance, also reflected in the times of polarity reversal

The polar coronal hole is probably related to the poloidal field of the dynamo

Coronal Holes & Geomagnetic Storms

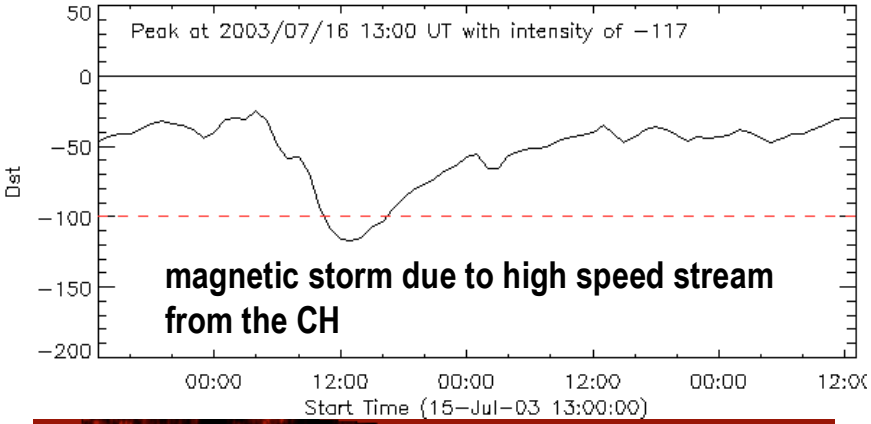

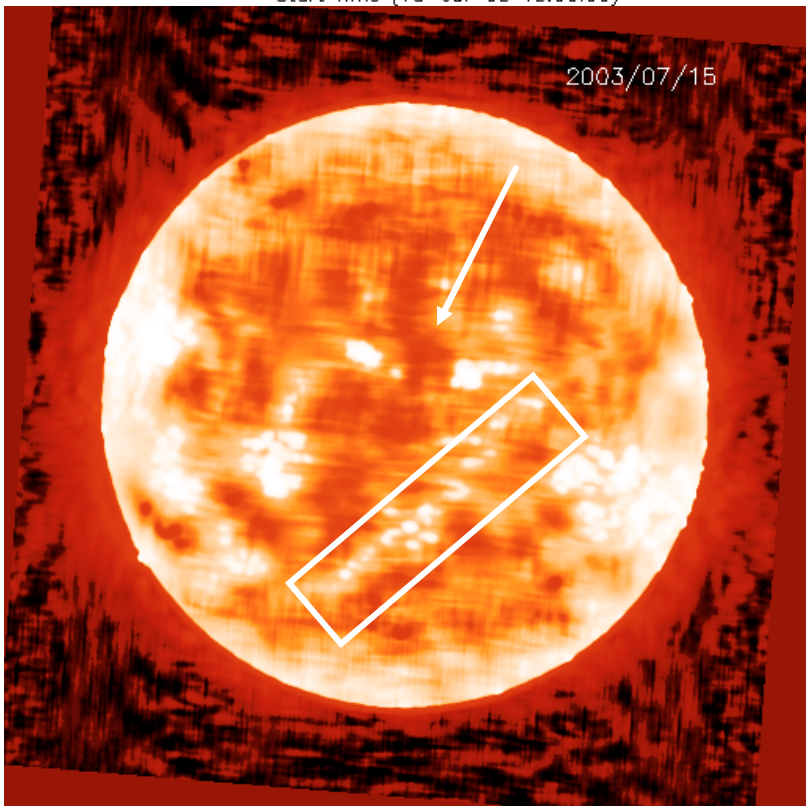

Nobeyama Radioheliograph 17 GHz image; Filament is dark unlike coronal hole. There is something special about the chromosphere under coronal holes: hotter?

SOHO/EIT 284 A image

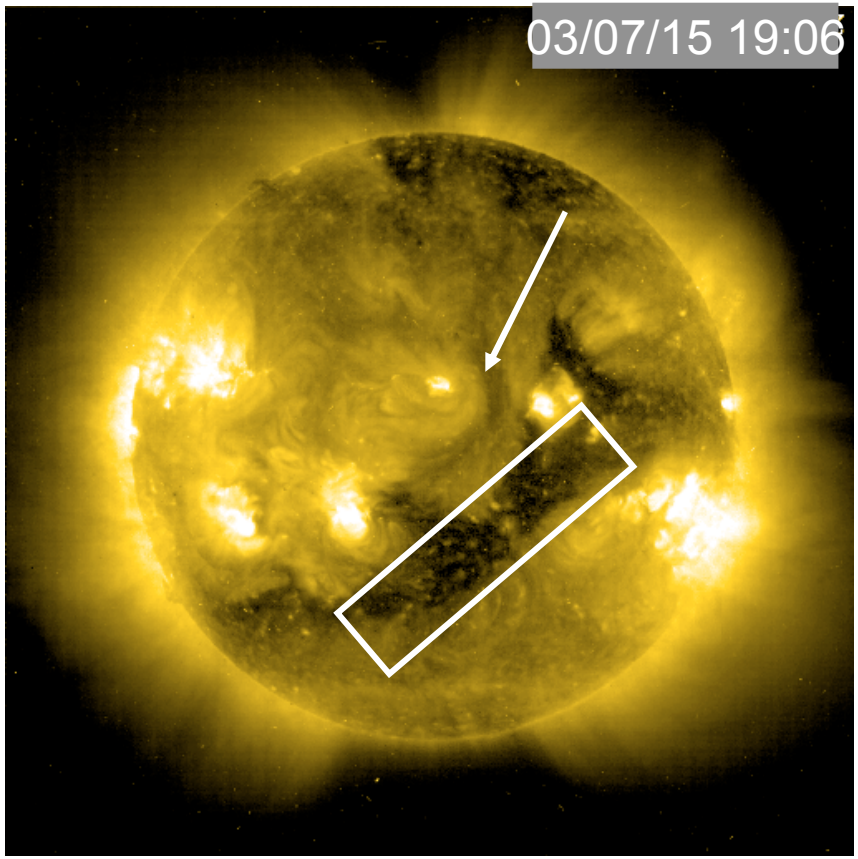

Filament is dark as coronal hole

Radio Enhancement in Coronal Holes

- **Below ~ 15 GHz, TbH < TbQ and the coronal hole appears dark relative to the quiet Sun.**
- **At frequencies > 15 GHz, TbH > TbQ, so the coronal hole appears brighter than the quiet Sun.**
- **Enhancement has been observed both in the polar and equatorial coronal holes.**
- **Associated with enhanced magnetic flux underlying the coronal hole (Kosugi et al, 1986, Gopalswamy et al, 1998a,b; Yoshiike & Nakajima, 2000).**
- **May be intimately related to the heating and acceleration of the fast solar wind.**
- **Typical enhancement is ~ 10%; Occasionally ~20% in compact structures.**

TbH – Brightness Temp of coronal hole
TbQ – Brightness Temp of quiet Sun

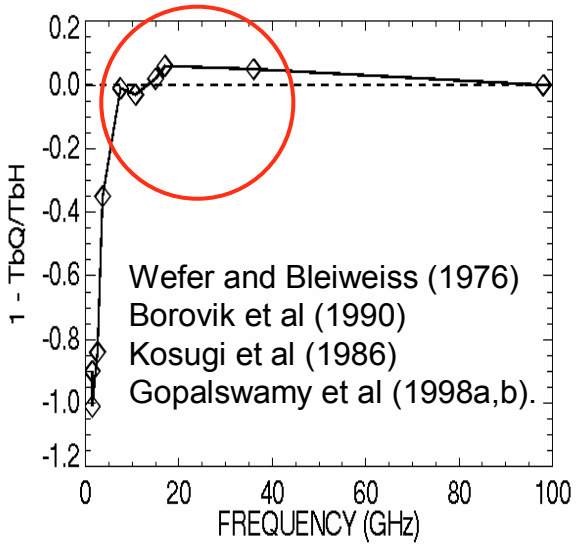

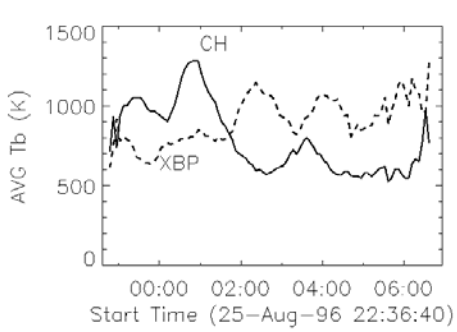

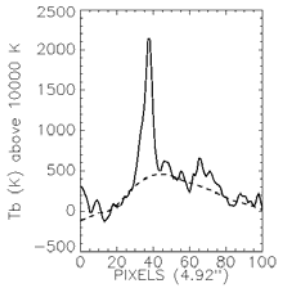

Solar Wind Acceleration

Tu et al. 2005

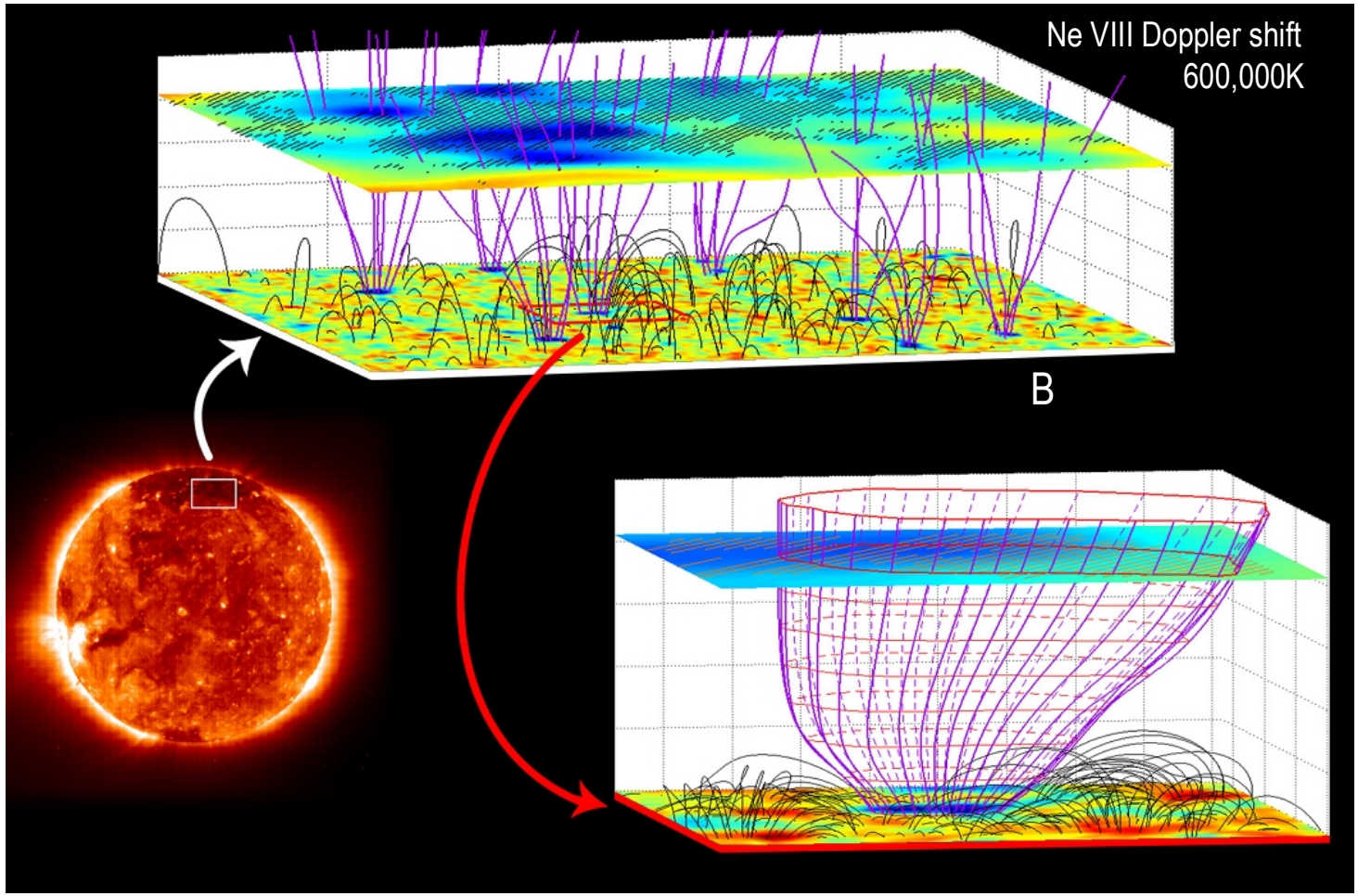

Bulk outflow not yet a height of 5,000 km, but present at 20,000 km. Closed magnetic loops are swept by convection to funnel regions where they reconnect with open field lines, releasing the plasma in the closed loops along the open field lines as solar wind (10 km/s at ~ 20,000 km). Microwave data indicate some connection to the chromosphere

Coronal Hole & Solar Wind

- Slow find from streamers ~300 km/s fast wind from coronal holes up to 800 km/s
- Slow and fast finds often collide producing corotating interaction regions
- While fast wind emanates from coronal holes, the speeds from all coronal holes are not the same.
- Skylab data indicated faster wind from larger coronal holes, which seems to saturate at large areas
- Wang & Sheeley (1990) related the solar wind speed (V) to expansion factor (f) of the coronal holes at the source surface (V ~1/f)
- Fisk et al.(1999) related the solar wind speed to the magnetic field (B) in the coronal holes (V ~B)
- Kojima et al. (2004) found significant exceptions when various populations of coronal holes and expansion factors are considered (polar holes, equatorial holes, mid-latitude holes).
- They also found a universal relationship between V and a combination of B and f: V ~ B/f
- In fact, Kojima et al. plot can be approximated by V = 300 + 550B/f km/s

Importance of B in CH

- Wang and Sheeley (1990): V~ 1/f

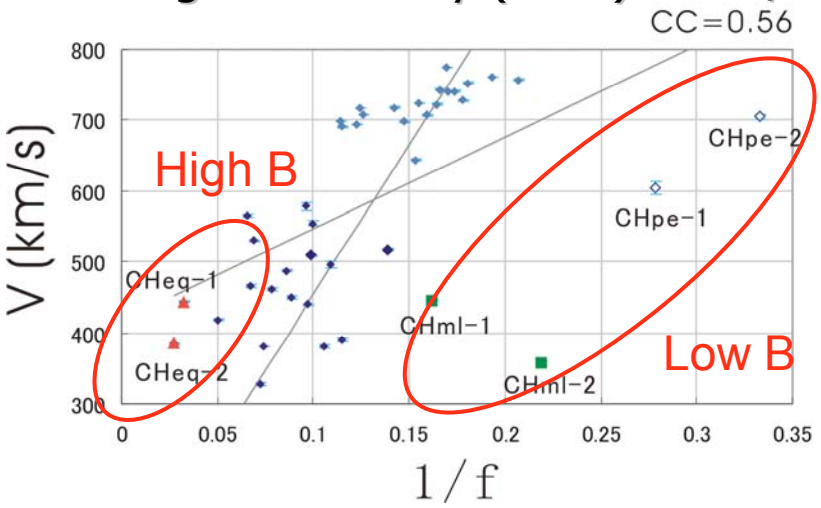

- Fisk et al. (1999) V → B via Poynting flux

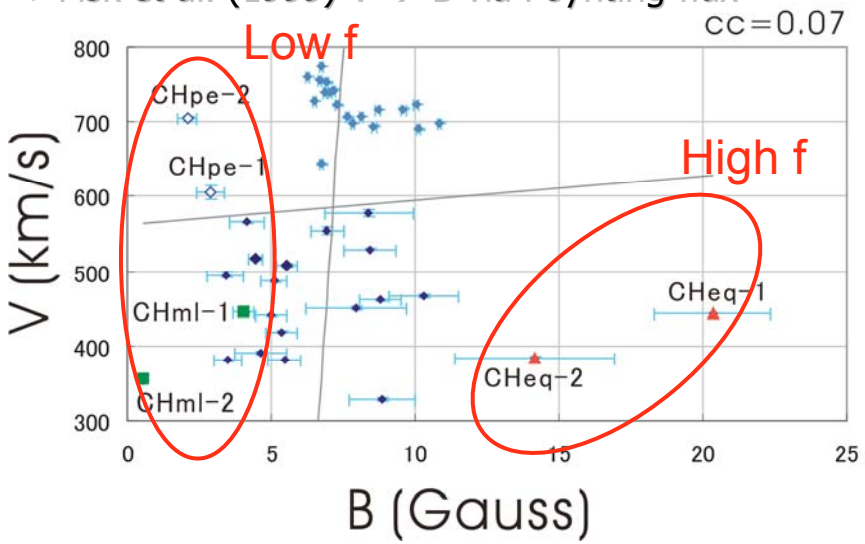

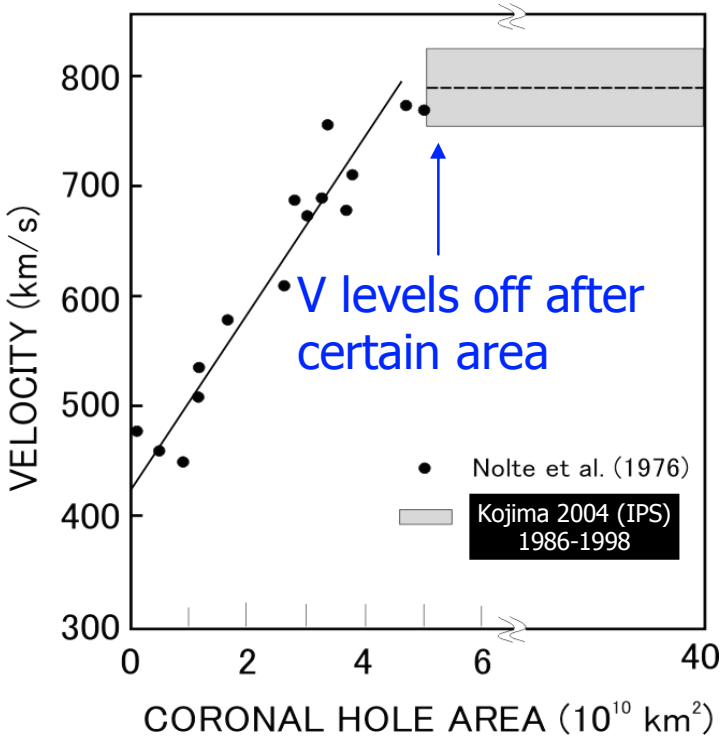

Hirano 2004, Kojima 2004

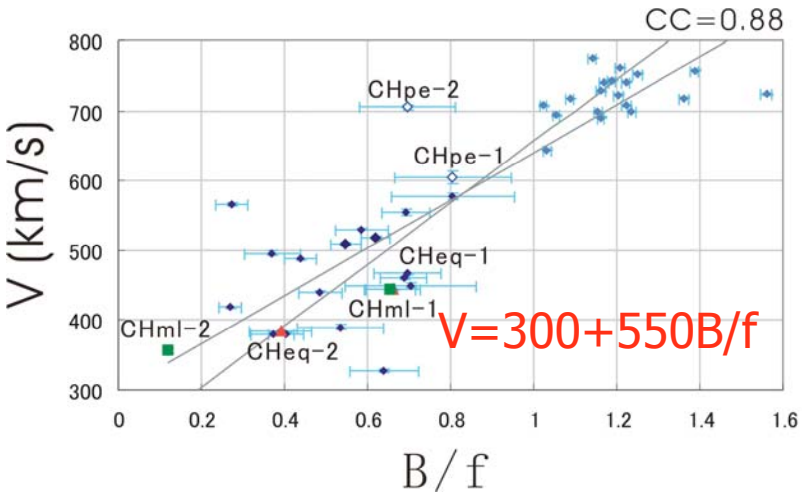

CMEs

Sunspots, Active Regions, Prominences

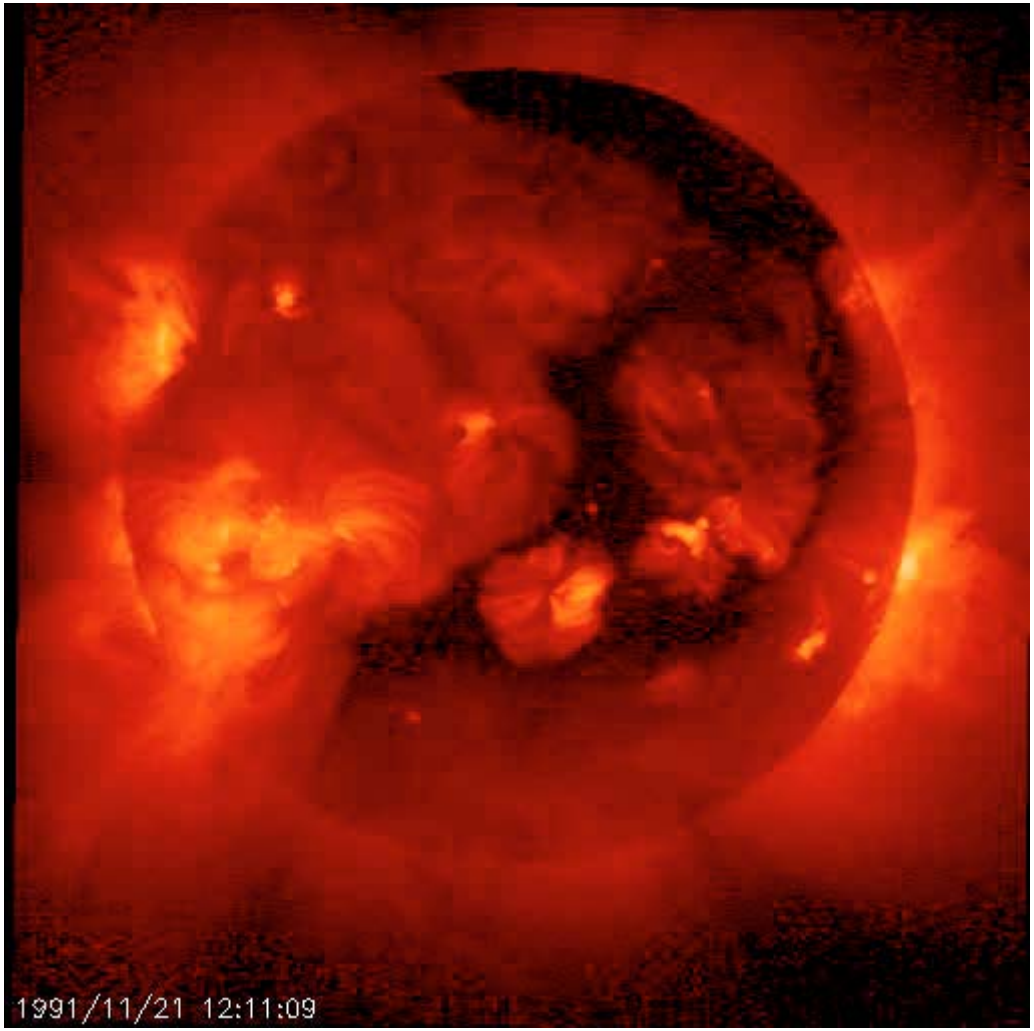

This Yohkoh/SXT movie shows the development of solar activity from minimum to maximum. Both coronal holes and active regions are seats of solar mass emission in the form of solar wind and coronal mass ejections that impact Earth's magnetosphere

CMEs with the corresponding changes in active regions

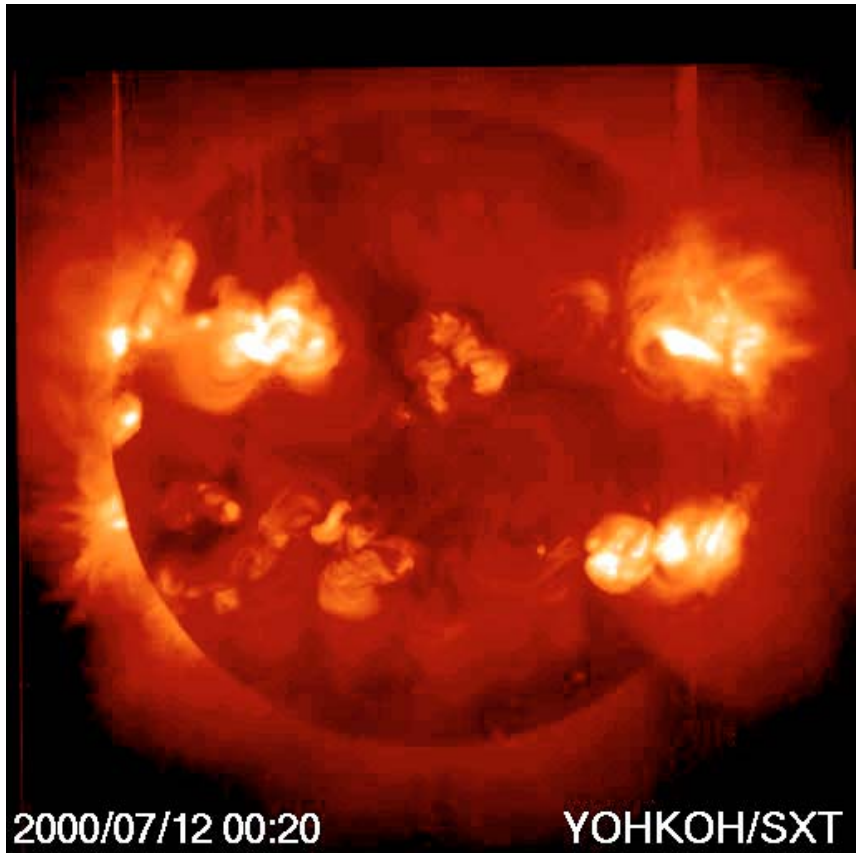

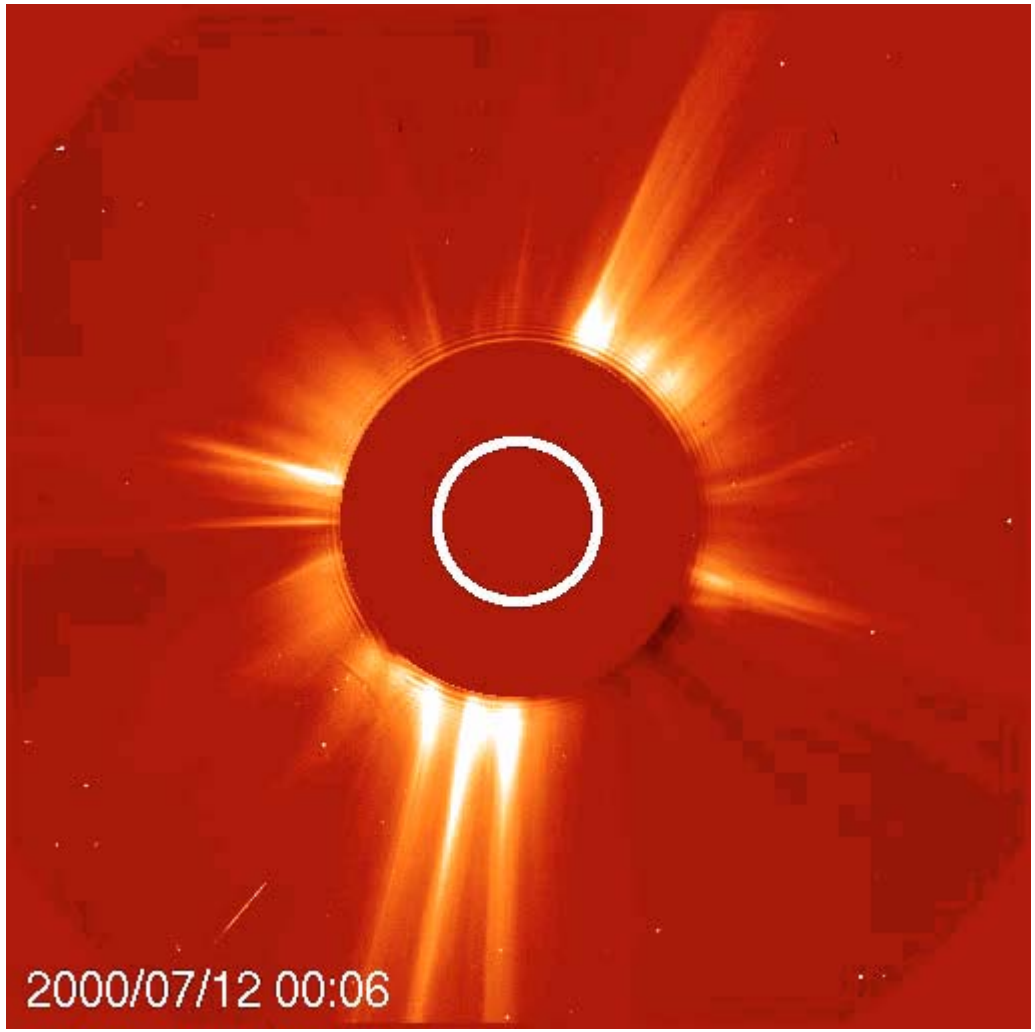

High Energy Plasmas & Particles

This movie taken by the C3 telescope on board the SOHO coronagraph shows how CMEs affect our ability to operate in space. The coronal mass ejections appearing on the solar disk accelerated solar energetic particles that reached the SOHO spacecraft in tens of minutes and blinding the detectors (the “snow storm” effect). Further observations of CMEs were hampered by this for several hours. The CMEs themselves arrived at Earth in less than a day to cause superintense geomagnetic storms.

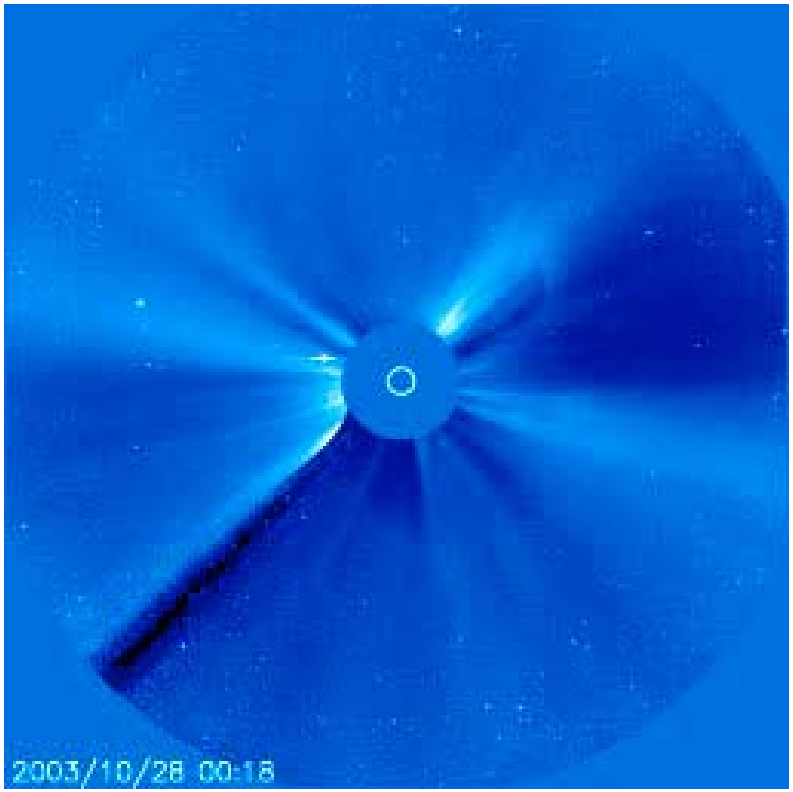

CME Structure

CMEs consist of the coronal features we discussed: the ambient corona with the permeating magnetic field and prominences. It also contains a dark void (cavity), which may be a region of enhanced magnetic field. The prominence erupts in association with the CME and becomes the inner bright core of the CME.

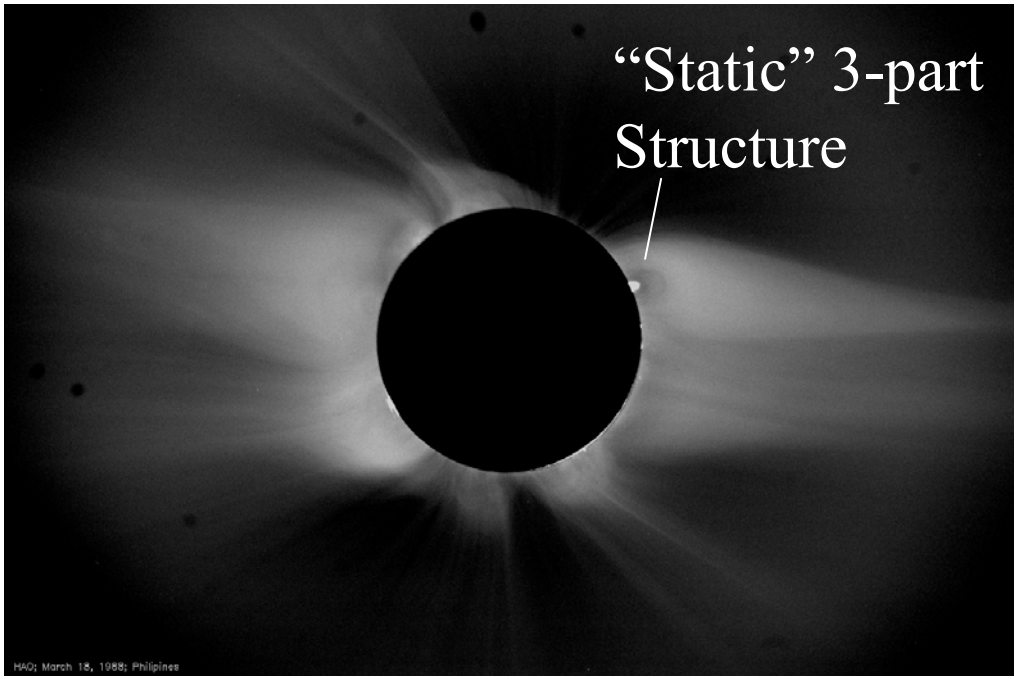

March 18, 1988 Eclipse Philippines. Courtesy: HAO

A 3-part CME

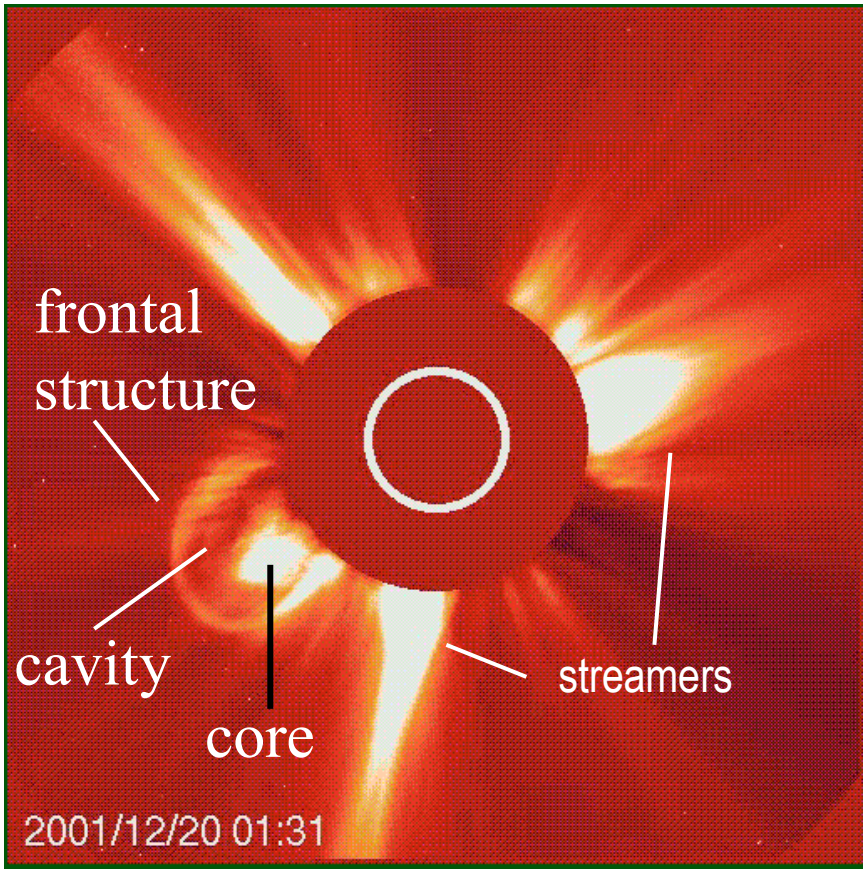

Post-eruption Structures: Scars of Eruption

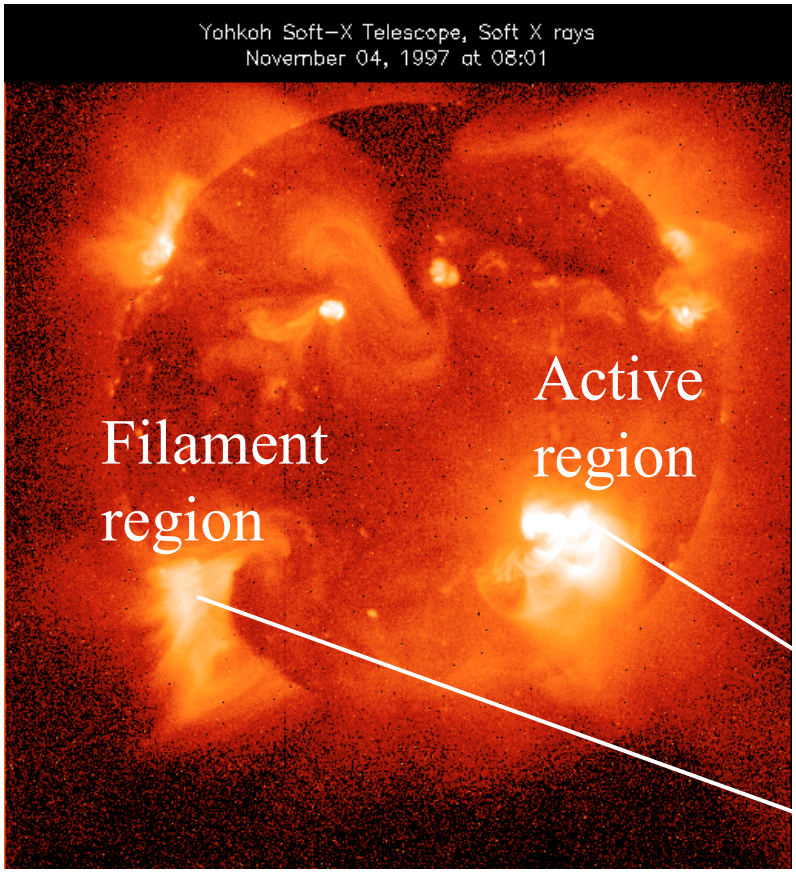

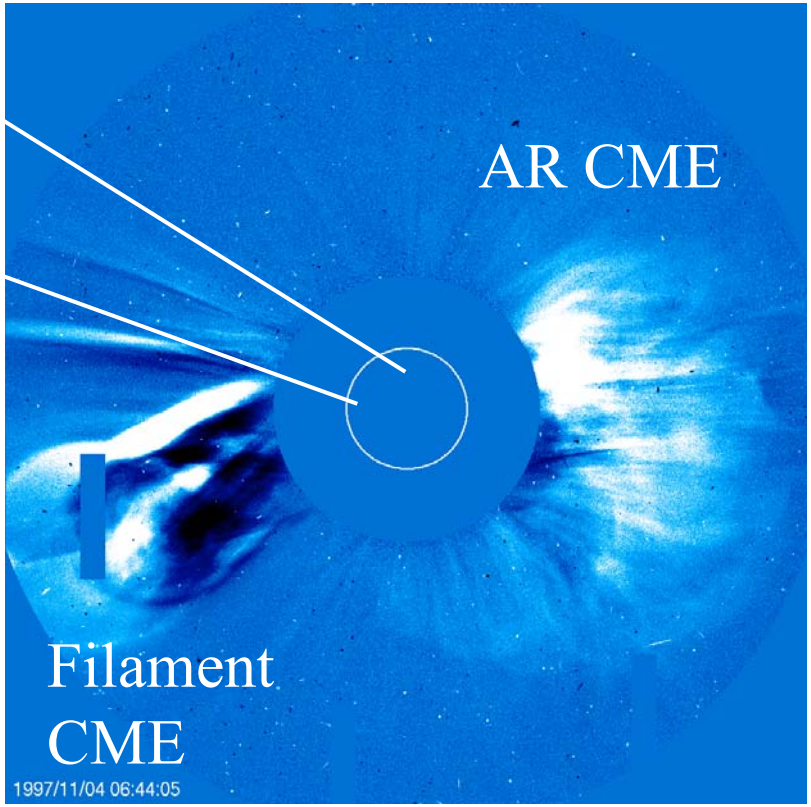

Flares happen at the time of CME onset. The bright loops observed in X-rays are the post eruption structures thought to be formed beneath the CME structures and confined to the eruption region. Filament regions generally have arcade of loops, while active regions have compact but brighter loops

CME Near the Sun: What We Observe

- The three-part structure becomes four part (with a shock forming at the leading edge of the CME) if the CME motion is super-Alfvenic. The shock is inferred from radio bursts of type II, SEPs or detected by in situ observations in the solar wind. Also Moreton waves in the chromosphere or EUV brow waves in the corona
- The CMEs carry information on their hot origin: Heating in the flare region → high Fe charge state in 1 AU flux ropes.
- The flux rope near the Sun seems to become the interplanetary CME or magnetic cloud (MC)

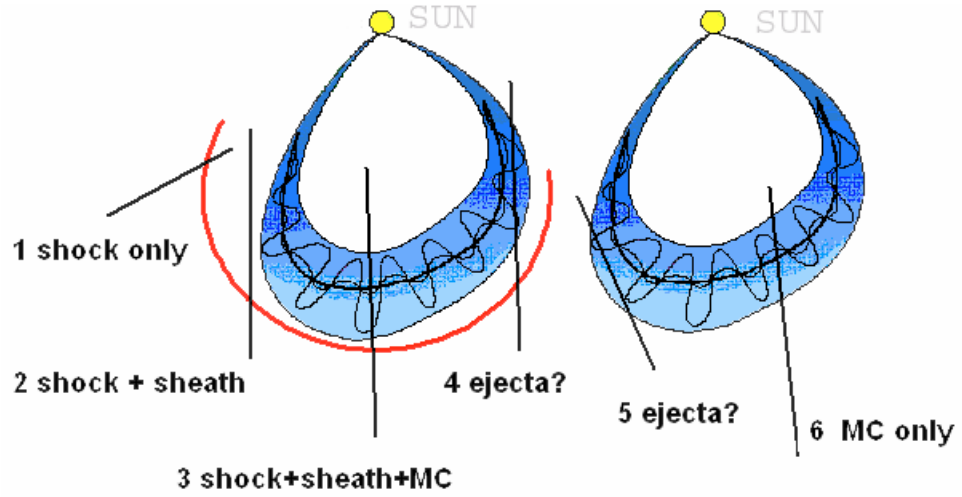

Burlaga, Lepping

Cliver et al 1986

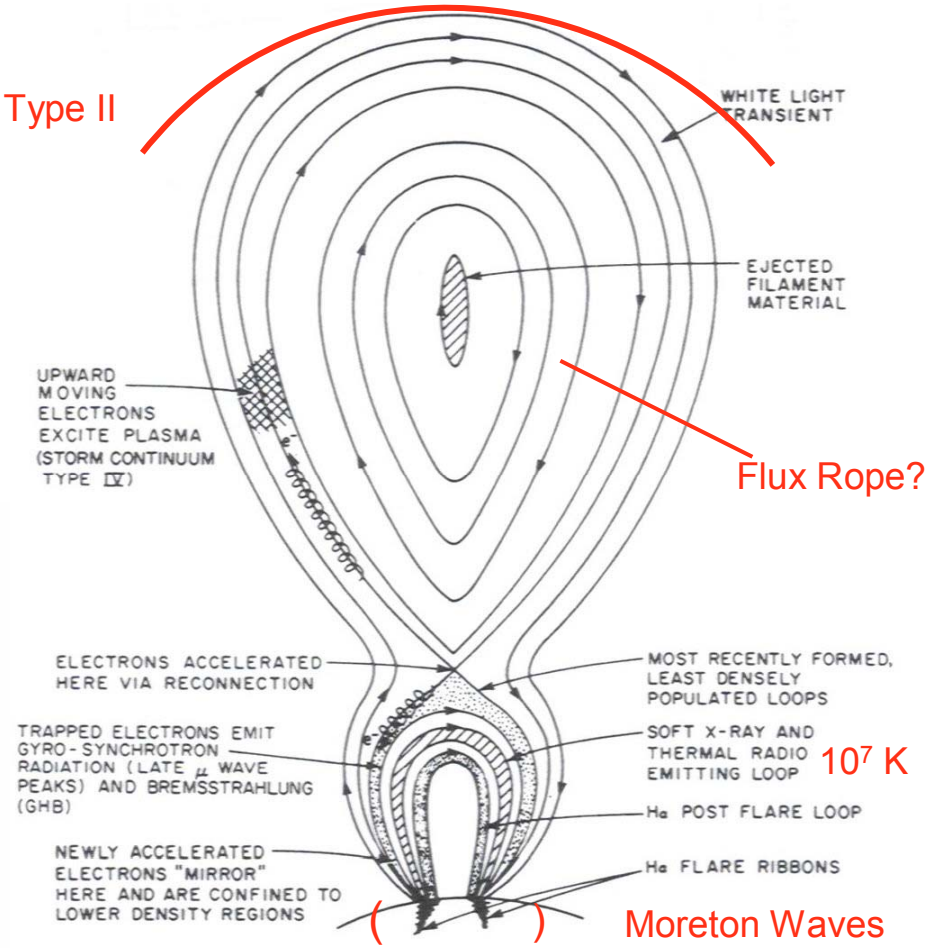

Type II Radio Burst due to a CME-driven shock

- Very intense type II radio bursts indicate Shock-driving capability of CMEs.
- 1-14 MHz crucial because the associated CMEs just leave the Sun.
- Type II bursts can track a CME-driven shock from sun to earth
- In the example below, Sky-plane height of the CME is ~9 Ro when the radio emission is at 800 kHz. This is the plasma frequency of the corona at a distance of ~9 Ro

Type II bursts are due to electrons accelerated in the shock front. These electron distributions are unstable to Langmuir waves, which convert to electromagnetic waves observed as type II bursts

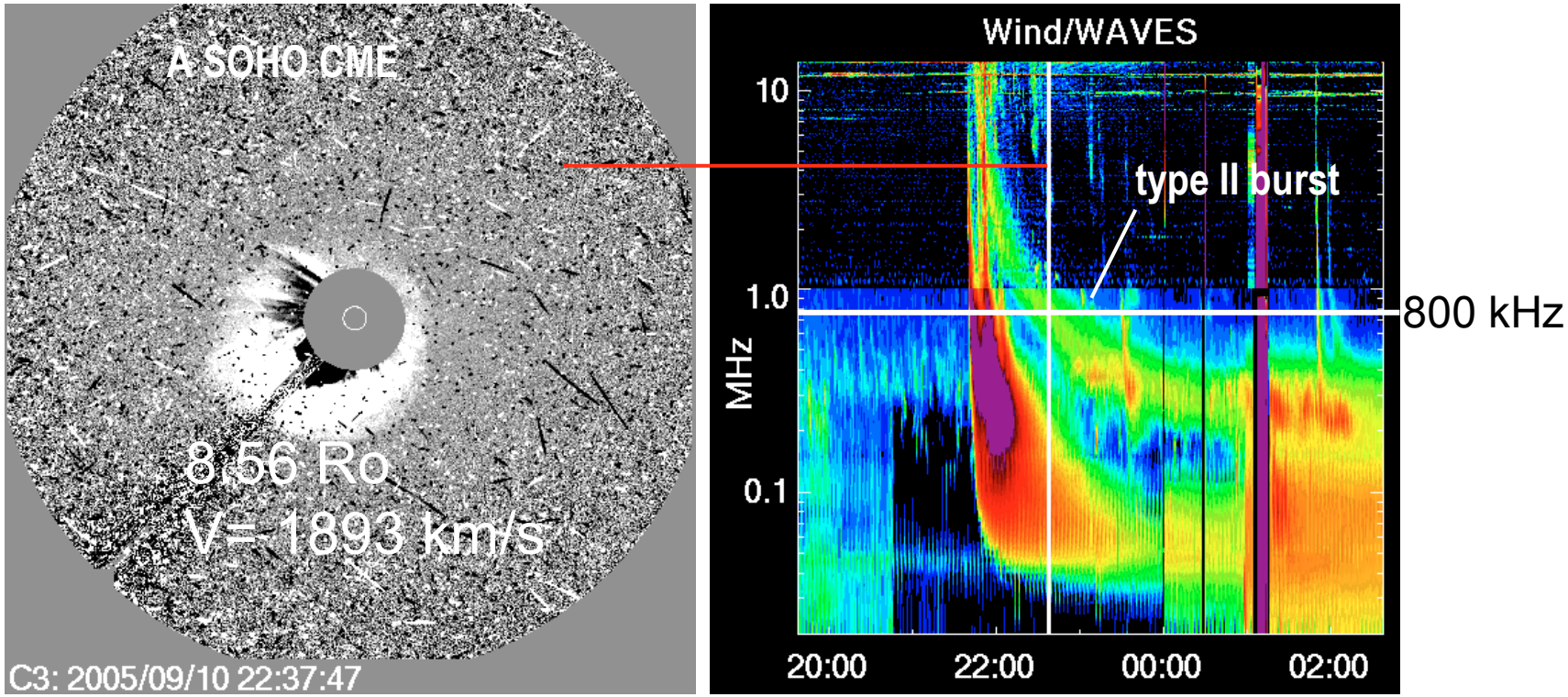

1-14 MHz radio range is called decameter-hectometric wavelengths or DH for short

Physical Properties of CMEs

- Temperature: 8000 K – 10^7 K (Prominence core to flare ejecta)
- Density: Coronal in the leading edge; higher in the prominence; cavity in between ?
- Magnetic field: High in the prominence (up to 150 G) and cavity; low in the frontal?

Statistical Properties

Speed & Width

- < 20 km/s to 3387 km/s (avg = 487 km/s)
- Highest speed observed on 2004/11/10
- <50 CMEs with v > 2000 km/s – CME speed not too much higher than ~ 3000 km/s
- Apparent width ranges from a few deg to 360 deg
- Average width of non-halo CMEs (W < 120 deg): 47 deg
- Full halos: ~3%
- Wide (W>120 deg) events: ~11%

  - implications for CMEs in the heliosphere

1996-2004 CMEs

Speed

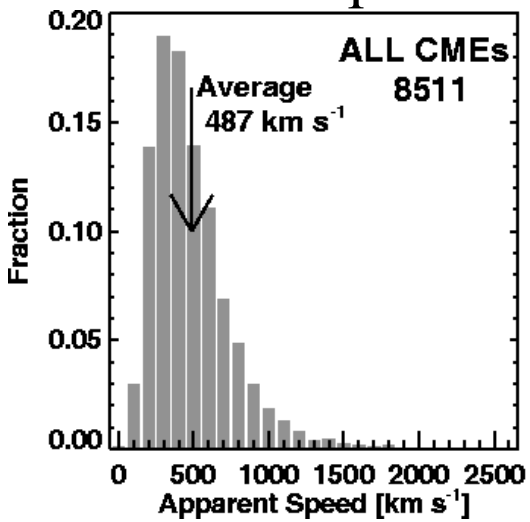

Width

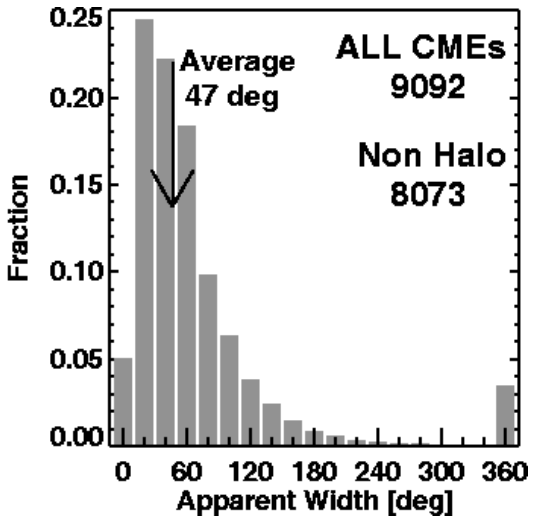

Speed & width are in the sky-plane. No attempt was made to correct for projection effects

It is not possible to measure the speeds of some CMEs due to poor quality or lack of at least two frames

CME Mass and Kinetic Energy

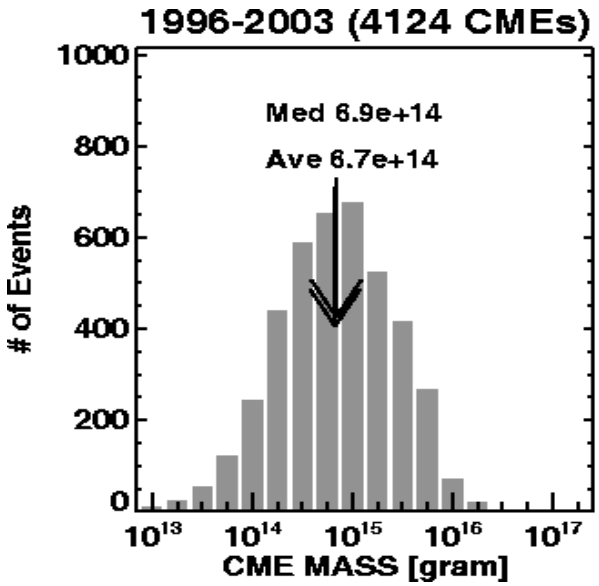

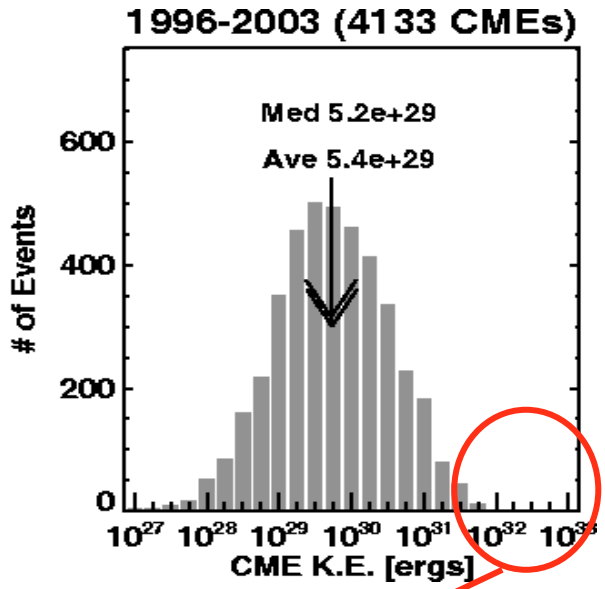

AR	Area (msh)	$VB^2p/8\pi$ (erg)	Max KE (erg)
AR0484	1750	3.66E+33	2.4e+32
AR0486	2610	4.57E+33	1.2e+33
AR0488	1750	2.76E+33	1.3e+32

Active region area in millionths of a solar hemisphere

magnetic potential energy from some large active regions and the kinetic energy of the largest CME from the regions.

Gopalswamy et al. 2005 JGR

Acceleration

Comparing the speeds of CMEs near the Sun and ICMEs (magnetic clouds) at 1 AU

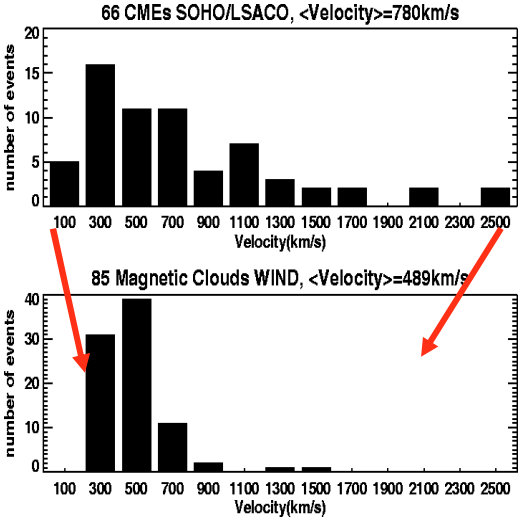

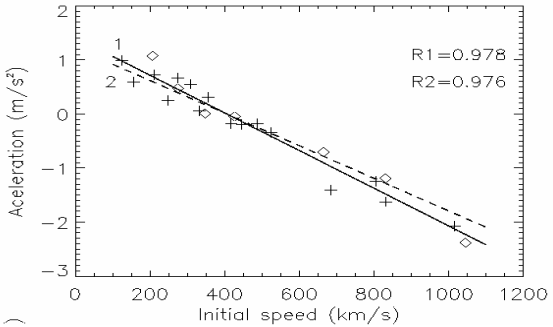

$a = -0.0054V + 2.193$

$a = -0.0054\,(V - 406)$

$a = 0$ for V=406 → CMEs riding on the solar wind

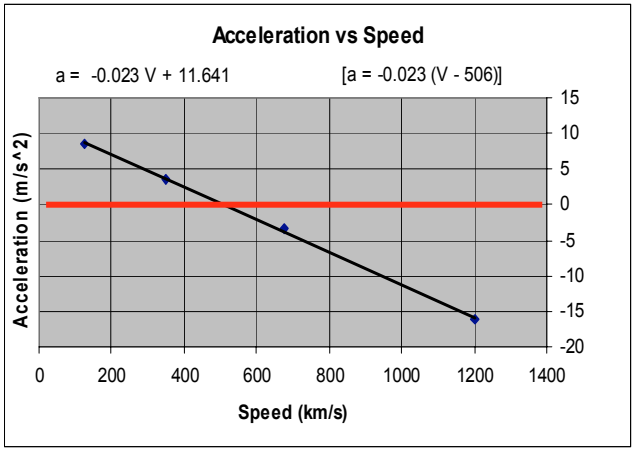

$a = -0.023\,(V - 506)$

- The dependence of acceleration *a* on speed *V* is similar in the LASCO FOV and over the Sun-Earth distance
- Very slow CMEs accelerate
- Very fast CMEs decelerate
- CMEs near slow wind speed show little acceleration
- Near the Sun, *a* has propelling, gravity & drag components

Gopalswamy et al.2000; 2001
Yashiro et al., 2004,
Gopalswamy, 2004

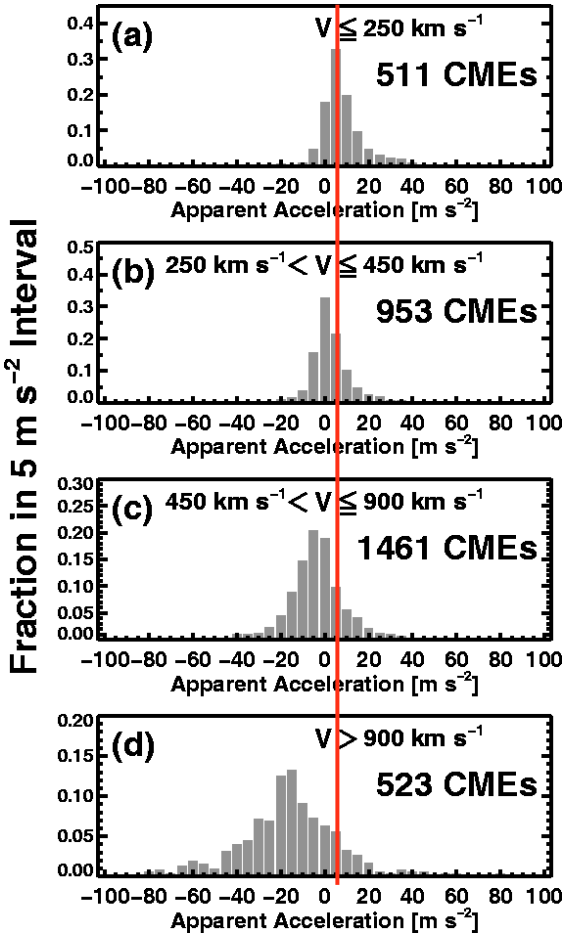

Transit Time of Shocks & CMEs

The IP acceleration can be used to estimate the CME transit time to Earth. The shock transit time can be obtained from the CME transit time by estimating the standoff distance.

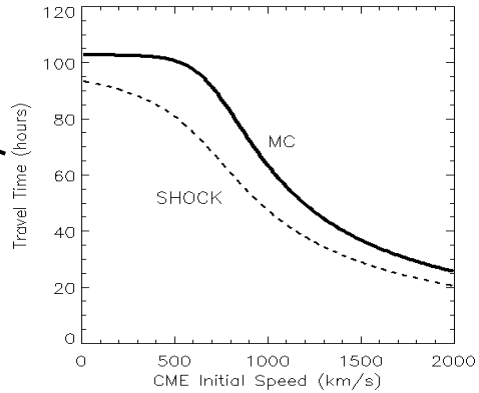

Empirical models for shock and CME arrival at Earth

SOHO contributed 2 events to the historical fast transit events compared with a simplified formula for the shock transit time.

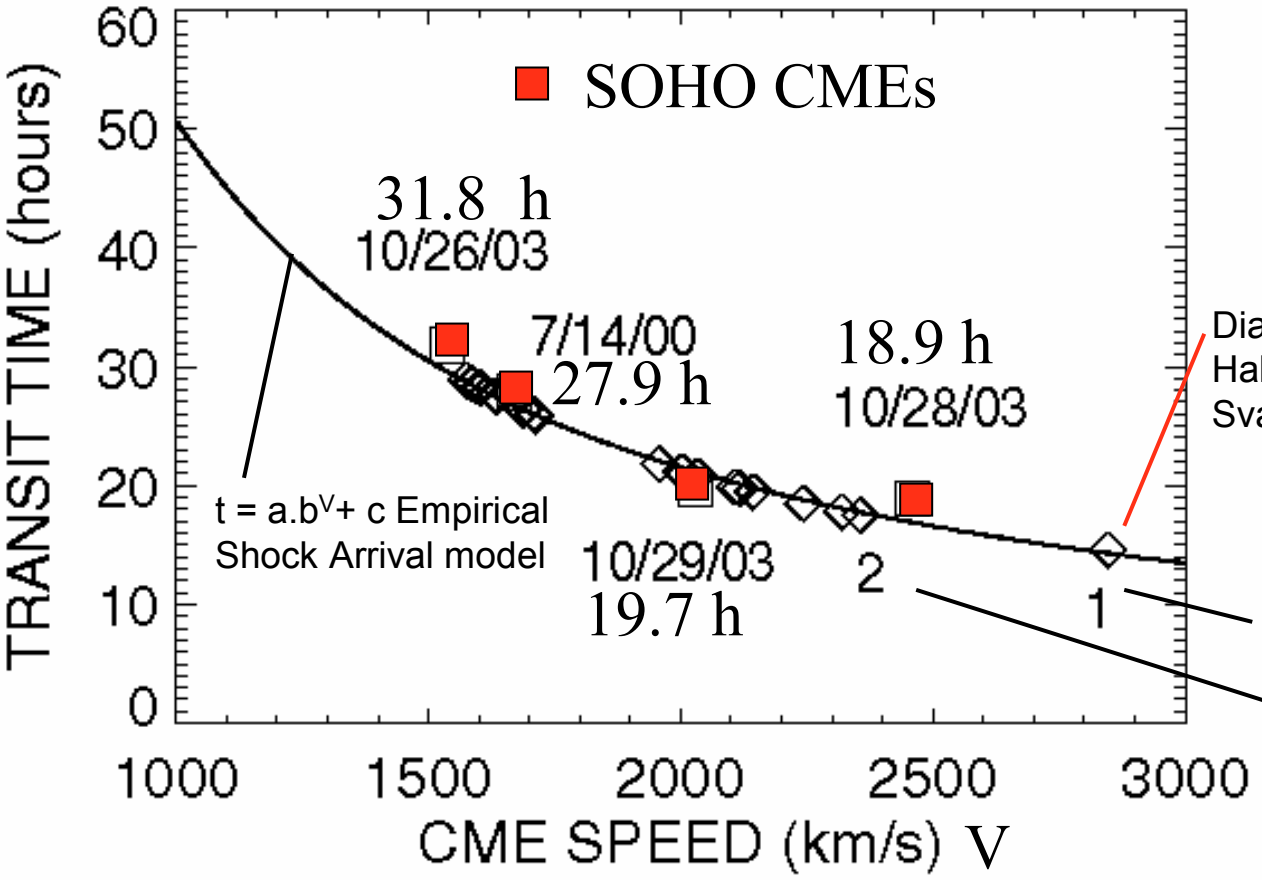

Diamonds: historical flare-SSC time from Hale 1931, Newton, 1943, Cliver & Svalgaard 2004, Gopalswamy et al 2005

Aug 4, 1972
Sep 1, 1859 Carrington

From Gopalswamy et al. 2005 JGR

Solar Cycle Variation of CME Rate and Speed

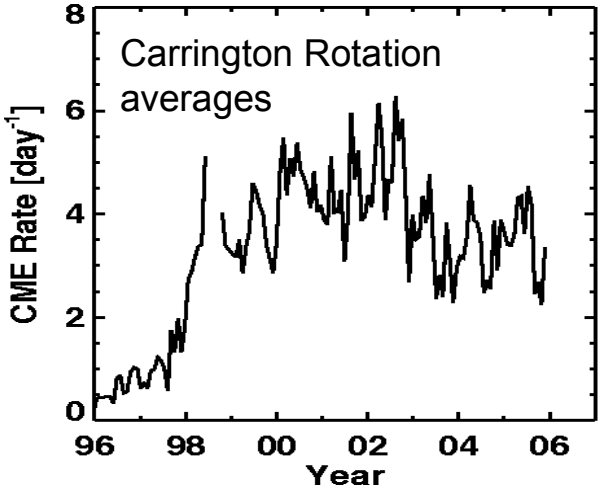

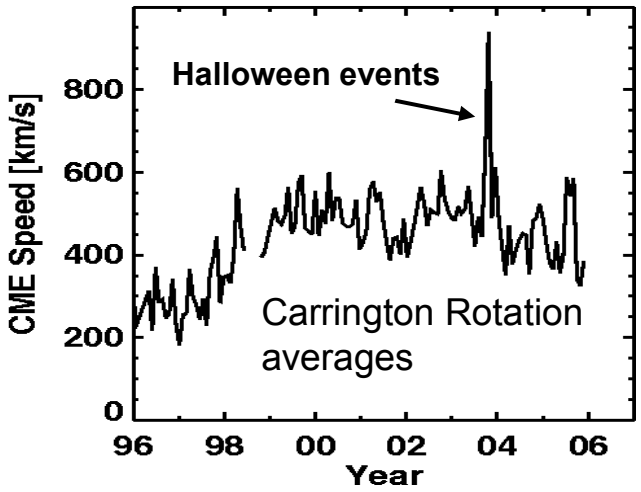

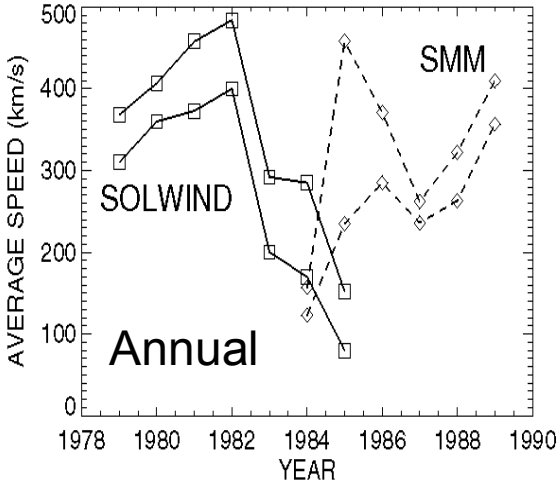

SOHO CME rate increased from ~0.5/day during solar minimum to ~6/day during maximum. The maximum rate is higher by a factor of 2 (pre-SOHO max rate ~3/day)

The pre-SOHO correlation between sunspot number and CME rate was confirmed, but the correlation was weaker. This seems to be due to the high-latitude CMEs that started in 1999 from polar crown filament region

The solar cycle variation of average CME speed was inconclusive in the pre-SOHO era. SOHO data confirmed the increase from minimum to maximum by a factor of 2. The spikes in the speeds are due to some active regions, which are copious producers of fast CMEs.

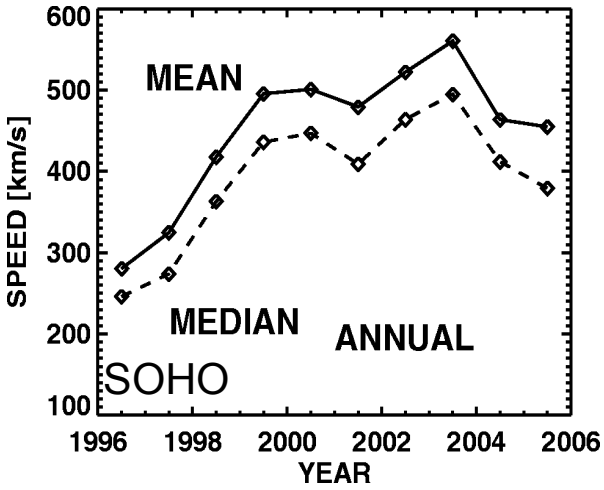

High & Low latitude CMEs

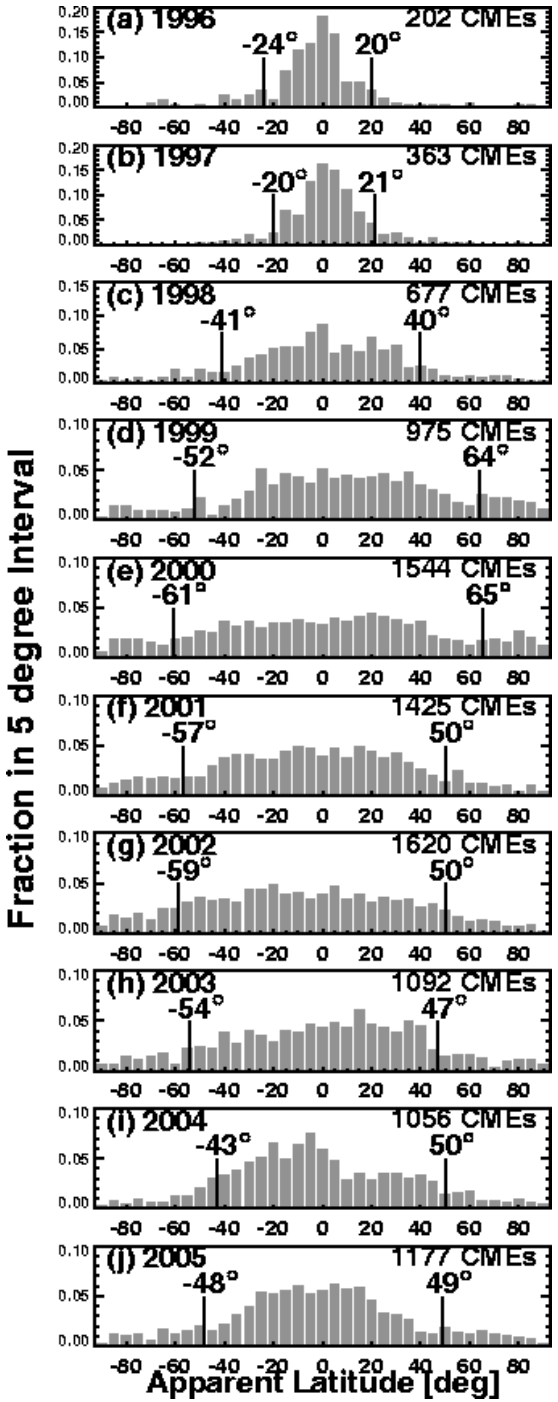

The average latitude changes significantly over the solar cycle

2005 distribution looks similar to that in 1998

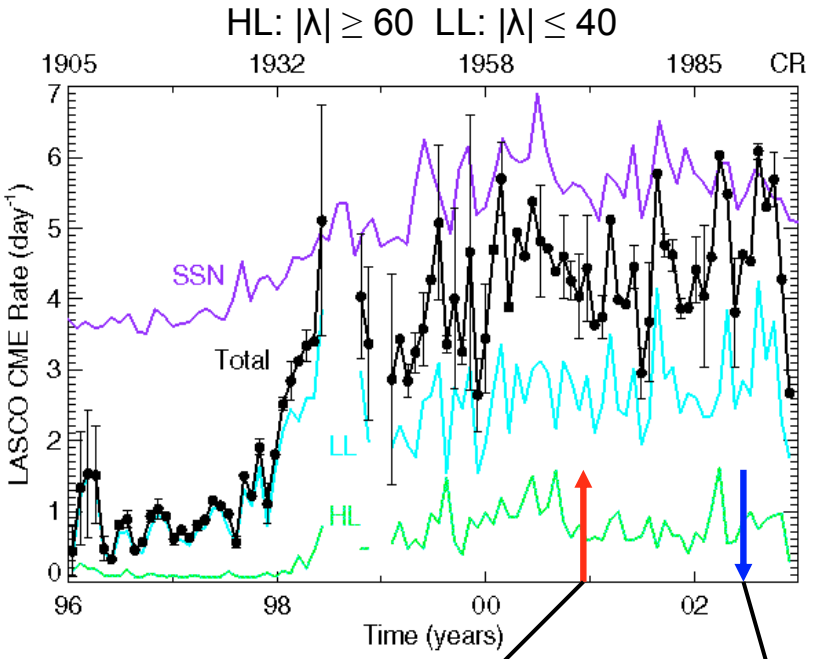

Polarity reversal in the northern hemisphere

Polarity reversal in the southern hemisphere

Polarity reversal coincides with the cessation of HL CMEs separately in the northern and southern hemispheres

CMEs & Cosmic Ray Modulation

An interesting consequence of the HL CME rate and polarity reversal is the connection to the modulation of galactic cosmic rays (GCRs). Newkirk et al. (1981) had identified CMEs as the solar origin of the low-frequency power in the interplanetary magnetic field fluctuations and suggested that the solar-cycle dependent modulation of GCRs can be explained by the presence of the fluctuations in the heliosphere. For effective modulation, a higher and more cycle-dependent CME occurrence rate (varying by factors up to 10) was required than pre-SOHO data indicated (Wagner, 1984). SOHO has demonstrated the higher and more cycle-dependent rate and hence the GCR modulation should be possible.

Cross-correlation between GCR intensity and high-latitude (HL) and low-latitude (LL) CME rates for (left) the A< 0 epoch of cycle 21 and (right) the A>0 epoch of cycle 23. Note the switching of the dominant correlation between cycles 22 (A<0) and 23 (A>0).

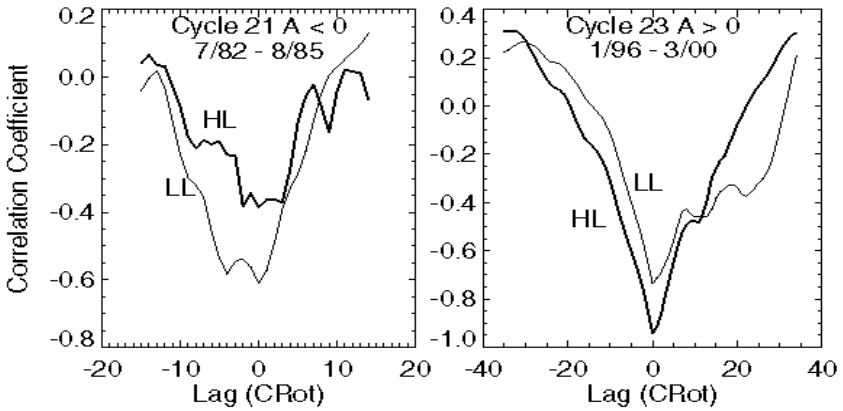

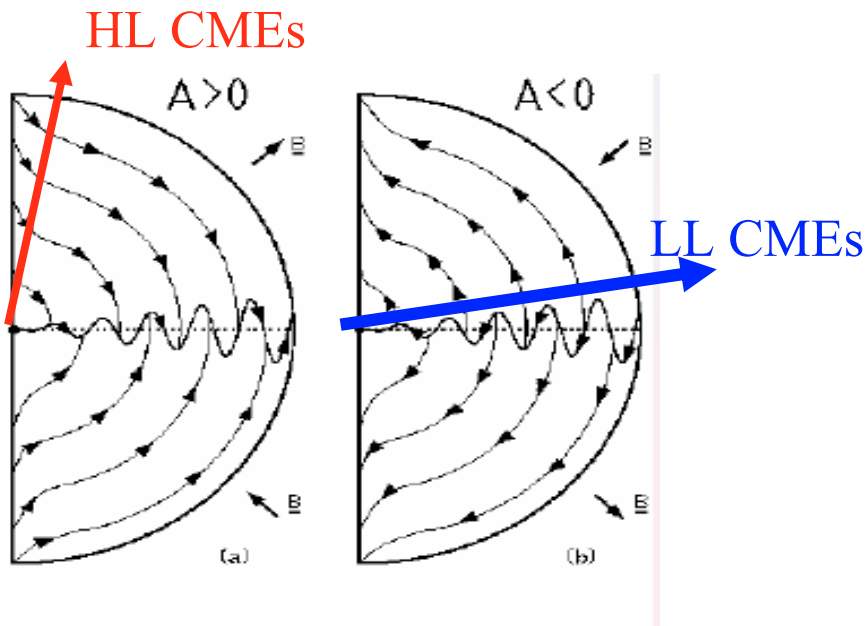

Gopalswamy, 2004

Sources of geoeffective & SEPeffective CMEs

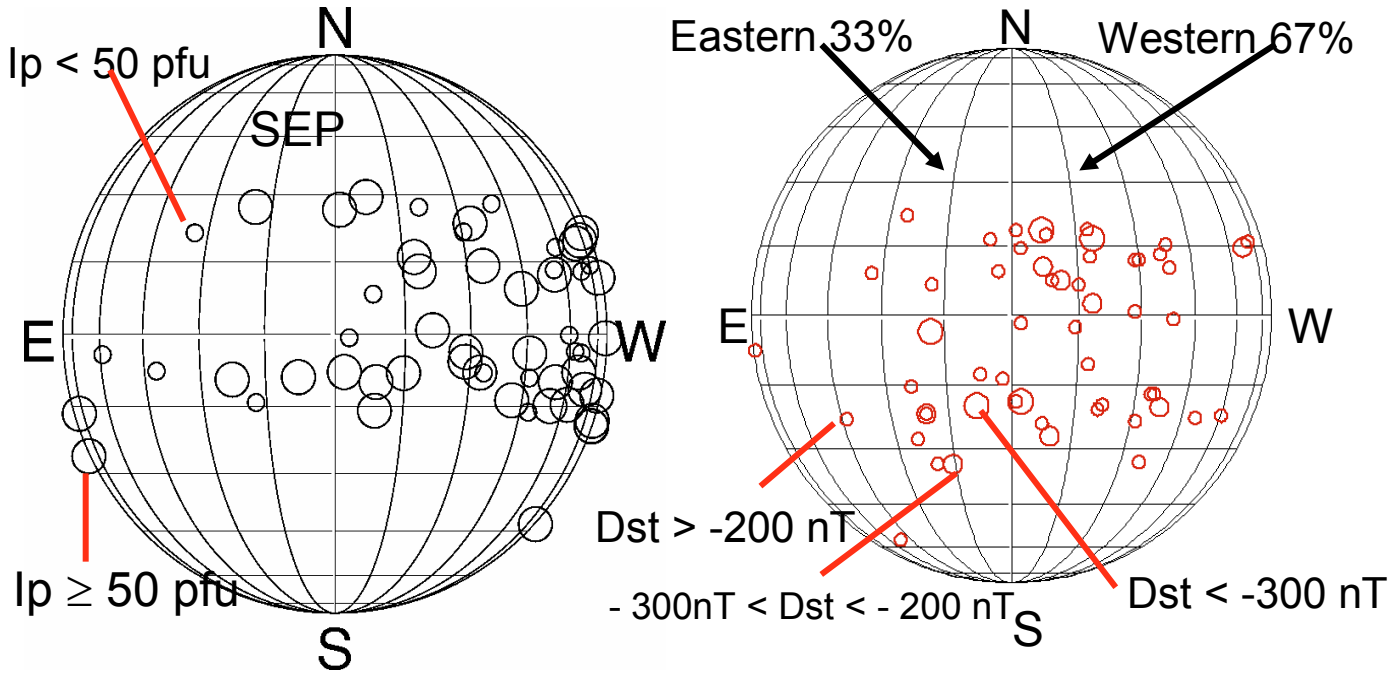

SEPeffective geoeffective

Disk center source for plasmag impact; western events for SEPs

CMEs Relevant for Space Weather

All – All CMEs in cycle 23
km - CMEs associated with kilometric type II bursts
m - CMEs associated with metric type II bursts
GEO – geoeffective CMEs
HALO – Halo CMEs, which appear to surround the occulting disk of the coronagraph
DH – CMEs with DH type II bursts
mkm- CMEs with type II bursts from m to km wavelengths
SEP – CMEs associated with solar energetic particles
GLE - CMEs associated with ground level enhancement of SEPs

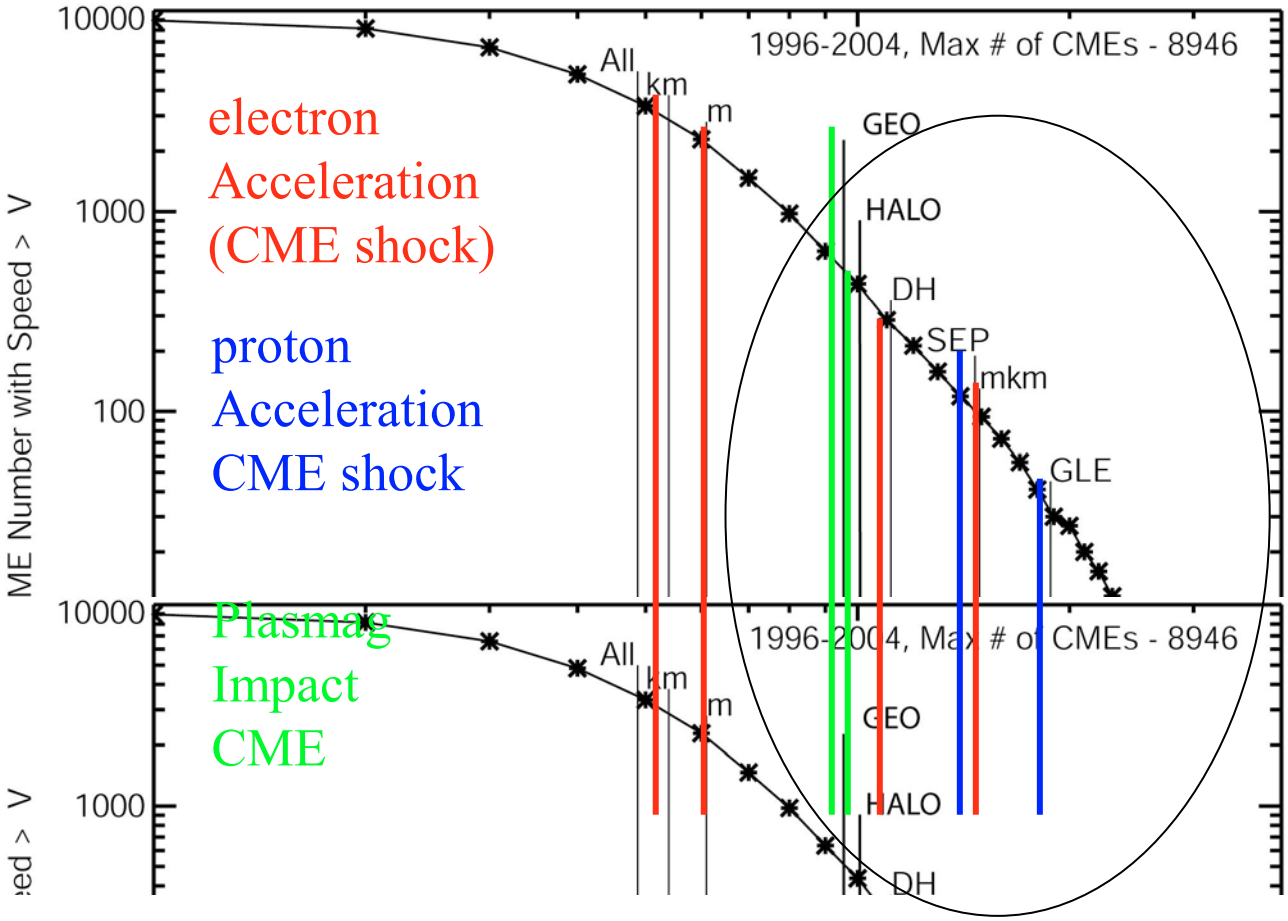

Even though > 10,000 CMEs have been observed by SOHO, only about 10% of them have heliospheric consequences These have speed ≥1000 km/s

Solar Disturbances can affect the extent of the heliosphere

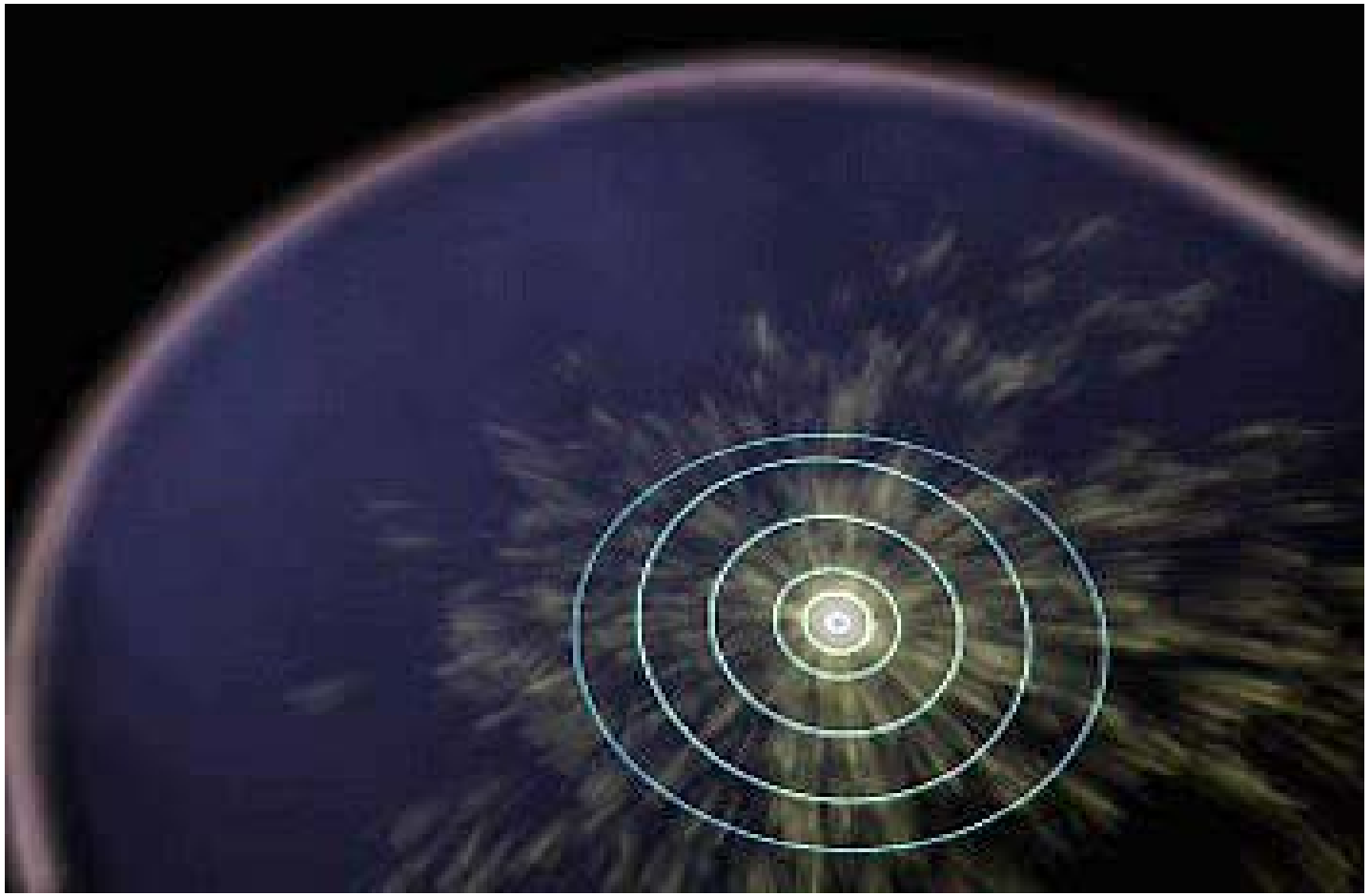

Animation showing the 2003 October November solar eruptions (based on Voyager 1 and 2 observations. Demonstrates the impact of solar events throughout the heliosphere
courtesy: T. Zurbuchen

Reference Material

- E.L. Schatzman & F. Praderie, The Stars, Springer-Verlag (1993)
- A. C. Philips: The Physics of Stars
- J. T. Schmelz and J. C. Brown (editors): The Sun: A Laboratory for Astrophysics (1992)
- A. Hanslmeier, The Sun & Space Weather, Kluwer, 2002
- J. Christenson-Dalsgaard: Lecture Notes on Stellar Oscillations, 2003
- Living Reviews
- http://cdaw.gsfc.nasa.gov/publications

List of movies

- slide# file name
- 33 puls_l8m4
- 36,40 hr_V_short.mpg
- 43 ray20.mpg
- 62 DYNAMO.AVI
- 70 gran_mov27M_99_crea.mpg
- 75 sunspot_june593_SVST_lapalma.mpg
- 76 movie02.mpg
- 77 spinspot2.mpg
- 103 sxt_wwwmovie_060425_092110X.mpg
- 104 sxt_almg.20000712.mpeg
- 104 000712_c2.mpeg
- 105 c3cmesm.mpg.mpeg
- 120 heliopause3.mpg